Process Integration of Electrolysis, Gasification and Syngas Upgrading for Biofuel Production

A techno-economic assessment

Andrej Milisav

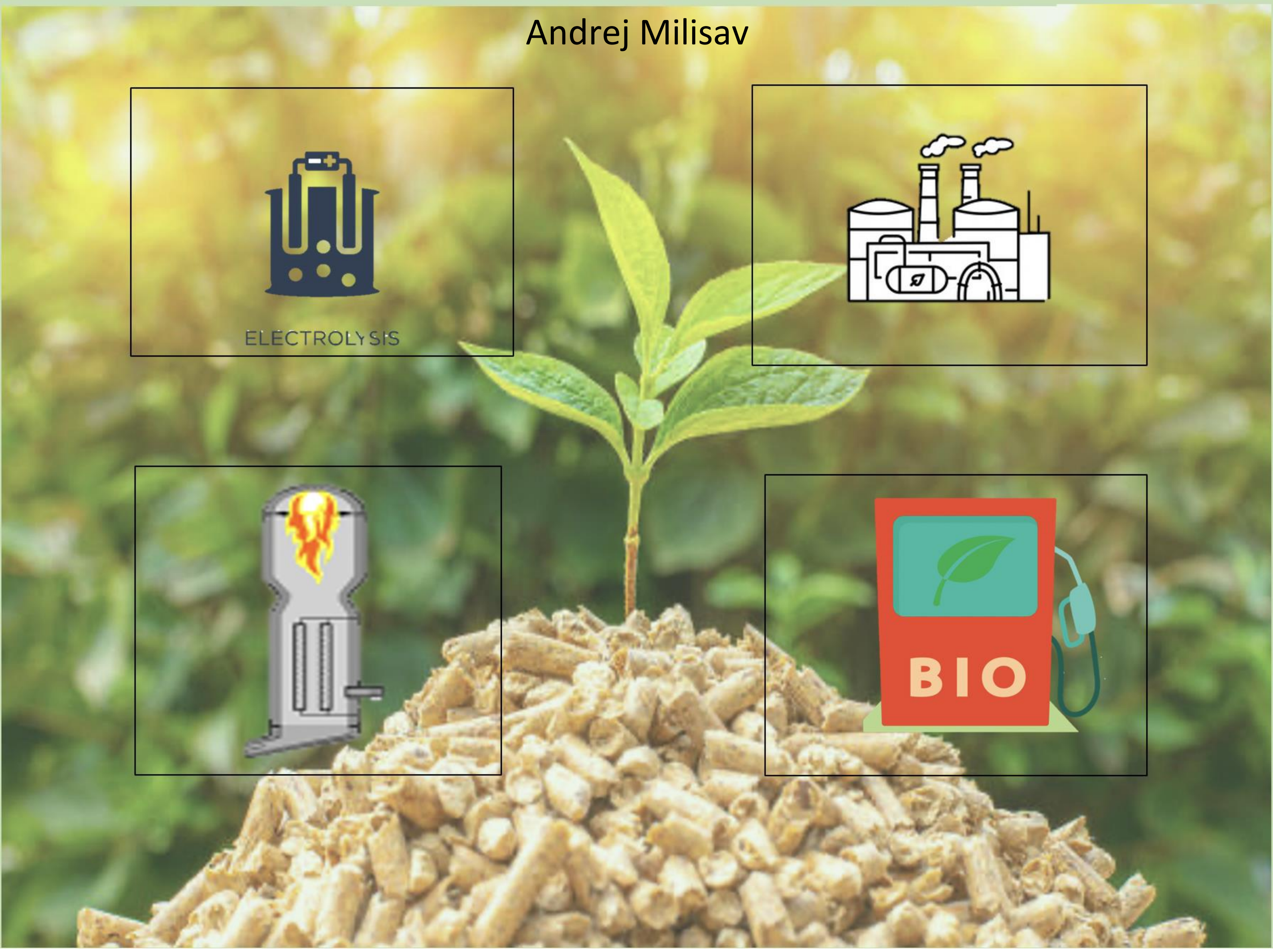

TU Delft

Process Integration of Electrolysis, Gasification and Syngas Upgrading for Biofuel Production

A techno-economic assessment

By

Andrej Milisav

in partial fulfilment of the requirements for the degree of

Master of Science
in Sustainable Energy Technology at the Delft University of Technology

to be defended publicly on May 22nd

Studentnumber: 4478045

Supervisor:	Prof. dr. ir. W. De Jong	
	Dr. ir. W. Guo (external)	
	Prof. dr. ir. M. Ramdin	
Thesis committee:	Prof. dr. ir. W. De Jong	TU Delft, supervisor
	Prof. dr. ir. M. Ramdin	TU Delft, supervisor
	Prof. dr. ir. MdM. Pérez-Fortez	TU Delft

TUDelft

Preface

This thesis represents my final fulfillment of the Msc Sustainable Energy Technology program. I have a bachelor's background in the field of chemical engineering, I decided to go on the sustainable path, because I aspire to be a part of this energy transition the world is going to phase. Emulating the ways of nature itself. This work was a combination between the sustainable side and the chemical engineering side which I desired. It will probably also be a type of field I would like to work in.

It proved to be quite a challenge though, which I now in the final stages look back upon with joy. The main reason for it going more difficult than I would have liked, started around the year 2018. I started severely abusing narcotic substances which lasted for years, was physically unrecognizable and mentally in a bad place. Sometimes I feel it has perhaps irreversibly damaged my ability to concentrate and the capacity of my memory and cognitive capacities. But actively working and focusing is giving me hope that the damage is limited. In these 5 years I have made tremendous progress, completely avoiding drugs and just sometimes drink excessively. I like being proud of myself again. A testament is this work as well. I still have a long journey to go and enough potential to grow, but I'm on the right track for sure.

I want to thank God and my lord and savior Jesus Christ for the strength He gave me to finish this work and help me during my bad times. Secondly, I want to thank professor Wiebren de Jong, for having the patience to work with me and guiding me through the project. The same gratitude goes out to doctor Wenze Guo, who helped me set-up the model and give me the fundaments to write this thesis. Lastly professor Ramdin has also provided me with insightful ideas and helped me finishing the work.

My family and beautiful girlfriend also deserve a special thanks. I was not easy to deal with in day-to-day life on (too) many occasions. But they had the patience and belief in me and I can see the pride in their eyes. Almost 8 years at the TU Delft are coming to an end, I am very ready for the next phase in my life and look back on 8 years that I will probably remember for the rest of my life.

Andrej Milisav
Rotterdam, a day before my 26th birthday.

Abstract

The transport sector remains one of the largest CO_2 emitting sectors globally. Decarbonizing the transport sector is an important aspect in the energy transition. The word transition is key, since it will take several decades or more to transition to a fully sustainable world. During this transition mainly heavy-duty vehicles and probably most vehicles in third world countries will rely on liquid transportation fuels. Affordable and competitive biofuels are the way to fill this need in a sustainable way.

This study will focus on integrating several sustainable units and feedstocks to produce gasoline and diesel, starting with a pyrolysis oil feedstock. The integrated units consist of a gasifier, whose gasifying agent, oxygen, is produced by a SOEC electrolyser, running on renewable electricity. The syngas produced in the gasifier is produced during a low temperature Fischer Tropsch process over a cobalt catalyst. The aim is to choose operating conditions resulting in a large chain growth probability factor to produce heavier hydrocarbons chains, which can be refined to mainly yield diesel. The hydrogen required to upgrade the syngas formed in the gasifier is supplied by the SOEC electrolyser as well. The final upgrading of the produced crude oil is performed by separating the fractions in distillation columns and using a hydrocracker to raise the yield of the desired products. The end products are diesel and gasoline, meant to be blended in with gasoline and diesel from conventional oil refineries. The gasoline and diesel are sulfur free and especially the diesel is of high quality, due to tuning the process to predominantly produce paraffinic hydrocarbons.

The assessment of the process will be a techno-economic analysis based on a model made with Aspen plus. 5000 $kg \cdot hr^{-1}$ of bio-oil produced by BTG was converted to 990 $kg \cdot hr^{-1}$ of high-quality diesel and 557 $kg \cdot hr^{-1}$ of gasoline. The overall carbon conversion of the process to the end products was 57.6 %. By designing a heat exchanger network, optimizing the energy produced and needed by the heat sources and sinks respectively, an overall energy efficiency on LHV base of 57.2 % was reached. The process in the current day and age was found to not be profitable yet, but will definitely be in the future.

Contents

List of figures

List of tables

Nomenclature

Abbreviation

ASR area specific resistance
AWE alkaline water electrolysis

Chapter 1

Introduction

The introduction will consist of 4 parts. In part 1.1 the problem will be explained. Section 1.2 will show the framework in which the problem is tackled. Section 1.3 will introduce the reader to the research questions designed to help solve the problem as structured as possible. Lastly in section 1.4 the reader will have an overview of what to expect in the upcoming chapters of this thesis.

1.1 The problem

Climate change is by now one of the most popular words used in politics. Different opinions upon top ranking politicians and society in general exist, but the consensus is that mankind has been responsible for changing the climate, in a negative way. Starting from the industrial revolution mankind discovered the potential of switching from making products on a small scale by hand, to, at that time, unprecedented production capacity by using machines and new fossil-based energy carriers. This resulted in a rapid development of almost all aspects of life and the quality of life for many people. Populations started growing exponentially. One of the main working horses used to sustain this rapid development and growth was the use of this fossil-based energy. Sunlight is the only energy source Earth has received over the ages. Organisms, predominantly plants or biomass, use sunlight to fixate its energy into matter, all organisms are mainly made up of three elements, oxygen, carbon and hydrogen. The lifetime of each organism and biomass type that ever existed is incomparable to the lifetime of Earth itself. When the organisms perished and the once living fixed solar energy was returned to Earth as matter, high quantities of stored tangible energy were stored. Eons of high pressure and temperature changed the composition of the three main constituents to only two, carbon and hydrogen. When exposed to their third companion, under certain conditions, tremendous amounts of once stored energy can be released. The downside is that one of the products resulting from this combustion of fossil-based products is carbon dioxide, CO_2. One of the most important greenhouse gases in the atmosphere. Figure 1 shows the increase of CO_2 in the atmosphere when over the last centuries.

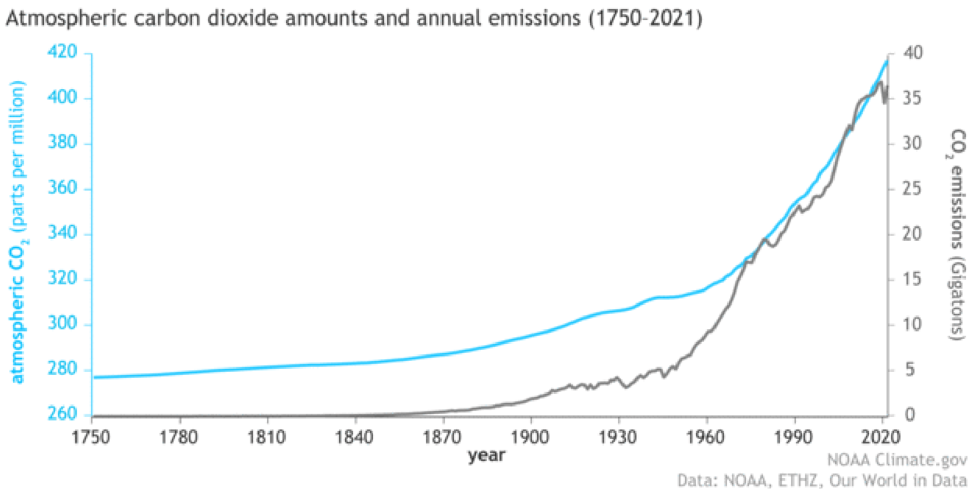

Figure 1: atmospheric CO2 amounts and annual emissions from 1750 -2021.[4]

A strong correlation can be seen with the atmospheric CO_2 levels and the CO_2 emitted by mankind into the atmosphere. The negative sides of these rising CO_2 levels are also well documented. For example the briefly mentioned term climate change. This causes loss in habitat for many different organisms, extreme and dangerous weather phenomena and inherently a loss in quality of life for many people and wildlife around the world. With an ever-increasing global population, measures have to be taken sooner than later. The problem is very clear, global greenhouse gas emissions, in particular CO_2, must be brought down. This can be achieved by de-fossilizing the economic sectors responsible for the emissions.

Measures and agreements have already been made globally, for example the net zero scenario 2030, in which the United Nations agreed to decrease the CO_2 emissions by 50%. [5]

As was said before, sunlight is the only primary energy source that is received by the Earth. Many new technologies have been developed to use the energy from the sunlight directly or indirectly, to transform it into useable forms for everyday life. The umbrella term for these techniques are renewable energy sources. Different renewable energy sources can be combined with each other. For example, biomass, which is the best at converting sunlight into tangible energy, can take over the role of carbon source from fossil fuels and the energy needed for processing it can come from PV modules or wind turbines. Biomass in its strictest definition is the total quantity of organisms in a specified area or volume.[6] As explained before these organisms are made up of carbon, which has been fixed into their structure and can thus be used as a carbon source. Biomass has been used for different purposes over the millennia. To this day, globally, it is still mostly used for cooking, heating and building. The more modern applications of biomass are mainly the production of biofuels. Three main classes or generations of biofuels exist[7]:

1. First generation biofuels come from biomass that is directly useable as food source. Usually first generation biomass is strictly used for consumption, since agricultural area is finite. But areas of land can be dedicated to cultivating fast growing biomass that can be processed further, if it does not compete too much with the consumption demand.
2. Second generation biofuels come from a wide array of different feedstock. However this non-edible biomass is usually considered as waste or in other words is not directly useable. For example agricultural residues and municipal solid waste or forest residues.

3. Third generation biofuels are related to using algal biomass. Since algae are cultivated in water, no competition for food production occurs. It also shows potential in the biotechnology sector. However, the technology and mainly yield are not mature yet.

When one thinks about fuels the first thing that comes to mind is the transport sector. One of the main sectors that is responsible for these CO_2 emissions, is the transport sector. It has a roughly equal share as the industry sector. The main polluting sector still remains the power industry, for the production for heat and electricity. Figure 2 shows that around 22% of the global greenhouse gas emissions come from the transport sector. The figure also shows how the different subsectors of the transport industry contribute to these emissions. It can be seen that decarbonizing the transportation sector would be an important factor, since it has enough room for improvement. Most of the vehicles and planes used in the transport sector transport goods and people and are run on fossil-based fuel.

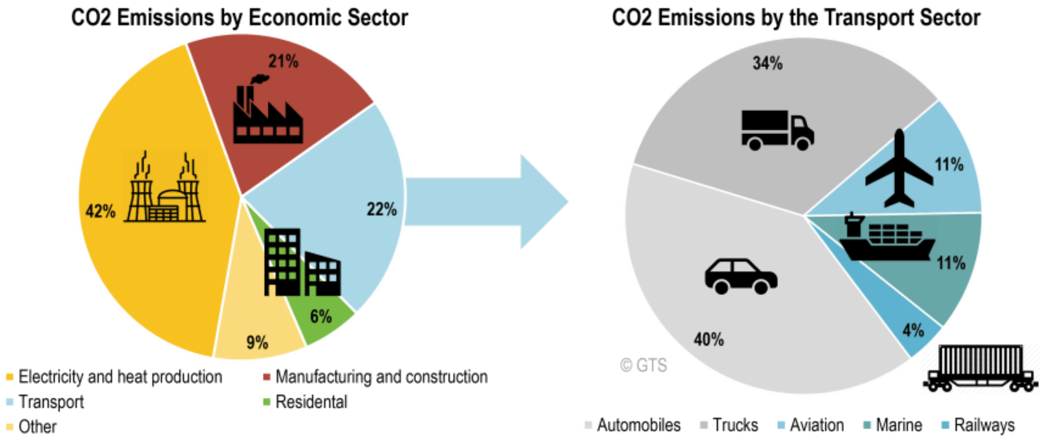

Figure 2: Global greenhouse gas emissions by the transportation sector.[8]

The transport sector almost solely relies on liquid fuels to power the engines used to propel the vehicle. This has been the case shortly after the invention of these vehicles, the engines are built that way. Up until a decade ago only fossil fueled cars existed. Electric vehicles are making a fast rise on the market but are globally still just a small fraction of the way in which vehicles are powered.[9] The infrastructure around the transport sector is almost entirely set up around liquid fuels. This combined gives plenty of initiative to still produce liquid fuels but now from biomass as the feedstock. The fuels produced from biomass can be blended with the current fuels and used in a majority of the vehicles, also relying on the same infrastructure. In 2021 biofuels represented 3.6% of the global energy demand in the transportation sector. If the net zero 2030 scenario is achieved biofuels could contribute up to 15% of the total demand. [10]

Now that the problem is clear and a brief introduction of biomass derived fuels is provided, the next section will dive into the research framework and what will be researched in this thesis.

1.2 Research framework

Producing liquid transportation fuels is not a new idea. Much research has already been performed on the topic. There are also many different routes in which this can be achieved, many combinations of feedstock, intermediary products and conversion technologies are possible. The boundary conditions are limited to the area and resources available in which the biofuels will be produced. For example social and environmental impacts need to be considered. But the main limiting factor in all the processes is the price competitiveness with traditional production of biofuel. Most of the “stock” fossil fuels can directly be implemented in a process to produce liquid fuels, cleaning some of the contaminants is one of the only steps required.

Biomass is not so ready to use, it contains high levels of oxygen, it has to be adapted, physically dried to be useable as feedstock, needs to be harvested and transported and must grow to fixate the carbon.[11] All of these processes need energy, more than conventional production methods, which makes the price of the end product significantly higher. The main difference however is that the production from biomass is a sustainable if the energy for the process is retrieved from somewhere else than fossil fuels.

Reaching sustainability is not so straightforward when it comes to biomass. Biomass needs to grow, so to ensure a constant and sustainable supply of biomass the amount harvested has to be regrown, a specific and maximum consumption rate has to be upheld.
The energy required for the land management around the biomass should also not emit more carbon-dioxide than is captured by the biomass. Specific types of biomass and land management techniques ensure that these constraints are met. This would be considered 1st generation biofuel problems. The 2nd generation biomass is already considered as waste, so using it is always better than not, however the amount of waste is limited. The vast majority of the current feedstocks for biofuel production are of the 1st generation type and include mainly soybeans, corn and sugarcane. In the net zero 2030 scenario the contribution of 2nd generation biomass is increased to 50% however. Limiting the inevitable impact on land use, food and feed prices and other environmental factors of 1st generation biomass. Nevertheless, reaching a fully sustainable process is a very important advantage over the conventional production.

A second advantage of using biomass is that the capture of CO_2 is much easier during biofuel production pathways. Because some pathways do emit CO_2, ethanol fermentation and bio-Fischer Tropsch for example. The high concentration of CO_2 in these pathways keeps the costs low since no additional purification is required besides dehydration. The captured CO_2 is then compressed and can be transported to other industries. Most commercial applications of CO_2 today involve the direct use, for example food and beverage production, metal fabrication, cooling, fire suppression and stimulating plant growth in greenhouses.[12] But pathways transforming CO_2 in fuels and chemicals are being developed.

As mentioned in the previous section the problem of sustainable energy production is tackled on many fronts. By integrating renewable energy technologies with the biomass feedstock a sustainable process for the production of biofuels can be designed. In many of the pathways, on top of heat or electricity as energy requirements, hydrogen gas is needed. When electricity is overproduced by renewable energy sources, it can be used for hydrogen generation, via electrolysis. The compatibility of the biomass conversion with renewable energy sources in this way is another advantage.

It is clear from these advantages and the described potential, that research on the topic of converting biomass to liquid fuels is worthwhile. Research is needed to mitigate the previously described limitations and make the products price-competitive, which can be achieved by further improvements in the technologies. One of the companies that concerns itself with such research is the Biomass Technology Group (BTG), they have set up a national scale project to advancements in the field of Biomass to Liquid (BTL) technology.

It was said that many different routes and combinations exist for the process. Four of them have been selected by BTG, as high potential candidates. In figure 3 the different routes considered by BTG are shown:

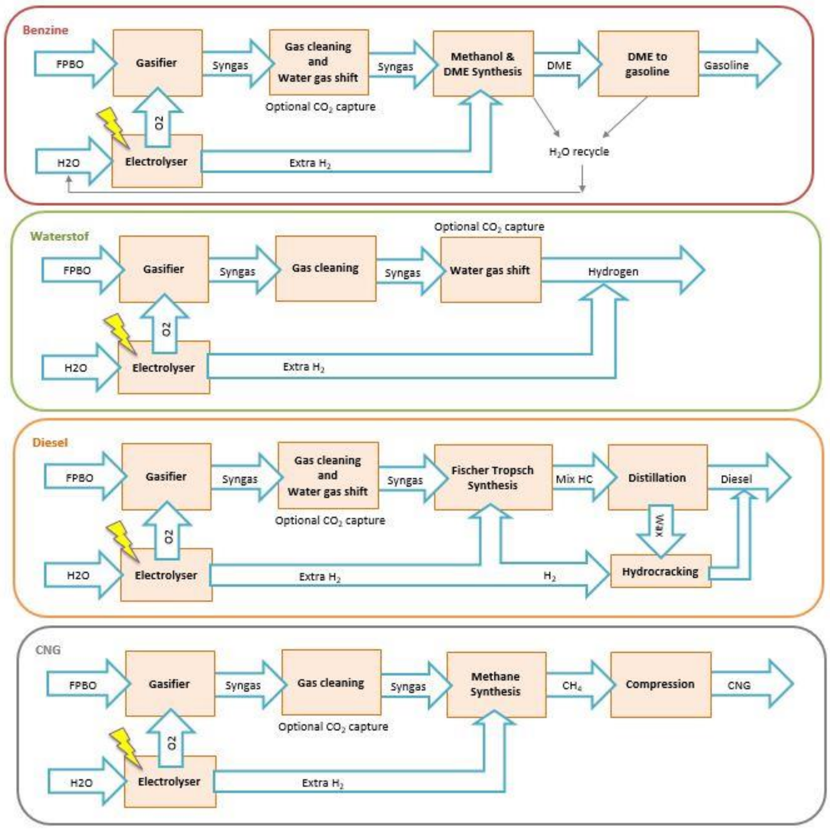

Figure 3: BtL routes considered by BTG.[1]

As can be seen in figure 3 all of the processes have the same two inputs, water and bio-oil. Secondly, they have the same two blocks that receive the inputs. The gasifier and the electrolyser. These two units are used to produce so called synthesis gas, which is a mixture of carbon mono oxide and hydrogen gas, CO and H_2, respectively. The syngas has very versatile applications, but here it will be cleaned and further processed to liquid fuels. This thesis will be a part of this national project, called “biomass4transport”, it is a collaboration between the BTG and the TU Delft. Peers have already investigated several of the routes as seen in figure

[1] the figure is taken from another thesis by Onsi Hanafi who referenced it as follows: “taken with permission from dr. E. Leijenhorst. Reference: proposal of the 'Biomass4transport' project, contract no TBBE119005. “

3. In this thesis the method of choice will be to the FT method to convert the syngas. The process is supplied with 5000 kg·hr^{-1} of fast pyrolysis bio-oil. The goal is to model this conversion pathway in Aspen Plus to perform a techno-economic analysis. One of the more important aspects will be to optimize the energy efficiency of the process. The next section will present the research questions developed to aid towards this goal.

1.3 Research questions

The previously discussed topics were as follows. Global warming is correlated to human global gas emissions, one of the main contributors is the transport sector. Biomass and renewable energy can be combined to form biofuels. The pathway chosen is the conversion of bio-oil to diesel and gasoline via the FT process.

The main research question:

How to integrate an as energy efficient possible system that incorporates electrolysis run on renewable electricity and bio-oil as feedstock for the production of diesel and gasoline via the Fischer Tropsch process?

Several sub questions will be used to distill the problem even further and to aid in the modelling of the process, section by section.

Sub question 1:

What gasifier design and specifications deliver the best quality of syngas, aiming for a high CO yield, for further upgrading while integrating the high-quality heat produced with the provided bio-oil?

The carbon in the bio-oil is the backbone of the fuels to be produced. Since it is the only carbon source that will enter the process a high CO yield will produce the highest quantity of liquid fuels. Hydrogen is the second most important molecule but will be supplied later on. CO_2 -production is to be minimized since it is a greenhouse gas and does not contribute towards the production of the fuels. The quality of the dry syngas will be assessed by the concentrations of these three molecules.

Sub question 2:

Which type of electrolyser is most suited for efficient energy integration in this process?

The electrolyser is run on renewable energy. It converts water into hydrogen and oxygen gas. The hydrogen gas will be used to upgrade the produced syngas and the oxygen in the gasifier. The FT process is known for its heat production, some types of electrolysers can benefit from this.

Sub question 3:

How to optimize and integrate the Fischer Tropsch process towards the production of gasoline and diesel constituents and use its exothermic reactions in the system?

The FT process is a well-developed technology. Its reactions release large quantities of heat which can be used to increase the overall efficiency of the process.

Sub question 4:

How will the FT reactor's products be extracted and converted to the desired products, while maximizing their yield?

The FT reactor will produce a mixture of hydrocarbon molecules, not all of them are suited to be used as diesel or gasoline. Techniques from the oil-refining industry are a good starting point.

Sub question 5:

Is the process technologically and economically feasible?

Just like any other company, BTG wants to maximize profit while ensuring a sustainable process. The economics behind the process need to be clear. The simulation will display whether or not the process is technologically feasible and if it is financially feasible.

1.4 Thesis overview and methodology

To get a thorough understanding of all the concepts and important parameters of the different sections of the process an extensive literature research was performed. The literature reviews can be found in chapter 2. Building further on the knowledge gained a basis of design will be presented in chapter 3. The basis of design is a first review stage to test the feasibility of the process, looking at different pathways that can be chosen to get from feed to product. Suitable locations, adequate logistic possibilities, product specifications, reactors, machinery and preliminary thermodynamic and kinetic calculations are considered. Chapter 4 will introduce the process system model. How is it set-up, why is a certain type of reactor chosen, what needs to be considered for the modelling and how are the units connected. For each of the different units an explanation will be given. Chapter 5 will present the results obtained in the plant, together with some sensitivity analysis. Chapter 6 will be about the heat integration of the process and how to raise the energy efficiency as high as possible. Chapter 7 will perform a financial analysis on the model. The last part, chapter 8, will answer the proposed research questions, draw conclusions and lastly provide suggestions for further research on this important topic.

Chapter 2

Literature review

The literature review is a collection of relevant and timely research on the relevant topics. The working principles, knowledge and findings on topics within the scope of the research are bundled and explained to the reader. This serves as a basis to build upon for the other chapters. Familiarity with the current knowledge is the field is obtained, as well as an understanding of boundaries and limitations in the field. It also shows which pathways have been tried but were not fruitful, so that one does not waste time exploring these. By having a broad understanding of the topics and what research has already been done, helps to find an own unique to the topic.

The literature review exists of 5 sections. Section 2.1 will discuss the principles of gasification and different types of gasifiers. Section 2.2 gives a summary on the methods to clean produced gas from contaminants and will cover the operating of a pressure swing adsorber for the cleaning of CO_2 and H_2S. Section 2.3 presents the principles behind electrolysis and presents different types of electrolysers with their limitations and advantages. Section 2.4 talks about the different pathways of going from syngas to gasoline and diesel, going in depth on the Fischer Tropsch process and the refining steps of the FTS product. Lastly section 2.5 will present the working principles of a reaction turbine and generator.

2.1 Gasification[13]

Bio-oil is the main feedstock of the entire process, that is why the first part of this literature review will target the conversion of the bio-oil to raw syngas. Before discussing this, a quick overview of the conversion from biomass to bio-oil will be given in section 2.1.1. The actual conversion of bio-oil to syngas will be done via gasification. A brief introduction to the working principles of gasifiers, the reaction taking place and their kinetics will be given in section 2.1.2. After this, different types of gasifiers will be discussed, highlighting their advantages and disadvantages, in section 2.1.3.

2.1.1 Pyrolysis of biomass

Biomass is converted to bio-oil via the pyrolysis process. The pyrolysis process takes place in an oxygen free environment. It is the thermal decomposition of the biomass, meaning that it is an endothermic process. Since it is performed in an oxygen free environment no combustion takes place and with enough heat the though biopolymers can be converted. The products of this conversion are solid char, liquid bio-oil and permanent light gases, like H_2, CO, CO_2, CH_4 and different C_2-based molecules. Depending on the temperature gradient increase and the residence time of the biomass inside the pyrolysis reactor the ratios between the solid, liquid and gaseous products can be manipulated. At temperatures above 200° C devolatilization starts, firstly producing the permanent small gas molecules. By ramping up the temperature and breaking down the biopolymers, lignin, hemicellulose and cellulose all kind of different molecules are produced which are classified as tars. When these molecules are condensed, they form bio-oil. This is the starting feed of this thesis. Bio-oil is produced by fast pyrolysis, which operates in the temperature range of 450-550 °C. In these conditions, depending on the biomass composition, around 60-70 wt% of the products is bio-oil. 10-15 wt% will be gas and 15-25 wt% char.

Bio-oil consists of a large amount of different carbon-based molecules. The main advantage of going through the trouble of making bio-oil is the substantial increase in volumetric energy density up to a factor 3-10.[14, 15] Bio-oil also contains a lot of water, between 5-35 %wt. This gives it its liquid form, even though it is highly viscous. The decrease in volume makes it easier to handle and more cost efficient to transport. The oil can be co-fired in fossil based powerplants to produce heat and power. But it can also be supplied as feedstock to a gasifier to be further upgraded.

The production of the bio-oil used in this thesis is performed by BTG, it takes place on a small scale and it is decentralized from the actual plant.

2.1.2 Gasification process

Gasification itself is a thermochemical reaction process, that can convert solid or liquid fuel into a combustible product gas. This is done under high temperature conditions in the presence of a gaseous agent. In most cases the gaseous agent is oxidizing the supplied fuel. Examples of several oxidizing agents are air, pure oxygen, steam and CO_2. When using these oxidizing agents in combination with a carbon-rich fuel the resulting product is referred to as biosyngas. It is observed that the gasifying agent used affects the heating value of the product gas. Using air, a low heating value of around 4-7 MJ/Nm3 is observed. While for oxygen it is close to 10-18 MJ/Nm3.[16, 17] Gasification is performed at high temperatures; the range is typically around 700-1500 °C. These high temperatures are needed to minimize the number of heavier hydrocarbons in the product gas and the tar content. The pressure applied is varies between atmospheric pressure up to 7 MPa. During the gasification a large number of reactions occur, the main reactions are presented in table 1.

Table 1: Main gasification reactions.[18, 19]

Heterogeneous reactions	**Reaction heat, relative to $\Delta_r H^0_{298}$ (kJ·mol^{-1})**	**Reaction name**	**Reaction number**
$C(s) + O_2 \rightarrow CO_2$	- 394	Complete combustion	R1
$C(s) + \frac{1}{2}O_2 \rightarrow CO$	- 111	Partial combustion	R2
$C(s) + CO_2 \rightarrow CO$	+ 172	Boudouard	R3
$C(s) + H_2O \rightarrow CO + H_2$	+ 131	Water-gas	R4
$C(s) + 2H_2 \rightarrow CH_4$	- 75	Methanation	R5
Homogenous reactions			
$CO + \frac{1}{2}O_2 \rightarrow CO_2$	- 283	CO partial combustion	R6
$H_2 + \frac{1}{2}O_2 \rightarrow H_2O$	- 242	H_2 combustion	R7
$CO + H_2O \rightarrow CO_2 + H_2$	- 41	Water-Gas Shift (WGS)	R8
$CH_4 + H_2O \rightarrow CO + 3H_2$	+ 206	Reforming	R9
H_2S and NH_3 formation reactions			
$H_2 + S \rightarrow H_2S$		H_2S formation	R10
$3H_2 + N_2 \rightarrow 2NH_3$		NH_3 formation	R11

There are two main working principles. Firstly, the production of producer gas, H_2O and CO_2 by partial oxidation. Secondly, reducing the producer gas to mainly CO and H_2, using the fuel molecules. The heat needed for the endothermic reactions, R3, R4 and R9 can be produced in the reactor itself by the other reactions of table 1. Or it can be supplied via an external unit, direct and indirect gasification is what this is called respectively.

The gases produced by the gasification process can be used in different processes and for different applications. The three main applications are to use the products for heat generation, for power production and lastly to produce different chemicals or biofuels. The latter will be done in this study.
To obtain a good quality of raw syngas the ratio between the fuel and gasifying agent is of importance. One parameter that is used to characterize this, is the stoichiometric oxygen ratio, with symbol λ. It is defined as:

$$\lambda = \frac{external\ O_2\ supply\ /fuel\ supply}{stoichiometric\ O_2\ requirement/\ unit\ of\ fuel\ input} \qquad \text{(Eq. 2.1)}$$

The numerator is the amount of external oxygen supplied to the process. The denominator is the stoichiometric amount of oxygen required for complete combustion of the fuel molecules. Three different regimes, commonly referred to as oxidation regimes, can be distinguished. If $\lambda > 1$ the regime is a combustion reaction. If $\lambda = 0$, the regime is that of a pyrolysis reaction and lastly if $0 < \lambda < 1$, a gasification reaction process occurs. Two opposing factors are of importance during a gasification reaction and finding the optimal oxygen equivalence ratio. First of all, the goal of a gasification is often to produce syngas. The reaction that lead to this product are endothermic reaction. Heat is needed to keep them going. This heat can be supplied by combustion of the fuel, but requires a larger oxygen supply to initiate the combustion reactions. In other words the reaction heat needed can internally be supplied, but at the expense of carbon and hydrogen that instead of forming H2 and CO are now forming CO2 and H2O since they are combusted. This problem can be tackled by using an external heat supply. But this in its turn means higher external energy requirements. Typical λ-values are between 0.4 and 0.5.
As mentioned before, biomass upgraded to the form of bio-oil, will be the feedstock for the gasification reactor. The gasifying agent will be pure oxygen, coming from an electrolyser, more on this will be discussed in the next section. The gasification products will almost entirely exist from syngas. Bio syngas is a raw product and needs to be cleaned downstream in the process.

2.1.3 Types of gasifiers

In this subsection different types of gasifiers will be discussed. From extensive experience over the years in the application of gasification, three main categories of suitable reactors have been found. These categories are based on the transport processes that are present in the reactors. The three categories are:

1. Fixed beds/ moving beds
2. Fluidized beds
3. Entrained flow (EF) reactors

Before continuing about the three different types, it is important to note that even though all of these types can host a gasification reaction, the product outcome will be different. For each of these reactors compromises for a list of important factors have to be made. These factors are the conversion efficiency, product gas quality, suitability for handling different feedstock, scalability and complexity of design and operation and investment cost. But the main criteria in finding a suitable gasifier for a specific process are:

- scale of the energy conversion process
- feedstock flexibility (particle sizes and fuel composition
- sensitivity to the amount of ash and its composition
- tar generation characteristics

There is also work being performed on newer types of gasifiers, examples are a cyclone gasifier, vertical vortex gasifier and The Blue tower. In the field of process intensification, the focus lies more on what can be achieved or rather upgraded in terms of the unit operational, functional or phenomena levels. The latter can be achieved by introducing plasma in the gasifier. But these technologies mostly excel in combining two or more steps. For example, the cyclone gasifier focusses on combining gasification and product separation. The vortex gasifier combines pyrolysis and gasification. The plasma technology is yet to be investigated. Since it is set in the boundaries of this thesis that bio-oil is the feedstock and considering that tars and ash will be the main groups that need to be separated, the choice has been made to focus on the three previously mentioned types of well-known reactors/gasifiers. Starting with the fixed bed gasifier.
The supply of fuel and gasifying agent differs for fixed beds. One can have a countercurrent updraft, cross-draft or co-current downdraft. The fixed bed gasifiers are considered as the small-scale class of gasifiers. The downdraft fixed bed reactor has a capacity of producing roughly between 0.1 MW and 1 MW. The updraft fixed bed reactor of 1 MW up to 10 MW. The cross-draft gasifiers are almost solely used for the gasification of charcoal. Since the future goal of the work done in this thesis is for it to grow to an industrial scale of biofuel production that can rival the traditional refineries, more production capacity is needed. This is why the other two categories of gasifiers, the fluidized beds and the Entrained Flow reactors, will be discussed more thoroughly.

Entrained flow gasifiers:

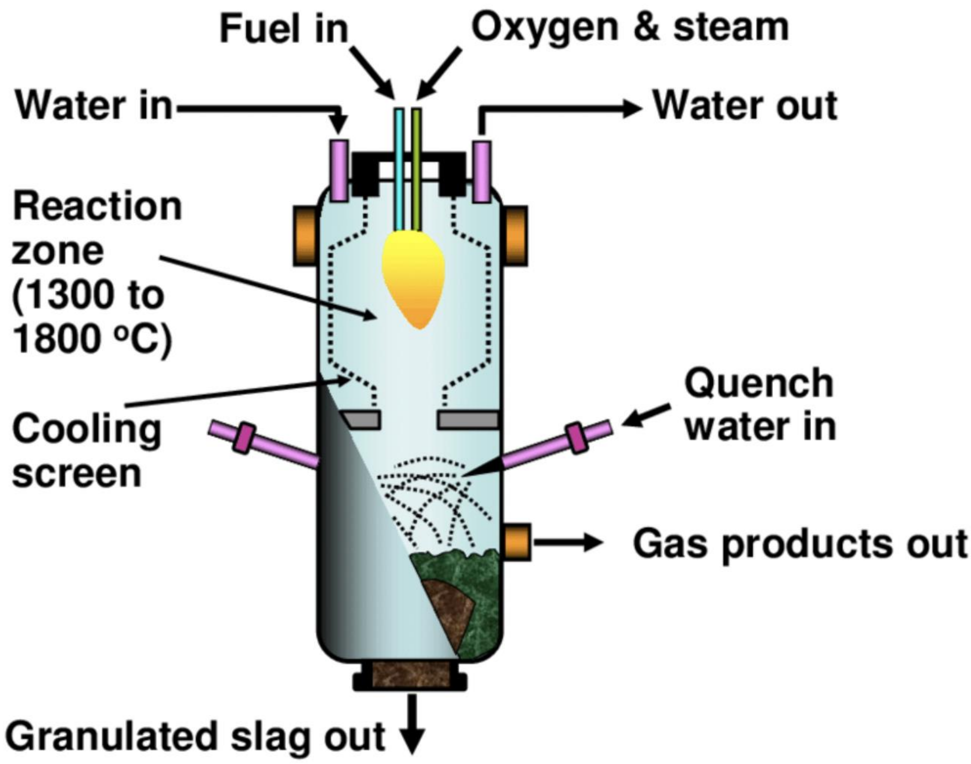

Figure 4: Schematic Entrained Flow gasifier[20]

Entrained flow gasifiers were originally designed for coal gasification and still operate with mainly varying types of coal. EF's operate at relatively high temperatures ranging from circa 1200 to 1500 °C. The pressure applied varies between 20-80 bar. The feed and oxidant enter the reactor in co-current flow. The fuel is typically supplied as a fine powder or slurry. In the case of biomass gasification using a EF the biomass also has to be ground to a powder. In the case of the gasification of bio-oil, it still has to be fed in slurry or powder form. This allows for high mass transfer to and inside the particles. These three factors combined, high temperature, high pressure and fine particles, are needed to keep the residence time low while having a high carbon conversion. Residence times are often in the order of a few seconds, while achieving a conversion of >98%. The short residence time shows why entrained flow gasifiers can be used for large-scale operation, well over 100 MW_{th}. To maintain the high temperature a large oxygen supply is needed, the stoichiometric oxygen ratio is usually higher than for other types of gasifier. Because of the very high operating temperatures the amount of tars formed that end up in the syngas is virtually zero. The ash present in the biomass is melted to so called slag because of the high temperatures. This slag deposits on the surface of the materials of the reactor and deteriorates the equipment and lowers the efficiency. So the downside of these conditions is that the capital and operating costs of an EF are significantly higher than that of other types of gasifiers. These cost stem from the previously discussed points, summarized these are. The required pre-treatment of the biomass, large oxygen requirement, large pressure and temperature requirements and slag formation.

Fluidized bed gasifiers:

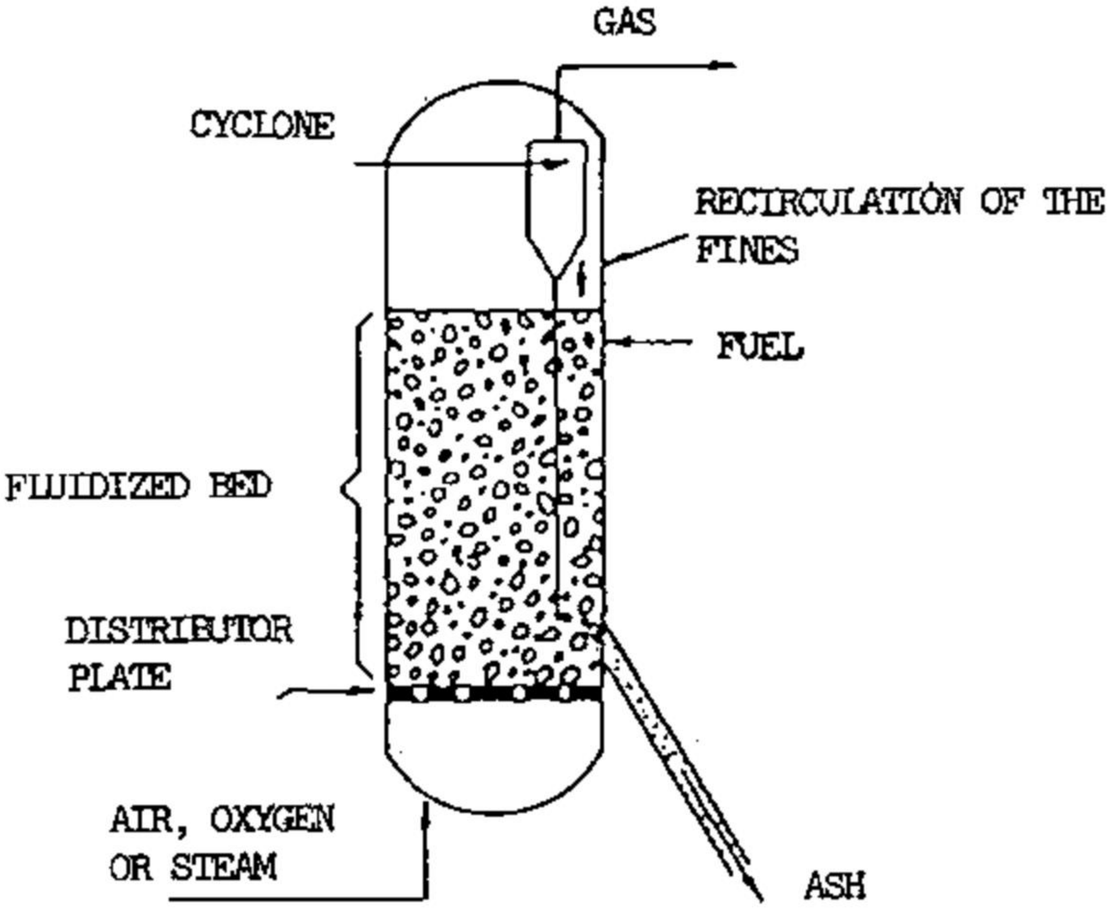

Figure 5: Schematic fluidized bed gasifier.[21]

Like the entrained flow gasifier, the fluidized bed gasifier was initially made to use coal as fuel. The 1970 oil crisis forced experimenting with biomass as a feedstock, successfully. Fluidized bed reactors have a capacity starting at around 10 MW_{th} up to 100 MW_{th}. The two main types of fluidized bed gasifiers are the BFB and CFB, bubbling fluidized bed and circulating fluidized bed respectively. The working principle of a fluidized bed reactor is as follows. A bed of small solid particles is present inside the reactor, usually the material is an inert or has catalytic properties. The most used inert is silica sand, the particles are very small and loose and the low specific heat capacity allows for it to heat up and cool down quickly. This bed facilitates heat and mass transfer inside the reactor. The next step is introducing the gasifying agent and fuel inside the reactor. The gasifying agent is blown with a high enough velocity to make the bed and particles float. The resulting mixture now acts as if in a fluidized state.

The temperatures are kept within a range of 700-900 °C. The pressures are between 0 and 7.0 MPa. Fluidized bed reactors operate in back-mixed mode, meaning that “fresh” feed is thoroughly mixed with feed molecules already undergoing gasification. This and the high turbulence in the bed means that the heat is very well distributed in the reactor, allowing for a very constant temperature throughout the reactor. For good operation it is necessary that the bed keeps floating. Two principles counteract this, agglomeration and sintering. Both principles can be seen as the small particles sticking together to form unwanted larger particles, which limit mass and heat transfer and can even become too large to stay afloat. Most commonly this is caused by the eutectics formed by the silica sand and the alkaline molecules in the ash. The relatively low temperature is usually below the ash melting temperature. This is the temperature where the ash slowly transforms into a sticky liquid, which wants be minimized since this would increase agglomeration. The lower temperature does mean that more tar will be formed than for the EF gasifier, but still significantly lower than in fixed bed reactors. The tar molecules can negatively affect the downstream equipment since it operates a lower temperatures, here the tars will condense and create slag.
The BFB reactor operates at an gasifying agent velocity above the minimum floating velocity, but most of the solid material remains inside the reactor, so it does not leave with the product gas. BFB are in the medium scale range <25 MW_{Th} .The high residence times inside the reactor allow for efficiencies >90%.
In a CFB the velocity is so high that solid particles leave the reactor together with the product gas. These solids are separated externally and after that recycled back inside the reactor. A CFB reaches efficiencies up to >95%.
The choice has been made to use a fluidized bed reactor in the design.

2.2 Gas cleaning[13]:

In this section the cleaning of the raw syngas will be described. The raw syngas leaving the gasifier has many impurities, that could be detrimental for the downstream units in the process. The composition of the fuel and the reaction conditions inside the gasifier determine the concentrations and presence of the contaminants in the product gas. The downstream equipment mainly dictates the maximum allowed concentration of these contaminants. Since the next downstream unit is a Fischer-Tropsch reactor and the hot gas will be part of a heat exchanger system, cleaning the gas is very important. Six main classes of contaminants that typically need to be removed after gasification are:

- Particulate matter
- Tars, particularly polyaromatic hydrocarbons
- Sulfur species
- Chlorine species
- Alkali and other trace elements
- Nitrogen compounds

Every single class will be briefly discussed in general, what the molecules are, why they have to be cleaned and how this is done. After which its relevance and need for cleaning for the system of this thesis will be discussed.

2.2.1 fundamentals for different contaminants

Particulate matter

Particulate matter is an umbrella term for all kinds of solid or liquid particles. These can be ash, attrited bed material, carbonaceous solids and even fine liquid droplets. These particles are typically in the 0.1-100 µm. The majority of these particles will be alkaline earth metal compounds, silica, alkali species and iron compounds. The lesser amount of inorganic particulate matter consists of Zn, Pb and Cu- particles. Many different methods for the clearance of particulate matter exist. These methods operate in three different temperature ranges. LT, low temperature, which is around the ambient temperature. IT intermediate temperature, which is up to 350° C. Lastly HT, high temperature, operating above the 350 °C. The minimum particle sizes that can be captured differ per cleaning technique. The settling chamber and impingment separator operate in the HT spectrum and filter relatively large particles 10-50 µm, the level of gas cleanup is low. Cyclones, multicyclones and a scrubber filter smaller particles and achieve a moderate level of gas cleanup. The rotating particle separator, electrostatic filter, Baghouse filter, Ceramic filter and Metal filters are able to capture the smallest particles of the spectrum, they achieve a high level of gas cleanup. The conditions, energy requirement and cost in most cases increase with a higher level of gas cleanup. But this also depends on the integration of the unit in the whole process.

Since the Fischer Tropsch reactor is the next unit, the tolerance for particulate matter is virtually zero. All of it has to be removed. Since it can lead to catalyst deactivation by fouling and erosion of the equipment. To achieve high level of gas cleanup and leave enough heat in the raw syngas stream for heat transfer, a scrubber is chosen to perform the cleaning at low temperature conditions.

Tar

Tar is one of the more challenging classes of contaminants that need to be removed. A definition for tar that is currently mostly accepted is that it is a name for all organic compounds present in the product gas, excluding molecules with carbon numbers 1 through 6. Problems associated with tars are that they are present in the gas-phase under the gasifying conditions, but they start to condense when the temperatures drop, as in most if not all the downstream equipment and piping. This causes clogging of pipes, fouling of heat exchanger surfaces and also the formation of soot, which negatively impacts the emissions of particulate matter and CO.

The first factor that will limit the amount of tar in the raw syngas stream are the gasifier conditions. Above temperatures of 1200 °C, most of these organic molecules thermally decompose into CO and H2 or other permanent gasses, meaning that the overall tar content leaving the gasifier will be lower. Since these conditions are only applied in EF gasifiers, cleaning techniques will be needed for other types of gasifiers.

Two stages in which the tar can be removed can be distinguished. The primary tar reduction stage, where the tar is removed inside the gasifier and the secondary tar reduction stage, where the tar is removed in downstream equipment.

Primary tar removal:

As mentioned, primary tar removal takes place inside the gasifier. The process conditions, temperature, gasifying medium, stochiometric oxygen ratio and residence time can be optimized for tar reduction. A higher stoichiometric oxygen ratio promotes a lower tar production. But at the same time the gas quality will be lower since more CO_2 is produced, instead of CO. Optimal ƛ values for tar reduction vary between 0.25-0.30. In the case of the gasifying medium used, it can differ the tar compositions. Even the gasifier design can change the tar production, adding a second oxidizer for example. Lastly many cheap catalysts have been tested to reduce the tar content in the product gas. Examples are different types of dolomites, magnesites, limestones, olivines and Ni-based catalysts. The catalysts have shown to reduce the tar contents, but in had a negative effect on the attrition behavior. The latter means that higher capacity requirements are needed to remove these particles. Preferably one would like to remove as much tar in the primary tar removal stage as possible. If still some tar is left the secondary tar removal methods have to be applied.

Secondary tar removal:

Secondary tar removals are units placed immediately after the gasifier. It is mostly needed for fixed bed gasifiers, but sometimes also for fluidized bed reactors. An example is a secondary

CFB reactor filled with dolomite. Even biomass-based char can be used. Newer techniques are Ni-based catalyst on a monolith structure. But the results at not yet adequate. Another problem is that alkali eutectics form sticky ash. Lastly particle cleaning can be combined with the tar conversion.

Considering that an EF gasifier will be used, most of the tar is removed primarily. The high operating temperature limits the amount of tar formed.

Sulfur Species

As for most chemical processes the tolerance for Sulfur is extremely low. For the Fischer Tropsch process a <10 ppb is needed. Sulfur poisons catalysts downstream and can corrode different materials, also the emission of Sulfuric compounds needs to be kept as low as possible. Sulfur mostly comes in the form of H_2S and in lesser amounts as COS and CS_2. Luckily most biomass types already contain (very) low amounts of Sulphur. But the amount of Sulfur in sewage sludge or municipal waste can be higher. Sulfur can again be removed in two stages. In the reactor or downstream, primary and secondary sulfur reduction methods respectively.

Primary Sulfur capture methods are catalyst based. The same materials as could be seen for the reduction of tars can serve as catalyst. These are the natural rock minerals, limestone and dolomite.

Just like for the primary Sulfur caption methods, the method used for reducing the Sulfur content is based on the use of a catalyst. Since this is secondary Sulfur capture it is performed in a unit outside of the reactor. The catalysts are mostly metal oxides. By undergoing the following reaction, the Sulfur in the H_2S molecules gets trapped:

$$\alpha\, MO(s) + H_2S\ (g) \rightarrow H_2O\ (g) + \alpha\, MS(s) \qquad \text{(Eq. 2.2)}$$

The two most important factors for good Sulfur removal are the sorption capacity and the operating temperature for the different metal-oxides. Each of them has their advantages and limitations. A combination of active carbon and ZnO has been chosen. ZnO has the best thermodynamic properties for high temperature H_2S cleaning.

Chlorine compound removal

Chlorine compound are another class of contaminants that needs to be removed. Chlorine is the predominant halogen in biomass and waste materials. The amount of chlorine differs significantly for different types of biomass. Alkali-induced slagging can occur during biomass gasification. It is also very detrimental for Cu and Zn catalysts downstream. Again sorbents are used to remove the chlorine. Once again these are the rock materials such as dolomite and limestone.

Alkali and trace metal cleaning

A lot of biomass contains high levels of alkali salts. Potassium being the most present, but Sodium and other alkaline earth elements are present as well. At lower gasification temperatures, between 550-600 °C, KCl and NaCl are solids and contribute to capturing Cl^-. When the temperature exceeds 700 °C, the salts begin to evaporate, straight into the gas phase. As they are in the gas-phase at elevated temperatures, competition with HCl formation starts. Meaning that KCl and NaCl also contribute to the levels of HCl. Since it are eutectic salts they will immediately condense as solid particles when the temperature in the downstream equipment gets lower. Causing unwanted deposition in the gasifier, piping and poisoning of the fuel synthesis catalyst. The alkali particles can be captured by cooling down the stream and applying different dry or wet particle removal systems. A problem is that some of the tar particles will also condensate which could again cause clogging. Lastly ash stickiness is also caused by lower-melting alkali-species. Because of these drawbacks it is preferred to have an upstream gas cleaning section. This would also counteract the problem of agglomeration forming in fluidized bed gasifiers as was discussed earlier.

Nitrogen compounds

The last of the six unwanted contaminants are the nitrogen compounds. The prevalent molecule that gets produced during biomass gasification is ammonia, NH_3. Hydrogen cyanide, HCN, is also formed, but in relatively lower concentrations. For both molecules, when it comes to a Fischer Tropsch process the tolerance is <20 ppb. HCN poisons the catalyst, leading to deactivation. If NH_3 remains in the stream, especially if the gasification is combined with power and heat production, NO_x compounds are formed. The latter being highly pollutant. NH_3 can be removed with a wet scrubber, this does result in a liquid waste stream though. Catalysts that were discussed earlier in the tar removal section, are also able to convert NH_3 to N_2. Lastly monoliths can be used to remove NH_3.

2.2.2 Pressure swing adsorber (PSA)

Pressure swing adsorption is a method used for the separation of different gases. The working principle is that under high pressure gases can be "trapped" on solid surfaces, adsorption. the higher the pressure, the more off the gas will be adsorbed. The solid material used will have different adsorption affinity for different gases. One the gas has flown through the pressure swing adsorber and the gas specie that was desired to be removed is removed from the flow stream, the pressure is dropped again and the adsorbed gas will desorb.

The solid material in the PSA is chosen to effectively discriminate between the gases present and it has to have a high active surface area. Typical adsorbent materials are zeolites, activated carbon, silica gel, alumina or synthetic resins.

Three variables are important for the effectiveness of the separation of the gases. The residence time in the adsorber, the pressure and the temperature. Longer residence times tend to increase the adsorption. Lower temperatures tend to increase the adsorption and finally higher pressures tend to increase the adsorption as well. [22]

The adsorption conditions for two molecules will be discussed CO_2 and H_2S.

PSA system for H_2S and CO_2

Methyldiethanolamine or MDEA is an aqueous chemical solvent that can react with CO_2 and H_2S as well. MDEA is useful in a set-up as shown in figure 6.

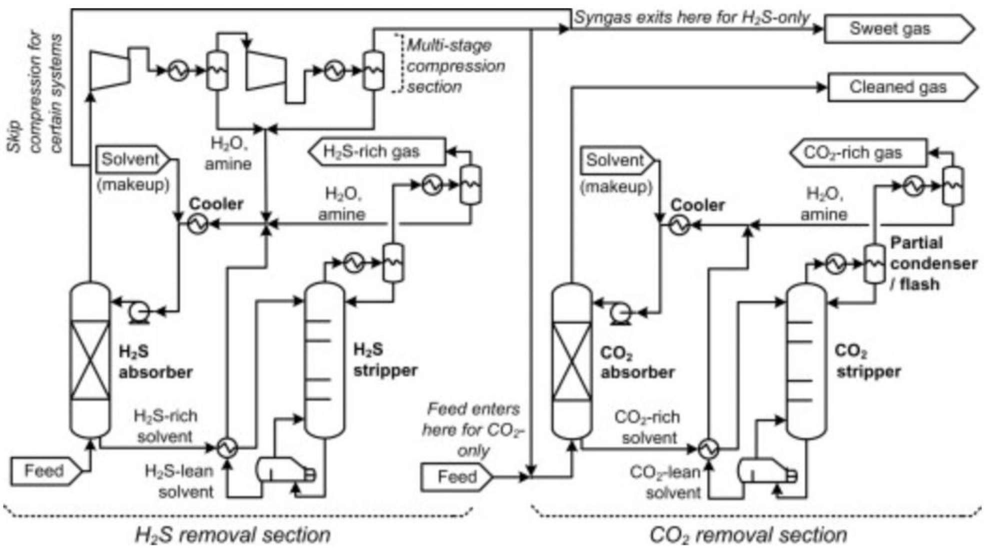

Figure 6: PSA system for H_2S and CO_2 removal.[23]

In the example as shown in figure 6, the adsorber section and the stripper section operate at a low pressure of 2 bar. The adsorption rate is higher at higher pressures, but at low pressures in the adsorber MDEA favors the adsorption of H_2S over CO_2, that was the goal here, to remove mainly H_2S. For the adsorption of CO_2 pressures exceeding 27 bar had to be used.

2.3 Electrolyser:

For the Fischer Tropsch to work optimally the ratio between H_2 and CO should be optimal, around 2.15 : 1. [24]The cleaned product gas coming from the gasifier however, has a ratio around 1:1. It is evident that more hydrogen gas needs to be added.

2.3.1 Hydrogen production

Hydrogen gas can be produced in several ways. Color codes are used to classify the method in which the hydrogen was produced. The three main and well-known classification groups are grey, blue and green hydrogen.

Grey hydrogen:

Grey hydrogen is hydrogen gas that has been produced from natural gas as feedstock. This is not the only fossil fuel-based hydrogen production method, although it does have the highest share. Syngas with a relatively high hydrogen ratio can be produced from natural gas, oil and coal. The respective shares are around 47%, 27% and 22% of the annual global hydrogen production.[25] Hydrogen produced from natural gas is done via steam methane reforming. From coal via the gasification process. It is to this date the cheapest method to produce hydrogen, around a factor 3 cheaper than renewable ways.

Blue hydrogen:

If the hydrogen is produced with fossil fuel as feedstock, but the CO_2 and other carbonaceous molecules are stored, opposed to emitted to the atmosphere. In practice around 10% of the carbon cannot be captured.

Green hydrogen:

Green hydrogen is produced trough electrolysis. The electricity needed comes from surpluses created by renewable energy sources. Only 1% of the global annual hydrogen production can be considered green. The main reason for this small share is the difference in price. This high price is determined by the four main factors [26]

- The CAPEX, capital expense
- The OPEX, operating expenses
- Lifetime or operating hours
- Efficiency of the electrolyser

The CAPEX is the one-time cost of the electrolyser, they come in all shapes and sizes. The two most important factors that need to be considered are the production rate of hydrogen during its lifetime and the electricity needed to produce a specific unit of hydrogen, the efficiency.

The actual operational hours of the electrolyser during its lifetime will show if the CAPEX costs made at the beginning for this type of electrolyser are the best choice.

The OPEX will consists of mainly the electricity, water and maintenance costs. Again the efficiency plays an important role, since the water and electricity used are less and effectively their cost. Even though renewable electricity prices are said to drop in the upcoming years, it will not be a cheap commodity. An efficient electrolyser, with a low drop in efficiency over its lifespan, will make significant savings in the OPEX. Some electrolysers can only operate on completely deionized water, also not a cheap commodity. A robust electrolyser that can use demineralized water for example opposed to deionized water lowers the OPEX over its lifespan as well. Lastly the maintenance costs, these vary significantly per electrolyser types. Most maintenance costs will be the changing the cell stack. The terms of Service-Level Agreement (SLA) or extended warranties are where these costs are captured and fixed. [26]

The start-up time, before the electrolyser can operate at full power, is also important, especially since the electricity supply from renewables is very intermittent. Lastly the downtime for maintenance to be able to be performed is important.

All these things considered make the price of green hydrogen high relative to grey and blue hydrogen. Lower CAPEX costs, scaling, lower electricity price and carbon taxes within the coming years should be able to level these costs in the future. This is largely what this thesis looks at.

Now that it is established how hydrogen can be produced and what dictates the cost differences and mainly limits a more competitive green hydrogen price it is time to look at what electrolysis is.

2.3.2 Electrolysis fundamentals

Electrolysis is the use of electrochemical energy to drive a non-spontaneous reaction. Electrolysis of water splits water into its two elemental constituents, hydrogen and oxygen. The only input required is electricity. The overall reaction for water looks as follows:

$$H_2O \rightarrow H_2 + \frac{1}{2}O_2 \qquad \text{(Eq. 2.3)}$$

Looking at the thermodynamics and combing the half reaction for the oxidation of water and reduction of hydrogen ions, these two half reactions are found:

$$2\,H_2O(l) \rightarrow O_2(g) + 4\,H^+(aq) + 4\,e^- \qquad E^0 = +1.23\,V \qquad \text{(Eq. 2.4)}$$

$$4H^+(aq) + 4e^- \rightarrow H_2\,(g) \qquad E^0 = 0.00\,V \qquad \text{(Eq. 2.5)}$$

Since the oxidation takes place at the anode and the reduction on the cathode, the thermodynamical cell potential of water electrolysis is found to be 1.23 V at 25°C and 1 atm.

However, in practice more electricity is needed. This so called overpotential comes from different resistances within the system. One can think of resistances of the cabling, resistance of the ions travelling through the electrolyte, but mainly about the ionic barrier around the electrode, which limits the mass transfer of the electrons. All the energy that encounters these resistances is lost as heat. If heat would be supplied to the system, these losses would become smaller. The previously mentioned loss factors would have higher mobility, the travelling ions and electrons and also through the ionic electrode barrier. This would result in an overall higher electric efficiency.

When comparing different types of electrolysers, the following parameters are important to compare:

- nominal current density
- operating temperature
- (stack) lifetime
- Cold start to nominal load
- Voltage efficiency

The current density is the amount of current flowing per unit cross-section area and is defined as:

$$j = \frac{I}{A} \qquad \text{(Eq. 2.6)}$$

With I being the current in Ampere and A the surface area in m^2.

A higher current means that more charge, more electrons are transferred through an area, which also implies that more water can be converted per available area. Since the active surface area of an eletrolyser is finite, this is an important parameter.

When it comes to the operating temperature the main link is with the reversible voltage U_{rev}, which is defined as:

$$U_{rev} = -\frac{\Delta G}{z \cdot F} \qquad \text{(Eq. 2.7)}$$

ΔG is the molar Gibbs free energy in $kJ \cdot mol^{-1}$
Z is the number of electrons that is being transferred in the reaction
F is the Faraday's constant, which equals 96485 $C \cdot mol^{-1}$

The thermodynamic relation $\Delta G = \Delta H - T \cdot \Delta S$ is well known. The enthalpy of the liquid water does not change drastically with increasing temperature. Except for when the temperature would reach 100 °C at 1 atm, the water would vaporize into the gas-phase. Since electrolysers need an electrolyte for the ions to be able to travel, water vapor is not sufficient. So pressure is needed to keep the water liquid. The positive part of increasing the temperature and keeping the water liquid is that ΔG will drop, also decreasing the reversible voltage level. In this way less electrical energy is required, since thermal energy can be used instead.

The stack lifetime is also a very important parameter for choosing an electrolyzer. An electrolyzer is not a cheap investment, one want to have it run as long as possible, close to its maximum capacity. However, the electrodes and membranes start to deteriorate under the applied conditions. The electrodes are often metals, metal-alloys or coated metals. The membranes need to be permeable for ions, but cannot allow the produced gasses to mix, usually it is a hydrophilic material that attracts polar molecules. The exact mechanisms for the deterioration are beyond the scope of this thesis. But one could think about less active electrode area due to crystallization of the electrodes or loss of matter. The same goes for the membrane which under the strong electric fields and in some electrolyzers acidic conditions deteriorates, this can be observed by the increase of the values of the previously mentioned resistances. It is also observed that the reduction of the stack lifetime, which can also be labeled as loss of performance essentially, differs with varying conditions. Rapid load changes, operating close to open cell voltage and start stop cycles, which are all inherent with intermittent energy, deteriorate the electrolyzer performance quicker. Observing the lifetime of an electrolyzer working at steady-state full capacity for example is not enough.

Unfortunately for electrolyzers it is not the case that they immediately when a current is supplied start to work at full capacity. The time it takes from cold start to operate at nominal load differs per type of electrolyzer. The precise reason of the mechanisms that cause this is also beyond the scope of this thesis. But one can imagine that before the right pressure and temperature are reached, the layers on the electrodes are set, the ions reach full mobility and the whole system is in steady state, time will pass.

The voltage efficiency is also a concept that has already been touched upon. It is the division between the reversible voltage and the reversible voltage plus the overpotential. The factors and concepts of what determines this have also been discussed. The voltage efficiency can be found if the overpotentials are known. Or alternatively, in a more precise way, by using:

$$\eta = \frac{\dot{m}H_2 * LHV\ H_2}{E_{electric}} \qquad \text{(Eq. 2.8)}$$

Where $\dot{m}H_2$ is the mass flow of hydrogen, in $kg \cdot s^{-1}$
Where LHV H_2 is the lower heating value of hydrogen, in $J \cdot kg^{-1}$
Where $E_{electric}$ is the electric energy supplied, in Watt

Some electrolyzers demand very noble or scarce elements to be used in the electrodes, this will increase the overall price dramatically.

Now that the criteria that an electrolyzer can be judged on have been discussed, it is time to review the potential candidates. Three main different types of electrolyzers exist.

1. Alkaline electrolyzer
2. PEM electrolyzer
3. SOEC electrolyzer

2.3.3 Electrolyser types

Alkaline water electrolysis (AWE)

The most mature technology of the three. The charge carrying ions, OH^- travel through an alkaline electrolyte, consisting of an aqueous solution of KOH and NaOH. The following half reactions take place:

$$Anode: \quad 2\,OH^-(aq) \rightarrow \; H_2O\,(l) + \frac{1}{2}\,O_2(g) + 2\,e^- \qquad \text{(Eq. 2.9)}$$

$$Cathode: \quad 2\,H_2O\,(l) + 2e^- \;\rightarrow OH^-(aq) + H_2(g) \qquad \text{(Eq. 2.10)}$$

The current density for an AWE is low and is limited to 0.2-0.4 $A{\cdot}cm^{-2}$. This is because of the high, previously described internal resistances. In the case of an AWE there is a minimum gap limit for the cell to be able to operate, the gap is the distance between the two electrodes. If the electrodes were to be put closer together, the electrolyzer would not function properly. The resistance coming from the distance of the gap is inherent.

The operating temperature is typically between 60-80 °C, often closer to 80 °C. This temperature has little potential to lower U_{rev}.

The electrodes have to be made of corrosive-resistant material, since the electrolyte is highly alkaline. The anode, at which the oxygen is produced, can be made out of pure nickel, or a nickel coating on a steel core, or lastly a nickel-iron alloy, coated on steel or nickel core. As can be seen nickel and steel are the foundational materials. Stainless steel has a lower overpotential for the production of oxygen than nickel, 0.28 V opposed to 0.61 V respectively. On the other hand, nickel has a significantly better electrical conductivity than stainless steel, 14.3 $MS{\cdot}m^{-1}$ opposed to 1.45 $MS{\cdot}m^{-1}$ respectively.[27] So determining the ratio between these two material or choosing on or the other is a trade-off process. The cathode, where the hydrogen is produced, has a steel coating with a catalytic coating. This coating differs between unactivated, activated nickel alloys like NiMo, NiSn and NiS or even platina groups. The overpotential for a platinum coating is 0.01 V. For the nickel alloys it ranges between 0.11-0.27 V. The membrane is a material trademarked as Zirfon Perl. The basis is an organic polymer, polyphenylene sulfide, with an open mesh structure. It is coated with circa 85% zirconium oxide and around 15% polysulfone. The lifetime of the electrolyzer is mainly determined by the electrodes, but also by the membrane. For an AWE the stack lifetime is between 60,000 and 90,000 hours. [28]

The time that it takes to go from a cold start to a nominal load is currently around <50 min. but expected to be <30 min by 2050.[29] An AWE is able to operate between 15% of nominal power and nominal power, with the efficiency increasing the closer one gets to nominal power. AWE’s are meant to be operated in a steady-state. Large variations in current can disrupt the system. The voltage efficiency of an AWE is currently 50-68%, with an operating voltage range between 1.8 and 2.4 V.

Proton exchange membrane (PEM)

The PEM electrolyser was invented to counteract the challenges faced when using an alkaline electrolyzer. For example low current density and low pressure operation. In a PEM electrolyzer protons are the charge carrying ions. The electrolyte is a solid polymer-based membrane which is gas tight. The following two reactions take place at the electrodes.

$$Anode: \quad 2H_2O\ (l) \ \rightarrow \ O_2\ (g) + 4H^+\ (aq) + 4e^- \qquad \text{(Eq. 2.11)}$$

$$Cathode: \qquad 4H^+\ (aq) + 4e^- \ \rightarrow \ 2H_2\ (g) \qquad \text{(Eq. 2.12)}$$

The current density achieved by a PEM electrolyzer is significantly larger than that of an AWE. The reason being that the relatively small protons are much more mobile in their electrolyte than the larger hydroxide ions. PEM electrolyzers are also able to operate at a higher pressure, up to 30 bar, which would make significant savings for the needed compression of hydrogen-gas for storage, if this would be the goal. The current density ranges 1-2 $A \cdot cm^{-1}$. Predictions are made that this number could rise up to 4-6 $A \cdot cm^{-1}$ by 2050, if changes in the design and membrane are successful. [29]

The operating temperature is also in the 50-80 °C range.

The electrodes are from both sides directly connected to the membrane. The conditions in a PEM electrolyzer are rough. The anode must be placed in a very acidic and highly oxidizing environment. The only material known to be stable at these conditions, while delivering high electrode activity is Iridium Oxide, IrO_2. This is also the main drawback of PEM electrolysis. Iridium is very scarce metal, with a concentration of about 1 ppb in the Earth's crust. The electrode itself usually has a platinum or titanium core, with an Iridium coating.

The cathode also operates in a highly acidic environment, but under reducing conditions. Making more materials suitable. Nevertheless the list remains short and the typical cathode in a PEM-electrolyzer is made from platinum black or platinum layers on a carbon core.

The membrane is a perfluorosulfonic acid (PFSA). A copolymer of perfluorovinyl ether groups, that have been terminated by sulfonate groups are structured as tetrafluorochtylene, this material has the simpler name Nafion, produced by DuPont. [30] Nafion is firstly treated with a base, after that the sulfonate groups are converted to sulfonic acid, by treating it with an acid. This gives it the ability to conduct protons.
The lifetime of a PEM electrolyzer is, even under the highly acidic conditions, between 50,000-80,000 hours.

Since the electrolyte is solid, the inertia is much lower than that for the liquid electrolyte used in AWE, to reach steady state. Also the protons travel much easier as mentioned. Meaning that the PEM system can much quicker react to power supply changes. The cold start up to nominal load time is roughly equal to <20 min. With future predictions estimated to lower the time to <5 min. [29]
The voltage efficiency is between 50% - 68%, identical to that of an AWE. The operating voltages are between 1.4 – 2.5 V.

Solid Oxide Electrolyser Cell (SOEC)

The SOEC electrolyser deals with both the limitations of the two previously described electrolysers. It can achieve high current density and no noble or expensive materials are needed, on top of that it reaches unrivaled efficiencies. SOEC stands for Solid Oxide electrolyser cell. In a SOEC electrolyser oxide-ions, O^{2-}, are the charge carriers. The electrolyte is a dense ceramic able to conduct the oxide ions. The following half reactions take place:

$$Anode: \qquad O^{2-}\ (g) \rightarrow \frac{1}{2}O_2\ (g) + 2e^- \qquad \text{(Eq. 2.13)}$$

$$Cathode: H_2O\ (g) + 2e^- \ \rightarrow \ H_2\ (g) \ + \ O^{2-} \qquad \text{(Eq. 2.14)}$$

The electrolyte is comprised of a combination of zirconia (ZrO_2) and yttria-stabilized zirconia (YSZ). Both materials are abundant and inexpensive. The zirconia has high conductive abilities and is temperature and corrosion resistant. The YSZ, Y_2O_3, is used to counteract material damage when cooling rapidly. Zirconia is a ceramic that is able to facilitate ionic conduction. The vacancies for the O^{2-} - ions to be filled are created by the doping with the YSZ, which is the driving force behind the ionic conduction. There is a temperature threshold though, only at temperatures above 600°C the ionic conduction starts. The electrodes are usually porous and are often either YSZ doped nickel or Lanthanum strontium manganate (LSM).[31]

Operating temperatures vary between 600 – 850 °C. This allows for the two most important advantages of the SOEC electrolyser. These are faster kinetics and more favorable thermodynamics. The former of the two allows for a current density of close to 1.5 $A{\cdot}cm^{-2}$ at thermoneutral potential. The high temperature also increases the electric efficiency, since now heat is assisting to the splitting of the water. Heat is a much less expensive and valuable form of energy.

The two main challenges of the SOEC-electrolyser are the durability or performance degradation and scale-up. Other problems are the robustness, start-up time and the costs. A quick overview on advancements for each of these problems will be provided.

The CAPEX costs are expected to drop significantly in the coming decades, based on the cost reductions due to economies of scale. [28]Studies have shown that electric energy will be the most contributing factor for the OPEX in the future, which is very favorable for the SOEC. This means that the cost will not be a limiting factor in the future.

The fuel electrode, the cathode, is mostly responsible for the degradation and decrease in performance. Studies showed that the electrocatalytically active sites can be blocked by silica-containing impurities. There is also a link between the initial performance of the fuel electrode and the degradation rate. If operation is performed over an extended time period at high overpotentials, Nickel can migrate from the electrolyte-electrode boundary to the support layer, this causes irreversible losses in the electrochemical performance.

Another aspect in the durability has to do with other components of the SOEC-system. An individual cell is about 100 cm^2 and can produce up to 30 L of hydrogen gas per hour.[32] To increase this performance the cell are stacked upon each other and connected in series. The flow channels, glass sealings and metallic interconnects for example. The environment of the SOEC electrolyser also has its wear and tear on this hardware, corrosion, accumulating impurities and inter-diffusing elements also change the electrochemical performance.

The robustness and start-up time, before nominal operation is achieved, are also known challenges from the early days of SOEC electrolysers. Their tolerance for temperature changes and emergency shutdowns was very low. By introducing metals into the cells all of the aforementioned problems are solved. Test have been performed and up to 2500 thermal cycles were performed by cells. The brittleness of ceramic layers also indicated that high pressure operation was not possible for SOEC. But when the pressure difference between the air-side compartments and the fuel-side compartments is minimized, the cells can operate at elevated pressure, up to 25 bar.

Lastly the scale-up issue. Improvements have been made on several areas. Cells with up to 550 cm^2 of active electrode area have been developed and tested, opposed to the beforementioned 100 cm^2. Also by optimization of the electrode microstructure and test conditions, has led to current densities up to 3 Acm^{-2}. And cell stacking technology is also advancing, proposals of 350 cells per stack are observed. If all these elements improve with the numbers described, electrolyser plants with industrial capacities can emerge.[32]

One more advantage of the SOEC electrolyser is that its also useable for the electrolysis of CO_2. Steam and CO_2 can even be electrolysed together, called co-firing. The resulting product is syngas. Having a process that uses CO_2 as a feedstock instead of having it as a polluting product is obviously desired. On top of that one attains a very desirable product that can be used for upgrading in many different applications, also for BTL processes. The half reaction of the CO_2 reduction looks as follows:

$$Cathode:\ CO_2(g) + 2e^- \rightarrow\ CO(g) +\ O^{2-}(g) \qquad \text{(Eq. 2.15)}$$

The reaction at the anode is the same for the electrolysis of carbon dioxide. Overall the following reaction at the cathode occurs and lastly the overall co-electrolysis reaction will be shown.

$$Cathode: H_2O\ (g) + CO_2\ (g) + 4e^-\ \rightarrow H_2\ (g) + CO\ (g) + 2O^{2-}(g) \qquad \text{(Eq. 2.15)}$$

$$Overall: H_2O\ (g) + CO_2\ (g)\ \rightarrow\ H_2\ (g) + CO\ (g) + \frac{1}{2}\ O_2\ (g) \qquad \text{(Eq. 2.16)}$$

2.4 Syngas to gasoline and diesel

Diesel and gasoline are basically hydrocarbon molecules. Different types of hydrocarbon molecules, like alkenes, isoalkanes, cycloalkanes and aromatics. For gasoline the length of these hydrocarbons ranges between molecules with four carbon atoms and with twelve carbon atoms. Diesel consists of mainly aliphatic hydrocarbons and aromatic hydrocarbons, accompanied by alkanes and alkyl-cyclohexane. The carbon numbers range from 8 to 28 carbon atoms in the molecule. Different routes towards the production of diesel and gasoline will be investigated and discussed in this section.

2.4.1 Pathways [33]

Firstly the biomass needs to be converted to bio-oil to be able to process it further. The previously described fast-pyrolysis process achieves this. The molecules in this bio-oil are mainly short hydrocarbons containing lots of oxygen. This oxygen needs to be removed and the carbon chains need to become longer. Several pathways are possible to achieve these two goals. These are summarized in the following block diagram and will be explained and why or why not they are chosen to be applied.

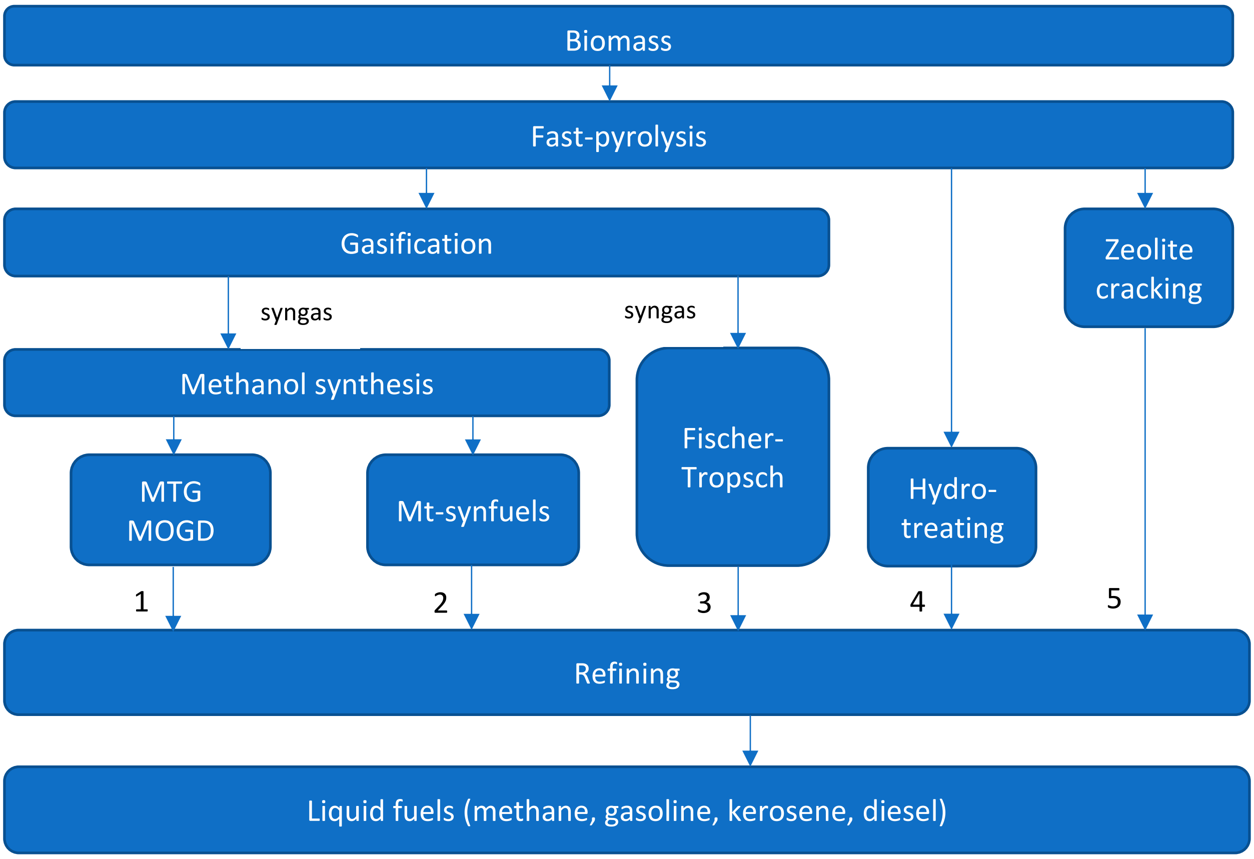

Figure 7: Alternative pathways of converting syngas to diesel and gasoline.

The first choice that needs to be made arrives after the fast-pyrolysis step. Two options are available:

1. A gasifier is used to transform the pyrolysis oil into synthesis gas. The synthesis gas is then upgraded and can be refined to form the final product.
2. A process is chosen that immediately makes the bio-oil ready for refining.

Two processes are available for the second case. These are hydrocracking and zeolite-cracking. Their pathway numbers in the diagram are 4 and 5 respectively.

4: Hydrotreating

A catalytic reaction takes place between the bio-oil and hydrogen molecules. The conditions are a high pressure of up to 200 bar and moderate temperatures of up to 400 °C. [34]A naphta-like product is obtained, around 33% of the original energy available in the bio-oil ends up as naphta. The naphta can be send to a refinery for further upgrading. The reaction looks as follows:

$$C_1H_{1.33}O_{0.43} + 0.77\ H_2 \rightarrow CH_2 + 0.43\ H_2O \qquad \text{(Eq. 2.17)}$$

A large hydrogen requirement is needed and when this comes from gasification of biomass the efficiency of the process drops even more. And if it comes from SMR it has a large carbon footprint. The high pressure brings high costs. Lastly precious metal catalysts on sturdy supports are needed to withstand the operating conditions.

5: Zeolite cracking

Zeolite cracking of bio-oil has the following conceptual overall reaction to remove the oxygen:

$$C_1H_{1.33}O_{0.43} + 0.26\ O_2 \rightarrow 0.65\ CH_{1.2} + 0.34\ CO_2 + 0.27\ H_2O \qquad \text{(Eq. 2.18)}$$

Several pathways can be followed, but the main interest is using zeolite-based cracking to produce aromatics. This process is operated at around 450 °C and atmospheric pressure. The low H/C ratio in bio-oils is the limiting factor for the aromatic hydrocarbons produced, suitable for gasoline blending. A yield of 45% in terms of energy is obtained relative to the biomass.[34] The product is only a fraction of what composes gasoline and CO_2 is emitted.

Both pathways show clear limitations and disadvantages for the purpose of producing mainly diesel and gasoline for the transport sector. That is why a gasifier is needed to transform the pyrolysis oil into synthesis gas. There are three different routes to get to the final product. Two of these, pathway 1 and 2, have the methanol synthesis as an intermediate step. During the methanol synthesis syngas is converted to methanol via three main reactions:

$$reaction\ 1: \quad 2\,H_2 + CO \rightarrow CH_3OH$$

$$reaction\ 2: \quad CO + H_2O \rightarrow CO_2 + H_2$$

$$reaction\ 3: \quad CO_2 + 3H_2 \rightarrow CH_3OH + H_2$$

1: MTG and MOGD [35]

MTG stands for methanol to gasoline. Three steps are identified. Firstly the methanol is dehydrated to form di methyl ether (DME). The second reaction step converts the DME to light olefins, with carbon numbers C_2 – C_4. The final step converts the light olefins to higher olefins, n/iso-paraffins, aromatics and naphtenes. This is summarized in the following simplified reaction mechanism:

$$2\,CH_3OH \rightleftarrows CH_3OCH_3 \rightarrow light\ olefins \rightarrow higher\ olefins, aromatics, naphtenes, n/iso-paraffins \quad \text{(Eq. 2.19)}$$

For the first step methanol is vaporized and fed into the DME reactor, which usually is a fixed bed. The reaction takes place at 310-320 °C, 26 bar over an aluminum catalyst. The equilibrium reaction is pushed as far as possible to the DME side and a mixture of mainly DME, methanol and water flows to the second reactor. The second reactor is filled with a zeolitic catalyst named ZSM-5. At 350-370 °C the conversion of DME to mainly raw gasoline, dissolved hydrogen, CO_2, light C_1-C_4 hydrocarbons and non-hydrocarbons. A distillation column is used to separate the raw gasoline from the other products and after one more unit, the heavy gas treatment unit, it meets the specified finished gasoline requirements. The carbon chains are limited to C_{11}, which is long enough to produce gasoline, but not diesel.

MOGD stands for Mobil olefins to gasoline and distillate. Mobil refers to Exxon Mobil, the investors of the MTG and MOGD process. Distillate refers to heavier hydrocarbons, in the range of diesel. The MOGD process is an extension of the MTG process. As was explained in the MTG process, the intermediate molecules are light olefins. The process that focusses on producing these olefins as product is called the methanol to olefins MTO process and is very similar to the MTG process. These olefins can serve as feedstock for the MOGD process. High octane numbers are desired and shape selectivity is applied to produce mainly methyl branched iso-olefins, ranging from C_5-C_{20}. The product distribution is determined by kinetic, shape-selective and thermodynamic limitations. The ratio between gasoline and raw distillate can vary between 0.2 and >100. Usually 4 fixed bed reactors are used in the MOGD section, these are filled with a special zeolite catalyst. Fractionation takes place after the MOGD. The output stream of the four fixed beds is split in three parts. The first part are the light hydrocarbons, with C_3/C_4, they undergo alkylation to enhance the gasoline yield and the rest is retrieved as propane. The second part is the gasoline fraction. The last part is that of the raw distillates. The raw distillate stream is hydrogenated in the heavy distillate treatment unit to form different products, amongst them is diesel.

A large number of reactors and units is needed to convert the olefins to the desired products. Methanol is also a toxic chemical.

2: Mt-Synfuels

Another pathway is that of the company Synfuels. The technology is still patented. What is known is that methanol is again the feedstock to produce the raw

2.4.2 Fischer Tropsch process

The final pathway, number 3 in figure 7, that will be discussed is the Fischer Tropsch (FT) process. Developed in 1926 by Frans Fischer and Hans Tropsch, hence where the name comes from. It gained interest because Germany needed liquid hydrocarbon fuels in between WW1 and WW2 and during WW2.[36] Germany is not rich in petroleum, but it does have a lot of coal. Via coal gasification, synthesis gas could be obtained, the FT process transformed it into large and oxygen free hydrocarbon chains. The mixture of these large hydrocarbon chains is called syncrude. The syncrude can be send to a refinery to produce the desired products. After WW2 it gained global interest and the commercialization of the process started when companies like Sasol and Shell started building plants in countries that are rich in natural gas and coal, with little reserves of petroleum oil. This started in the 1950's. The interest in the FT process regained interest, since biomass can be also be used as feedstock for the required syngas. Giving a carbon-neutral and renewable way of producing traditional liquid transportation fuels.

The Fischer Tropsch Synthesis (FTS) uses syngas as a feedstock. Different reactors, catalysts and operating conditions can be used, the goal is to produce long hydrocarbon chains. The propagation mechanism is not exactly clear, but it is clear that the two most produced products are paraffins and olefins.[37] This can be summarized in the following simplified reactions. Both reactions are highly exothermic.

$$Paraffins\!: \ n\,CO + (2n+1)\,H_2 \ \rightarrow C_nH_{2n+2} + n\,H_2O \qquad \text{(Eq. 2.20)}$$

$$Olefins\!: n\,CO + 2\,H_2 \ \rightarrow C_nH_{2n} + n\,H_2O \qquad \text{(Eq. 2.21)}$$

The simplified initiation of the chain looks as follows:

$$Initiation\!: (\,)^* \ + CO + \ 2H_2 \ \rightarrow (CH_2)^* + \ \ H_2O \qquad \text{(Eq. 2.22)}$$

The exact propagation reaction mechanism is still up for debate, but several pathways are available. Three of them will be presented. [2, 38]

a. The original mechanism was suggested by Fischer and Tropsch themselves. They believed the carbon chain is propagated by addition of -CH_2-. This implies that C + C coupling is achieved through polymerization of CH_2 intermediates on the surface. An example of this is shown in figure 8 a.
b. The next mechanism was proposed by Pichler and Schulz. During experiments the formation of oxygenates was observed, which could not be explained by the first

mechanism. That is why a CO insertion mechanism was proposed. When its time to form a new C + C bond to form on the active sites, CO is directly inserted to the adsorbed alkyl intermediates. This is shown if figure 8 b.

c. The last proposed mechanism is the oxygenate or enol mechanism. This time the adsorbed intermediates are hydroxyl methylene. By dimerization of the adsorbed intermediate C + C coupling is formed. This can be seen in figure 8 c.

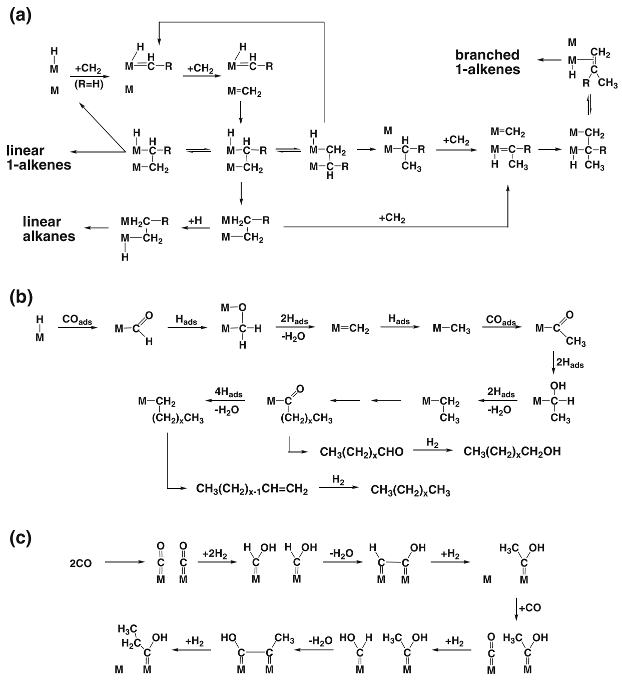

Figure 8: Proposed FT reaction mechanisms. [2]

The simplified termination of the chain looks as follows:

$$Paraffin\ termination: (CH_2)_n^* + H_2 \rightarrow C_nH_{2n+2} \qquad \text{(Eq. 2.23)}$$

$$Olefin\ termination: (CH_2)_n^* \rightarrow C_nH_{2n} \qquad \text{(Eq. 2.24)}$$

As mentioned earlier the goal is to produce relatively long, in the gasoline and diesel range, hydrocarbons. These molecules are often referred to as middle distillates and range from C_{5+}, to C_{20}. The molecules produced are mainly paraffins, olefins and other linear hydrocarbons. To prevent early termination and improve the selectivity towards longer chains a few factors are important. These are the operating conditions, catalyst type and the syngas composition, more specifically the H_2 : CO ratio. The temperature and syngas composition have the largest effect of these three factors and are quantified in the growth probability factor, denoted by α. [39]

Song et al. developed an empirical correlation to calculate α[40]:

$$\alpha = (0.2332\, \frac{\gamma CO}{\gamma CO + \gamma H_2} + 0.633)[1 - 0.0039(T - 533)] \qquad \text{(Eq. 2.25)}$$

This α can be implemented into the Anderson Schulz Flory method (ASF). With the ASF distribution the ratio of different length polymers, hydrocarbons in this case, can be determined by assuming an ideal step-growth polymerization process. The formula for the ASF distribution looks as follows:

$$Mc_n = \alpha^{n-1}(\alpha - 1) \quad \text{(Eq. 2.26)}$$

M_{Cn} represents the molfraction of the hydrocarbon molecule with n carbon atoms.

The ASF distribution gives a relatively good estimate, but during experiments a few stark deviations have been observed. These are[37]:

- The methane yield or selectivity towards methane is higher than predicted by ASF.
- The ethene yield or selectivity towards ethene is lower than predicted by ASF.
- α increases with increasing carbon number.
- An exponential decrease in the olefin to paraffin ratio is observed for C_{3+}.

To account for these deviations, new models have been developed. These new models can be grouped into two main categories. Hydrocarbon selectivity models and Langmuir-Hinshelwood-Hougen-Watson (LHHW) kinetic models. For the hydrocarbon selectivity models again two main categories exist from which different derivates exist in the academic world. These are the double-alpha and olefin-readsorption models. Even these are still simplified versions relative to LHHW models, which take every part of the reaction mechanism and the kinetic rates of the steps in the mechanism into account. Both of these approaches are beyond the scope of this thesis.

FT Catalysts: [41]

The metals from group VIII in the periodic table are mostly used for the FTS, they form the basis of the catalysts. Most of the FT related research of these catalyst has been done on iron, ruthenium, nickel and cobalt. This group can quickly be made even smaller, since ruthenium is a rare and expensive metal and nickel tends to transform to nickel carbonyl under high pressures, which are applied during the FT process. That is why iron and cobalt and their respective operating ranges will be the only one discussed. Before going to the catalysts two operating regimes of the FT process will be discussed.

There are two main types of FTS temperature regimes. Low Temperature Fischer Tropsch and High Temperature Fischer Tropsch, abbreviated LTFT and HTFT respectively. LTFT is an operation in the 200-240 °C range. A FT process is considered HTFT between 300-360 °C. Cobalt catalysts are only used in LTFT, the main products are linear waxes with a high molecular mass, but also molecules in the diesel range. High pressure increases the production of these linear waxes and decreases the degree of branching. Iron catalyst can operate in both regimes. In the LTFT iron operation the same products are the target as for the cobalt. HTFT processes on the other hand have more selectivity towards the gasoline range of hydrocarbons.

Iron (Fe) vs Cobalt (Co) catalyst:

Before diving in the elemental reactions that occur and how the catalysts react to them, the structure and re-assembly of the catalyst when the process starts will be discussed. The iron-based catalyst for the FTS is alkalized, usually with potassium. Cu can also be added for improved reduction properties or MnO, ZnO or alumina for improved performance. The catalyst undergoes a change when it is brought in contact for the first time with syngas. The catalyst re-assembling takes place. The iron reacts with the carbon that is available through CO-dissociation. A FT-active carbide surface is formed, which enables FTS. During the re-assembling the rate of the FT-reaction is increasing, but the selectivity does not change, meaning that the active sites appear to be static. The only parameter that influences the reactions is temperature.

The cobalt-based catalyst is usually promoted with zirconia. The re-assembly takes place by segregation of the metal surface and disproportionation takes place. The original Co-catalyst is now turned into two different compounds, one with a higher and one with a lower oxidative state then the original. One is meant for chain growth, while the other one facilitates the formation of the -CH_2- monomer. The structure of the active catalyst sites appears to be thermodynamically controlled. The time, how long the reaction is run, temperature and partial pressure all have effect on the elemental reactions. The Cobalt FT sites are of dynamic nature.

Methane formation is thermodynamically favored to be formed under FT conditions, opposed to higher hydrocarbon chains. Iron catalyst sites are static entities, with no methanation sites present, allowing to operate at higher temperatures without excessive methanation. Cobalt catalysts have dynamic methanation sites, causing excessive methane formation when the temperature and partial CO pressure are increased.

The primary products during the FTS are olefins and paraffins, with ratios of close to 4:1 or 3:1. This is true for both Fe and Co. But the secondary reactions, re-adsorption of olefins, double bond shifting in the olefins and olefin hydrogenation also take place. These secondary reactions intensively take place on Co catalyst, reducing the olefin to paraffin ratio drastically, paraffins now being the majority product by far. This also partly explains the ethene deviation from the ASF distribution discussed earlier. For iron catalysts these secondary olefin reactions are limited to some olefin re-adsorption on the growth sites. This makes iron catalyst the choice for producing olefins.

Lastly the earlier seen water gas shift (WGS) reaction is discussed. It looks as follows:

$$CO_2 + H_2 \rightleftarrows CO + H_2O \qquad \text{(Eq. 2.27)}$$

On the iron catalyst the WGS reaction is very fast. This has to do with the alkalized oxidative part of the catalyst that is created during re-assembly. Because of this iron catalysts are more versatile and can receive lower quality syngas. Lower quality means less rich in hydrogen in this case. Water is the majority by-product of FTS, with the CO from the syngas, hydrogen can be produced. This does however mean that the iron-catalyst is affected by the presence of water, which is present in vast amounts, and CO_2 is produced.

The WGS merely proceeds on the Co-catalyst. Meaning that it is almost unaffected by the presence of water and almost no CO_2 is produced. It does have as consequence that for the FT reaction to proceed H_2 rich syngas is required. Co-catalysts are also more sensitive to impurities and require a higher degree of cleaning than an iron-based catalyst.

It is evident that both catalysts have their up- and downsides. Depending on what the final product is the correct catalyst for the process can be chosen. Table 2 summarizes the previously discussed factors.

Table 2: Overview difference Iron and Cobalt FT catalysts.

Factor	Iron	Cobalt
Extensive methanation	No	At rising temp, lower γ CO
Catalyst re-assembly	Carbide formation	Surface segregation
WGS-activity	Yes	No
Olefin reactions	No (little)	Extensive
Promotion	Potassium	Zirconia
Alkali	Essential	No

FT-reactors [42]

The Fischer Tropsch reaction is very exothermic. The catalysts are off course in the solid state and the syngas is in the gaseous phase. Three (archetype) reactors can be considered for the FT process.

- Gas-solid fluidized beds
- Multi-tubular reactor
- Slurry-bubble column reactor

Gas solid fluidized beds:

The first commercial version of this reactor was developed in 1955 in Sasolburg, the process is known as the Synthol process. Fine catalysts between 40 -150 diameter were used. The bed was held up by high velocity gas, between 1-2 $m \cdot s^{-1}$. The reactor was a riser type, standing 46 meters tall with a diameter of 2.3 m. The production was limited to 1500 $bbl \cdot day^{-1}$.

Because the FT process is relatively slow a high catalyst bed density is needed so that the reaction has enough time and surfaces to react on. A riser type reactor, like the Synthol one, is not ideal due to low catalyst density inside the reactor. In 1989 a new version of the Synthol process was developed by Sasol, a bubbling fluidized bed reactor was developed for FT application. It operates in the bubbling regime and has internal cooling tubes. The advantages over the Synthol process, are more compact reactor for same production capacity, less attrition from the catalyst, easier operation and maintenance and less energy required for gas circulation. This added up resulted in significant reductions in capital and operating costs.

The benefits for a bubbling fluidized bed are the excellent heat transfer and uniform temperature distribution. This is needed for the highly exothermic FT process. The use of small catalyst particles also eliminates mass transfer limitations, mainly because of high pore diffusion. A serious problem is that heavier products can deposit on the catalyst surface. The syncrude is sticky and causes agglomeration of the catalyst particles, which hinders fluidization. To counteract this, high temperature and moderate pressure are used. As could be seen in the previous catalyst section this favors the production of lighter products. The ASF α is even limited to 0.71. In this regime gasoline range molecules, up to C_{11}/C_{12}, are the largest products.

Multi-tubular reactor (fixed bed)

This type of reactor is designed for the production of heavy, waxy FT products. The Shell Middle Distillate Process (SMDS) is the name and the first plant was installed in 1993. A specially developed catalyst and careful reactor design enabled a production capacity of up to 3000 $bbl \cdot day^{-1}$ of synthetic hydrocarbons.

A relatively large pressure drop is inherent in fixed beds. This in its turn requires larger catalyst particles, not to densely packed, so that the gas can still flow around them. The catalyst particles in this reactor are around 1mm in diameter. This negatively impacts the intraparticle diffusion, decreasing reaction rate. The shape and size of the catalyst is therefore very important for this reactor.

A multi-tubular reactor's cooling is achieved by surrounding the catalyst-filled tubes with a cooling medium. The reactor is to be kept isothermal and the heat is removed by conduction of the metal comprising the cylindrical tubes. The relatively poor conduction and limited heat transfer to the tube wall can create high temperature zones. This can cause reduction of selectivity or earlier catalyst activity decline, both undesired. The tube diameter, catalyst particle size and gas velocity are factors that determine the effectiveness of the heat transport and how homogenous the temperature throughout the bed is. The largest temperature peaks are usually near the inlet, closer to the outlet the temperature is more homogenous. The tube and catalyst particles have to be designed to handle the largest temperature peaks, meaning that for most of the tube it is overdesigned. Larger catalyst particle size and higher gas velocities increase the heat removal. But a trade-off has to be made since this also limits the mass transfer and increasing the pressure drop. Another way of creating a more homogenous process is by reducing the per pass conversion to around 20-30%, instead of 70% and introducing a recycling stream. This is combination with now the possibility of higher temperatures and pressures increased the reactor capacity factor 25 times, reduced the cooling area 12 times and the catalyst and steel used by a factor 7. The last improvement in radial heat conductivity can be made, by operating in the presence of a liquid. The condensable FT products already create a gas/liquid mixture and this already causes improvements towards the outlet region. By introducing liquid before the inlet, trickle flow mode can be achieved in the entire tube. A multi-tubular fixed bed reactor can be scaled-up safely and straightforward and is capable of very large production capacities.

Slurry bubble column reactor

A slurry bubble column reactor (SBCR) also has a very high production capacity and can produce heavier hydrocarbons. In 1993 Sasol, again, designed a commercial reactor for the FTS. With a diameter of 5 m and a height of 22 m, this reactor has a production capacity of 2500 bbl·day^{-1}. The SBCR is an advanced version of the previously described gas/solid fluidized bed. The name slurry implies the introduction of a third phase, opposed to the two phases of the gas/solid fluidized bed, namely liquid. The reactor is filled with a network of cooling tubes, with diameters of about 50 mm. The remainder of the reactor is filled with liquid and catalyst, referred to as slurry. The catalyst particles are small again, around 50 µm. These fine catalyst particles are intensively mixed with the surrounding liquid, the slurry can even be considered a pseudo-homogenous phase. This assumption holds for large diameter reactors and high superficial gas velocities of $U > 0.2$ m·s^{-1}.

Now it is time to introduce the reagent, syngas, also the last phase. The gas is blown into the slurry mixture. The liquid will respond by expanding and the height of the bed increases almost linearly with increasing U. Only very small bubbles, between 1-7 mm, are able to traverse through the slurry. The majority of these bubbles falls within this size range and this regime of operation if referred to as the bubbly flow regime. Once a certain superficial gas velocity threshold is reached, U_{trans} , coalescing of the small bubbles begins. These new and large bubbles travel significantly faster through the slurry and have sizes ranging between 20- 70 mm. Small bubbles are still present but have a hard time travelling through the slurry, they are almost entrained. The vast majority of the gas transferred, is done by the large bubbles. Since both bubble types co-exist, this is called the heterogenous flow regime.

Another important characteristic is the gas hold-up. This is the volume fraction of gas in the gas/liquid (slurry) phase. The name hold-up suggests that a high number is negative. This is indeed the case, since gas in this case is your reagent. If this gas is unable to traverse through the column or even entrained by the hydrodynamic behavior inside the reactor, the yield suffers, since it cannot react.

The amount of suspended catalyst also determines the degree of coalescence of the small bubbles. More catalyst suspended means more coalescence. At around 30 vol % of suspended catalyst for the FT process, the presence of small bubbles is negligible. Another factor that increases the coalescence is increasing the superficial gas velocity.

The last question was if these large bubbles provide good enough mass transfer. It was found that this is indeed the case, since these large bubbles did not reach the top of the reactor in one piece. Constant breaking-up and coalescing takes place, ensuring high mass transfer rates and enough contact with the catalyst particles.

Heat transfer and equalization of the temperature in the reactor is also good for SBCR, especially in the heterogenous mode. As said the reactor is filled with cooling tubes across its length, that take away the heat. Heat transfer coefficients of up to 1000 W·m^{-2}K^{-1} are reached.

The downsides of the SBCR are the separation of solids and liquid. Distilling of the product is not possible, filtration can be a solution. The separation problem increases if attrition affects the catalyst particles, this can be mechanical attrition or chemical.
A foam can be formed, which again increases gas holdup.
Too low velocities can indirectly affect the suspension of the catalyst particles, since concentration gradient of catalyst are formed at low velocities, which produces too much of the sticky products in a small volume, causing clusters.
Lastly upscaling of a SBCR is not so straightforward, a costly demonstration stage is generally considered to be necessary.

Table 3 summarizes the main parameters discussed for the reactors.

Table 3: Overview qualities of the different FT reactors.

Reactor type	Mass transfer	Heat transfer	Production capacity	Product range	Upscaling
Gas solid fluidized bed	Very good	Very good	> 2500 bbl/day	Methane up to C_{12}	straightforward
Multi-tubular fixed bed	Limited	Limited	> 2500 bbl/day	Methane up to heavy waxes	straightforward
Slurry bubble column	Good	Good	> 2500 bbl/day	Methane up to heavy waxes	complicated

2.4.4 Refinery:

Now that it is clear how the syncrude is produced, the next step is extracting the desired products. These are gasoline and diesel. The syncrude however is comprised of the whole range of hydrocarbons in ratios predicted by ASF based distributions. As could be seen in figure x the refinery is the next step after the FTS. This refinery operates just like the well-known oil refineries. Firstly, the working principles behind the distillation columns used will be described in this section. Secondly the hydrocracking unit will be discussed in the following section. Lastly the conversion of raw gasoline and diesel, reforming, to sellable forms will be discussed.

Distillation columns

Distillation columns separate molecules based on their differences in volatility, using their boiling points. Depending on the process, separation requirements and scale of operation, distillation columns vary greatly in length. Usually, they are the highest structure in an oil refinery and can reach up to 30+ meters.[43] The column is filled with trays, around every 0.3 or 0.6 meters. A schematic of the column looks as follows:

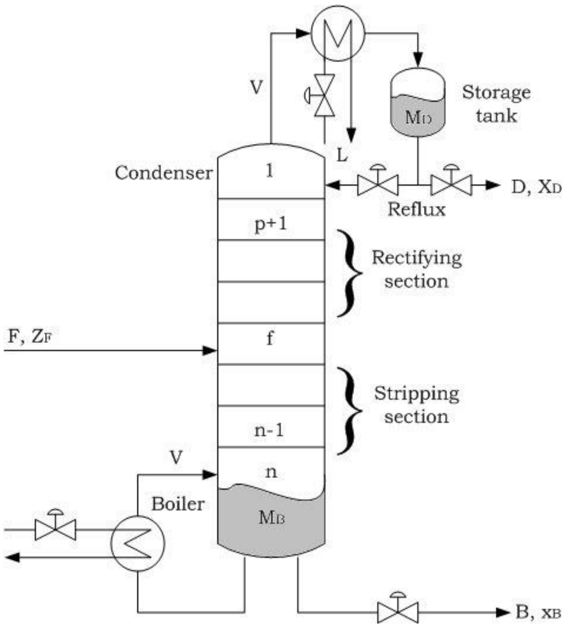

Figure 9: Schematic distillation column.[3]

Before the syncrude enters the distillation column it is heated up, creating a mixture of gases. The feed is delivered in a certain part of the column, the tray that is the first to interact with the feed is called the feed tray. Every part of the column above the feed tray is referred to as the rectifying section. The part of the column below the feed tray is the stripping section. The vapors of the feed flow up the column and the liquids counter currently down the column. As said before, the column is filled with trays. These trays are perforated, enabling vapor to flow through them. There are different tray designs, but the bubble cap tray will be discussed.

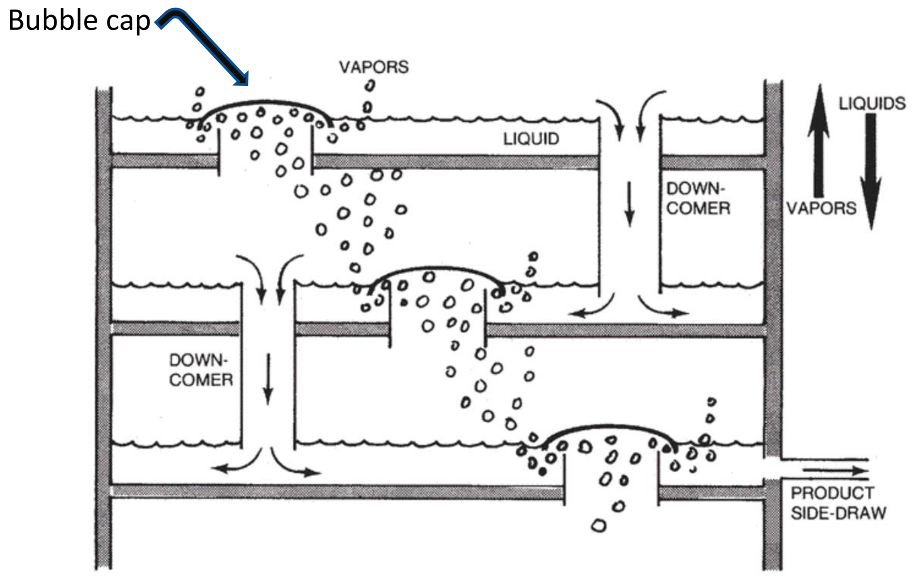

Figure 10: Schematic bubble cap trays. [44]

As can be seen in figure 10, the bubble caps force the vapor to flow through liquid present in the tray. This is the essence of distillation. Each tray provides intensive contact and allows heat exchange between the vapor and liquid. A vapor liquid equilibrium is reached and some of the vapor, will go up to the next tray, another part of the vapor which got below its boiling point will stay in the tray as liquid. The vapor that continuous rising is now cooler and will go through the same process in the next tray it encounters. The top trays are richest in the most volatile molecules, the bottom trays in the least volatile molecules, because excess liquid is able to flow down to a tray below, through the downcomer. The molecules that reach the top of the column will encounter the condenser, which cools down the vapor and sends a part of it back to the distillation column. The ratio between the amount of liquid send back to the tower and the amount of product removed from the process is called the reflux ratio. At the bottom of the column a reboiler does the opposite, liquid that flows to the bottom is heated and vaporized. In specified parts of the column product side-draws are installed. Here the products are extracted from the column and sent to downstream operations. Now that the basic principles are established, the distillation of syncrude will be discussed.
Lots of different molecules are present in the syncrude, which cannot all be separated individually. The syncrude is heated up to about 350 °C before entering the distillation column. The temperature of the trays is controlled. At certain trays the temperature is exactly the temperature at which the desired product condensates. These trays, their temperatures and the target products from syncrude are as follows: [45]

- At the bottom long paraffinic waxes, mainly liquid, are removed from the tower.
- Around 260 °C Diesel condenses out of the tower.
- Around 180 °C Kerosene condenses out of the tower.
- Around 110 °C Gasoline condenses out of the tower.
- At the top petroleum gas, LPG is removed from the tower.

The terms feed tray and reflux ratio where already discussed briefly. For most systems and process simulations modelling software is able to calculate these. The assumptions and method to calculate both for a binary mixture can be found in Appendix B, advanced software works on these principles to obtain the desired values for more complex systems.

2.4.5 Hydrocracker:

Hydrocracking is a tool to increase the desired yield of middle distillates. The feedstock for hydrocracking, are the carbon chains that exceed the length of the middle distillates, C_{20} and up, in the FT process these are the paraffinic waxes produced. It is a two-stage processes that occurs simultaneously inside the reactor. Under high temperatures, 400-820 °C, and high pressures, 70-140 atm, catalytic cracking of the long carbon chains take place, this is the first stage. [46]The second stage is that the cracked molecules are hydrogenated, since hydrogen gas is also present in the reactor, hence the name hydrocracker.

The catalysts used for the hydrocracking are bifunctional. They combine an acid function for the first stage and a hydrogenating function for the second stage of the process. Superfacial acidity and a large surface area are needed for the acid function. Halogenated aluminas, zeolites, amorphous silica-aluminas and clays are often used. For the hydrogenation part one or a combination of transition metals is used. These can be iron, cobalt, nickel, palladium, platinum and others. The typical hydrocracking catalysts are made up around a weak acid support. This promotes the production of high-quality middle distillates. [47]

<u>Hydrocracking and Fischer Tropsch [48]</u>

The previous could be seen as the typical hydrocracking process. In combination with the FT process it looks a bit different.

To achieve a good hydrocracking process several things must be the target:

- The length of the fragments that are produced from the cracking of the long wax chain should be predominantly in the desired product range.
- The hydrocracking of components above the desired range should be prioritized over those below the desired range.
- The production of commercially less desired species should be minimalized.

The products of the LTFT process are a mixture of hydrocarbon chains, syncrude. In the syncrude there are heavy paraffins, waxes, present. Overall the LTFT waxes are predominantly paraffinic and free of metals, sulphur and aromatics, making them ideal for hydrocracking. Hydrocracking these waxes serves two purposes, increasing middle distillates yield and improving the cold properties since the hydrocracked molecules are mostly branched. Highly linear molecules and a very low aromatic content are both favored factors for diesel, since this increases the cetane number and makes the diesel of high quality. This high-quality diesel can be blended with low value refinery products, like light cycle oil, to increase the amount of diesel.

The straight run diesel from the LTFT process has a cetane number of about 75. The main goal of the combination of the LTFT process with a hydrocracker is thus the production of diesel. Of the syncrude produced, diesel makes up about 20%. To focus on the diesel yield, the LTFT process is designed for maximum wax production, because downstream hydrocracking of the waxes under mild conditions is the largest contributor to the final diesel yield. The mild conditions include pressures between 35-70 bar. It has been found that the distillate yield firstly increases with increasing pressure, up to a maximum from which is starts to decrease. Another benefit of the high pressure is that secondary cracking into lighter molecules is inhibited. The conditions are referred to as mild, opposed to the hydrocracking of petroleum derived feedstock, which must be exposed to 150 bar.

A few other factors need to be kept in mind for selecting the proper catalyst.
Firstly the non-paraffinic compounds of the syncrude, mainly alcohols, have to easily and completely hydrodeoxygenated. Meaning that the catalyst should be resistant to the presence of water and that an inevitable production of smaller hydrocarbon is present.
The partial pressure of the hydrogen must be kept above a certain threshold. If this is not the case dehydrocyclization of the paraffins can take place, forming polynuclear aromatics which can cause coking of the catalyst. The catalyst should be able the selectivity of this dehydrocyclization. Lastly lower hydrogen/wax levels increase the product selectivity towards lighter hydrocarbons. The catalyst should be able to avoid this even at lower hydrogen/wax levels. Hydrocracking by using the previously described standard bifunctional catalysts under mild conditions, results in a diesel fraction of close to 80%. Some branching does occur which lowers the cetane number to 70, which is still very high. The noble metal containing bifunctional catalysts have another advantage, which is higher hydro-isomerisation activity, which has better low temperature characteristics for the diesel.

2.5 Turbine

This last section of the literature review will explain how a turbine can be used to produce electricity from steam. First the general working principle of a turbine will be explained. Then the basic working principles a reaction turbine will be shown, the reaction turbine is mostly used in power plants. Lastly a short explanation of the generator that produces the electricity will be given.

A steam turbine is able to convert thermal energy that is present in pressurized steam and convert it into mechanical energy, rotating an axis, called the rotor. This rotor in its turn drives the generator, which converts the mechanical energy into electricity.

The first element that is needed is pressurized steam, the temperatures and pressures differ for different turbine designs and scales. Low pressure steam does not exceed 1.03 bar and the temperatures are around 250 °C. Medium and high-pressure steam are usually in the order of 28-59 bar with temperatures varying between 400-455 °C, pressures and temperatures as high as 97-124 bar and up to 510 °C have been reached. [49] The steam holds three types of energy:

1. Kinetic energy, the velocity of the flowing steam.
2. Thermal energy, the temperature of the flowing steam.
3. Pressure energy, the energy stored by pressurization of the flowing steam.

2.5.1 Reaction turbine:

The reaction turbine has two sets of blades attached to the rotor. Moving blades and stationary blades, depicted in figure 12. The moving blades are shaped as airfoils, shown in figure 11:

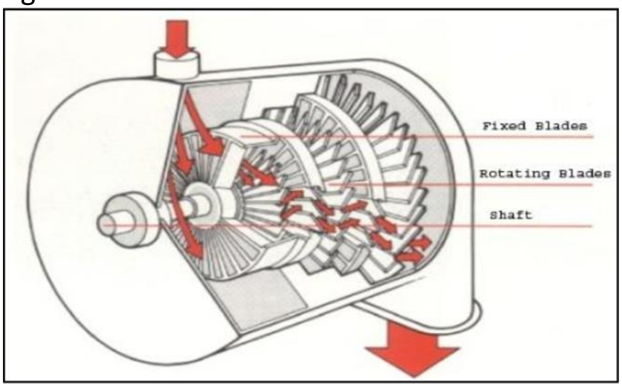

Figure 12: Schematic of reaction turbine.[50]


Figure 11: Illustration airfoil blades inside a turbine.[1]

When the steam passes the airfoil shaped blades a pressure difference is formed, this creates lift force, which rotates the turbine. Since energy can only be converted, all three types of energy present in the steam decrease. The second set of blades, which are stationary, do not move. The blades are positioned and shaped like a nozzle, in this way it forces the steam to flow from a large flow area to a small flow area, it expands. Now Bernoulli's conservation of energy principle applies which dictates that the kinetic energy increases if the pressure energy falls. The steam continues its way to a second set of moving blades. Again the set of blades rotates the rotor and all three forms of energy decrease. Then the steam meets another set of stationary blades and the same as before happens. A turbine has many sets of these moving and stationary blades. Figure x already showed that the blades keep getting bigger. Since the pressure is dropping, the steam is expanding and needs more area. Larger blades provide this needed expansion area. High-capacity power plants have different types of operating regimes, all connected to the same axle. The steam first enters the high-pressure turbine, then the medium pressure turbine and finally the low-pressure turbine, to extract as much work from the steam as possible. They all have the same working principle however. Eventually the steam has no more thermal energy left to drive the blades, since thermal energy can be seen as the source for the kinetic energy. [50]

In a reheat turbine, the steam is reheated after the first, high pressure, set of blades, to carry enough energy into the other two parts. This also helps in keeping the speed of the rotor constant, since the frequency of the electricity produced by the generator is directly related to the rotor speed. A mechanism is used to govern the steam flow into the turbine system. Now that is it clear how the rotor is rotated the next step, of electricity generation will be explained.

2.5.2 Generator:

The first principle is the creation of magnetic fields. When a current passes through a wire, a magnetic field is created around this wire. By shaping the wire into a coil, this electromagnetic field can be increased in strength, since each cross-section of the wire still produces an electromagnetic field. The current flowing through the coil also increases the strength of the electromagnetic field. The electromagnetic field has a north and a south pole, just like a magnet.

The opposite is also true, if a magnet is passed through a coil, a current will flow through the coil. The current flow can be increased if the magnet moves faster trough the coil, if its magnetic field is stronger or if the coil is larger. If an electromagnet is rotated around a coil, it will generate a single-phase alternating current (AC) in the coil. The alternating current is produced by the two poles of the magnet, which while rotating decrease or increase the current flow in the respective pole's direction, this has a sinusoidal shape. By placing three sets of coils, 120° from each other, around the electromagnet, a three-phase alternating current can be produced, this is shown in figure 13.

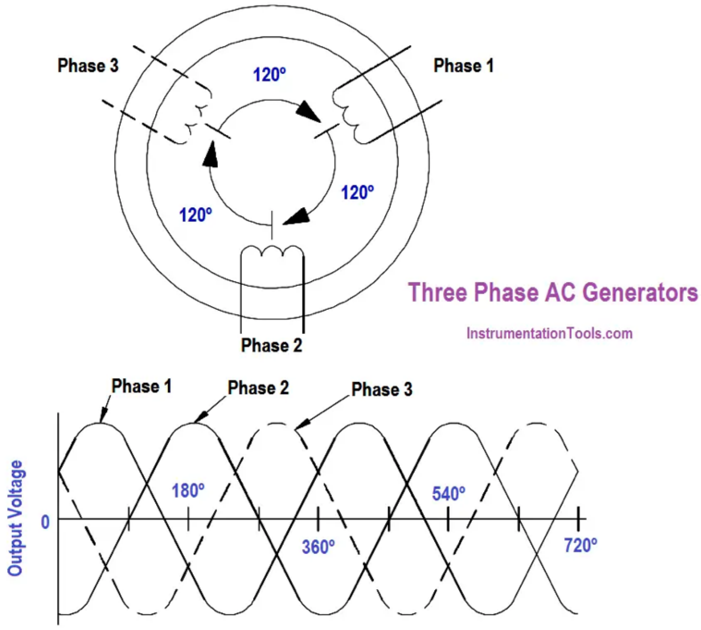

Figure 13: Visualization generator working principle.[51]

Summarized the combination of turbine and generator works as follows. The turbine rotates the rotor shaft. Onto the rotor shaft an electromagnet is connected, which spins around in the generator. High rotations per minute (RPM) of the rotor are needed to produce AC electricity with a useable frequency. Since an electromagnet is used, the strength of the magnetic field and thus the current can be varied.

This closes the chapter on the literature. In the next chapter the basis of design will be presented.

Chapter 3

Basis of Design

The basis of design (BoD) bundles the assumptions, rationale, criteria, principles and considerations used for calculations and major decisions to meet the Owner's Project Requirements (OPR). The BoD describes the technical approach towards the system design and is part of the projects technical specifications. The BoD serves as the fundament for design calculations and other design considerations. By preliminary investigating different routes and options from feed to end-product, the design takes shape. To aid in making a clear basis of design several aspects have to be discussed, these are divided into sections in this chapter. Section 3.1 presents the purpose of the design. Section 3.2 will delineate the battery limits of the system. Section 3.3 contains a description of the design for the individual units. Section 3.4 usually has a simplified block diagram, but since the thesis will present the model in the next section, this is unnecessary at this point. Section 3.5 will discuss the kinetics and thermodynamics used for the preliminary design. Section 3.6 provides the reader with the pure component properties. Section 3.7 will discuss the basic assumptions. Lastly section 3.8 will check the optimal economic margin, to see if the project can be profitable.

3.1 Purpose of design

Biomass and fossil fuels have lots in common. Both captured CO_2 from the atmosphere and fixated it in their structure. The latter did it eons ago and lost its oxygen through continuous pressure and heat. The former captures the carbon dioxide in real time and can serve as a renewable carbon source for versatile applications. Production of power, heat or different types of chemicals. Biomass can be grown with this purpose, but secondary biomass sources as residues and municipal waste could also be put to good use. The industry that concerns itself with this is getting more and more attractive, mainly due to renewable and improving economic reasons.

In this research biomass, more specifically bio-oil derived from pinewood, will serve as feedstock to produce liquid transportation fuels like diesel and gasoline. 5000 $kg \cdot hr^{-1}$ of bio-oil from BTG is the feedstock for the process. The goal is to design a continuous process that produces diesel- and gasoline-sized alkanes from biomass and has a decent share in the overall market. By combining old, well-known and thoroughly developed technologies from the petrochemical sector with new technologies and energy sources. The old technologies are gasification, which will be used to convert the bio-oil to syngas. The Fischer Tropsch process that will convert the syngas to syncrude. The last of the old technologies is converting the syncrude into the desired middle-distillates like diesel and gasoline in a refinery. The new technology will be the use of an electrolyser running on renewable electricity. Together they can facilitate the production of carbon neutral transportations fuels that can be implemented in the current infrastructure.

3.2 battery limits

The battery limits can be considered as the borders of the chemical process plant. Everything inside the fences of the plant is thoroughly designed and installed equipment used for the process. Everything outside the fences needs to be received or supplied, the product, to an external source. Preferably the plant is located in a place that makes the transactions with these external actors as efficient as possible, for example near a harbor, a main road or near train tracks.

A block scheme will be used to very schematically represent the figuratively described borders of the plant. The molecules entering and leaving the fences will be shown.
Within the fences, 5 units are used to create the end-product. A gasifier, a gas cleaning section, an electrolyser, a FT reactor and a syncrude upgrading unit. The end products are diesel and gasoline. Catalysts used in the FT- and hydrocracker reactor also come from outside the battery limit. Utilities like cooling water and air are assumed to be on site. The electricity used will be renewable electricity. Part of it will be produced within the battery limit by a turbine, the other part, to ensure continuous operation, will be bought from a hybrid PV plant, that has windmills, PV modules and batteries. The plant has a grid connection with this hybrid renewable energy plant. So, it will also be considered as outside the battery limit.

Storage tanks for the bio-oil and deionized water and other solvents are available on site. Their supply is via pipelines crossing the battery limit, running from the outside to the inside of the boundaries. Heat exchangers will also be available on site, making an efficient interplay between heat- sources and sinks possible.

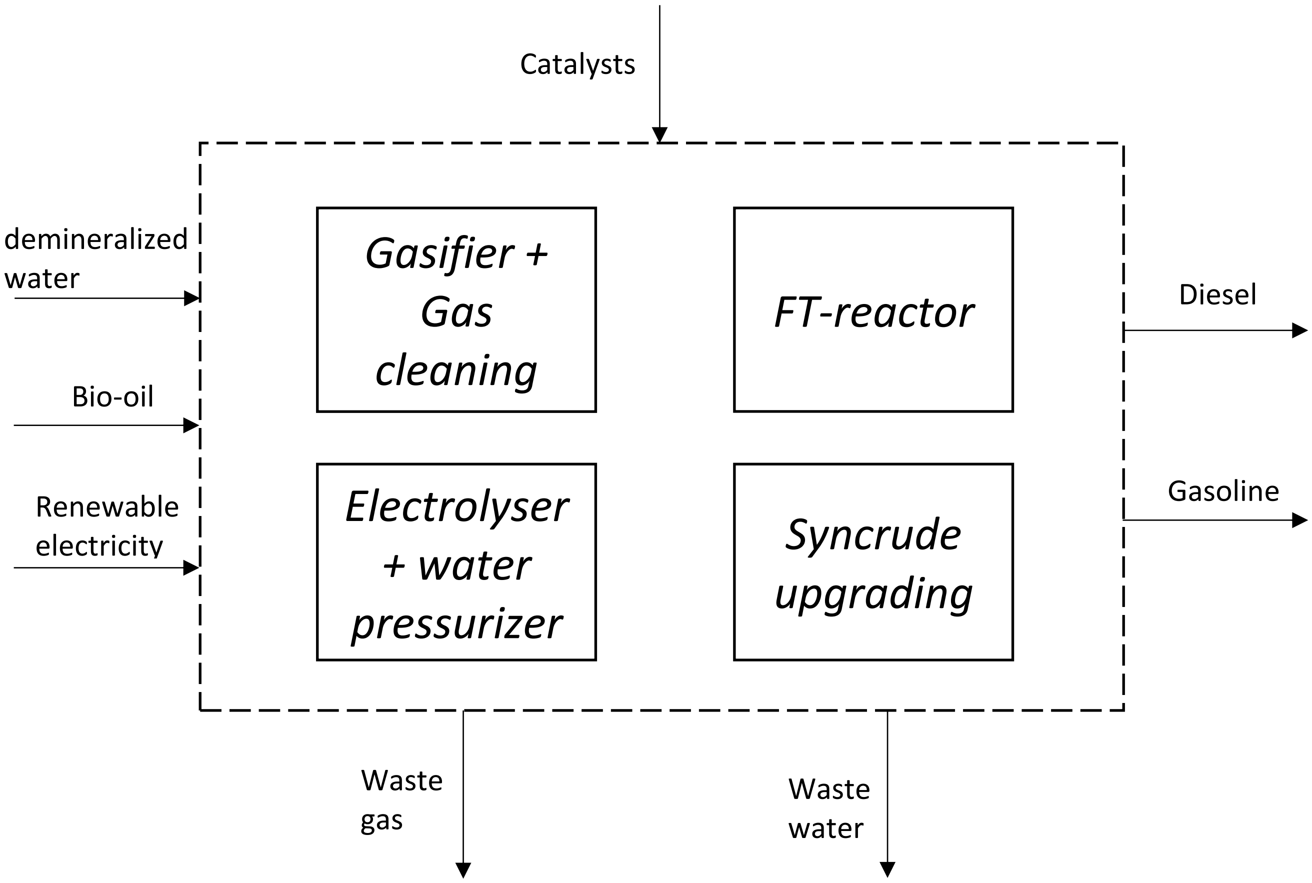

Figure 14: Battery limits of the process.

3.3 description of the design

The bio-oil entering the process is meant to be gasified, to produce syngas. Bio-oil needs no pre-treatment to be able to be gasified. But cleaning of unwanted species is needed after the gasifier, since the contaminant tolerance for the FT process equipment and mainly catalysts is very low. The deionized water and electricity are both directly supplied to the electrolyzer. The syncrude formed in the Fischer Tropsch process needs to separated and worked up in a refinery type unit. Small waste gases are combusted to supply steam to a turbine to further improve the energy efficiency of the process.

3.3.1 The gasifier unit

The bio-oil is mixed with oxygen and then the bio-oil and oxygen mixture enters the gasification unit in which it is converted to synthesis gas. The oxygen equivalence ratio is selected towards maximization of CO yield. The gasifying agent is pure oxygen, coming from the electrolyzer unit. The only contaminant that is needs to be reduced is the 46 ppm of sulphur present in the initial biomass, in the form of hydrogen sulfide. A pressure swing absorber (PSA) is used to remove H_2S. On top of that a PSA system is used to separate the hydrogen and CO from the CO_2 formed in the gasifier. The final raw syngas only consists of hydrogen gas and carbon mono-oxide.

3.3.2 The electrolyzer unit

The two other feed streams are deionized water and renewable electricity. Both are supplied to the electrolyzer that will convert water into hydrogen and oxygen gas. The vast majority of oxygen is used as gasifying agent in the gasifier, while the other part is considered as excess and vent off. The largest part of the hydrogen is mixed with the raw syngas from the gasifier to supply high quality syngas to the FT reactor. Another part of the hydrogen gas produced will go to the hydrocracker unit, in which it is needed. The final part of hydrogen is considered excess.

3.3.3 The Fischer Tropsch reactor

The Fischer Tropsch reactor will convert the upgraded syngas into hydrocarbon chains, with conditions set to maximize the production of middle distillates. This is best done in a LTFT process. The highest yield of middle distillates and highest CO conversion is achieved with the operating conditions, 220 °C and 25 bar.[24] A flash unit is used to separate the light gases up to C_9 from the other hydrocarbon chains that will stay in the syncrude. Water is the major byproduct and will be separated from the syncrude in a decanter. The syncrude will go to the refinery section. The other by product are light fuel gases, which will be combusted in the turbine section, described. The water contains minor mol fractions of the hydrocarbons formed in the order of 10^{-7}, this water can be used for steam production downstream.

3.3.4 Refinery unit

The syncrude enters the refinery unit. Three distillations columns are used in the model. In reality this could be achieved by one distillation column, but it was done in this way to make the modelling simpler. Four different hydrocarbon ranges can be observed in the syncrude. These are the light fuel gasses, the gasoline range, the diesel range and waxes. The first column separates the gasoline and flue gases from the diesel and the waxes. The second column the flue gasses from the gasoline. Lastly the third column will separate the diesel and the waxes. The waxes are sent to the hydrocracker unit, where in the presence of a catalyst and hydrogen the long wax molecules will be split into the three other groups, with the focus being toward the middle distillates diesel and gasoline. The diesel and gasoline are the final products. However, these diesel and gasoline molecules are almost only alkanes, which need further treatment to change the structure and make up a mixture that is used as commercial gasoline and diesel. That is beyond the scope of this thesis. That is why the battery limit is set at the raw forms of gasoline and diesel. Both are valuable products and can be mixed in with the other constituents to be useable, this can be done in a “classic” refinery. The fuel gas will be fed to the turbine section for combustion.

3.3.5 fuel gas combustion in turbine

The turbine is used to improve the energy efficiency of the process. The fuel gas from the FT section and the hydrocracker section are completely combusted with air, water and CO_2 are formed. This high-grade heat will be used to heat up pressurized water to steam, this water is the clean water stream that came out of the FT reactor and was then separated from the syncrude. The steam in its turn will be sent to the actual turbine, which will convert the mechanical energy delivered by the steam on the rotor of the turbine to electricity.

3.4 block diagram

In the next chapter the model will be thoroughly explained per section. Block diagrams will be presented in each respective chapter with the streams and their specifications.

3.5 Thermodynamics and kinetics

3.5.1 Kinetics

In the BoD phase, the kinetics were used to find the CO conversion in the FT reactor of the produced syngas. A simplified LHHW kinetic model was used to calculate the CO conversion of the produced syngas for a cobalt catalyst. With Diesel being the most wanted product, the choice was made to use a LTFT process with a cobalt catalyst. Hamelinck et al. [52] found the following simplified kinetics for a cobalt catalyst in the LTFT range:

Cobalt (220-240):

$$r_{FT}CO = \frac{\alpha P_{CO} P_{H_2}}{(1+\beta P_{CO})^2} \qquad \text{(Eq. 3.1)}$$

$$\alpha = 10^{10} \exp\left(\frac{-115}{RT}\right) \; mol \cdot (s \cdot kg_{cat} \cdot bar^2)^{-1} \qquad \text{(Eq. 3.2)}$$

$$\beta = 3.5 \cdot 10^{-23} \exp\left(\frac{192}{RT}\right) \; 1 \cdot (K \cdot bar)^{-1} \qquad \text{(Eq. 3.3)}$$

The kg in the expression for α refer to per kg of catalyst. The SI units for inputting LHHW kinetics into AspenPlus are Pa for the pressure instead of bar. So this needs to be converted, by dividing the pre-exponential factor of α with 10^{10} and that of β by 10^5. The other required SI units are J instead of kJ, so the numbers inside the brackets of the exponents need to be multiplied by a factor 10^3. The value of R is taken as 8.314 $J \cdot mol^{-1} K^{-1}$.
The form in which the kinetic factors have to be input in Aspen looks as follows:

$$K = \exp(A) \cdot \exp\left(\frac{B}{T}\right) \cdot T^{c} \cdot \exp\,(DT) \qquad \text{(Eq. 3.4)}$$

By putting the expression of α into this form the following inputs for A and B are found:

A = ln (1) = 0 and for B = (-115000 / 8.314) = -13832

Doing the same for β yields:

A = ln ($3.5 \cdot 10^{-28}$) = -63,22 and for B = (192000 / 8.314) = 23093

This is the input for the forward reaction. The reaction was assumed to be completely irreversible, so this is almost all the input needed for Aspen. The last input needed can be found in equation 3.1, which shows the exponents of the partial pressures of components CO and H_2. These are displayed in the table below:

Table 4: Exponent value of CO and H_2 for input in Aspen.

Component for α	Exponential
CO	1
H_2	1
Component for β	
CO	2
H_2	0

By modelling this in a CSTR reactor a CO conversion of 80% was found, which is in agreement with values found in literature.[53]

<u>3.5.2 Thermodynamics</u>

Thermodynamics were used to optimize the conversion of bio-oil to a high CO yield in the gasifier by varying the SC and OER ratio. This will be explained thoroughly in the next chapter. The same is true for the thermodynamics used to calculate the separation of the desired hydrocarbon ranges for the various products formed.

3.6 pure component properties

The pure component properties are given in Appendix C.

3.7 basic assumptions

To help simplifying the process where needed, without losing too much accuracy, assumptions were made. The main assumptions, which require more context, will be explained in this part of the basis of design.

3.7.1 Capacity

The plant receives 5000 kg of bio-oil per hour. Assuming yearly plant operation of around 8000 hours, this equal 40 kton of bio-oil per year. Assuming an overall FT process efficiency in terms of carbon conversion, based on the preliminary literature findings, of 60%, this would yield 24 kton of gasoline and diesel in a year. According to the CBS, a statistics bureau in the Netherlands, the total production of oil refineries is around 5000 kton per month.[54] Meaning around 60000 kton per year. Meaning that the contribution to the entire market would be close to 0.039%. This means that it will definitely not overfeed the market and that there are plenty opportunities to mix the produced diesel and gasoline.

3.7.2 Feedstock and product specifications

Deionized water:

Ions and minerals that are naturally found in fresh water are unwanted contaminants when it comes to electrolysis. The ions can have more favorable redox potentials interfering with the main wanted reaction, but also damage the electrodes and cause corrosion. That is why clean water is needed as input for an electrolyser. The best way to measure the amount of ions present is by determining the conductivity of the water. The American Society for Testing of Materials has set boundaries to distinguish between different water qualities.

Table 5: Water quality classification ASTM.[55]

Measurement unit	Type I water	Type II water	Type III water	Type IV water
Resistivity ($M\Omega cm^{-1}$)	> 18	> 1	> 4	> 0.2
Conductivity (μScm^{-1})	< 0.056	< 1	< 0.25	< 5.0
pH at 25°C	N/A	N/A	N/A	5.0 – 8.0
Total Organic Carbon (TOC) ppb or μgL^{-1}	< 50	<50	< 200	N/A
Sodium (ppb)	< 1	< 5	< 10	< 50
Chloride (ppb)	< 1	< 5	< 10	< 50
Silica (ppb)	< 3	< 3	<500	N/A

AWE usually has a conductivity tolerance of about < 5 $\mu S \cdot cm^{-1}$, meaning that type II water can be used. For PEM electrolysis this is already lowered to < 0.2 μScm^{-1}, meaning that is has to be grade I water.[56] Opposed to PEM- and AWE electrolysis the water in SOEC electrolysis reacts as steam. Meaning that the ions which are present in the water will stay behind as the water is heated and vaporizes. The metal ions will stay behind and the vaporized water is ready for electrolysis. This means that a lower grade of water can be used than for the other two electrolysis types, lowering the OPEX. The metals will foul the pipelines that supply the steam to the electrolyser though. To minimize this ultrapure water is needed. In the ASTM standards for laboratory reagent water, type IV water can be used for SOEC electrolysis.

Bio-oil:

The bio-oil is produced from pinewood. The Pinewood tree is a common tree in the Netherlands and can mostly be found the provinces Drenthe, Brabant and Gelderland. But the pinewood comes almost entirely from the United states and is delivered as wood pellets. The pyrolysis oil derived from pinewood has the following specifications:

Table 6: Proximate analysis pyrolysis oil from pinewood.[15]

Proximate analysis	**Wt%**
Moisture (a.r.)	21.1
Solids (a.r)	0.01
Ash (dry)	0.09

Table 7: Ultimate analysis pyrolysis oil from pinewood.[15]

Ultimate analysis	**ppm**
C	$574 \cdot 10^3$
H	$66 \cdot 10^3$
N	$< 1 \cdot 10^3$
S	46
P	1.1
Sb,Cr,Mn,Sr	< 1
Pb	1.3
Se	2.4
Ca	6.4
Mg	2.1
Fe	0.7
Na	6.1
Al	3.9
K	8.7
Zi	9.5

Not every tree is the same and has the same content, but the numbers observed in tables 6 and 7 give a good indication of the average quality and composition of the bio-oil found by Leijenhorst et al. The FT process is very sensitive for contaminants, the tolerances for the most important contaminants are displayed in table 8.

Table 8: Contaminant tolerance FT process.[13]

Contaminant type	**FTS tolerance (ppm)**
Particulate matter	Non detectable
Tars	< 0.01
Sulfur species (H_2S)	< 0.01
Nitrogen species (NH_3)	< 0.02
Alkali compounds	< 0.01
Halides (HCl)	< 0.01

As can be seen from comparing table 7 and 8 the concentrations of some of the contaminants are too high and will need to be removed. The contaminant concentrations in the product gas after gasification are the ones that matter, which will change significantly.

The operating conditions of the chosen gasifier also play a large role in the contaminant levels. The different cleaning techniques were already discussed in chapter 2. The next chapter will present how the cleaning is achieved in this thesis, but it is convenient for the reader to already see the quality of the biomass and the standards it has to meet before entering the FTS.

Diesel commercial specifications:

The commercial specifications of diesel can be specified in more than one way, but the most used are as follows:

Table 9: Commercial specifications diesel.[57]

Property	Optimal/boundary value
Cetane number	40
Flash point (°C)	52
Water and sediments (%vol)	0.05
Kinematic viscosity (mm2·s^{-1} at 40 °C)	1.9-4.1
Density (kg·m^{-3})	876
Ash %	0.01
Sulfur %	0.025

The diesel produced from the biomass will have a high cetane number, since alkanes are the primary molecules produced. Also, the sulfur content will be very low, since the sulfur was almost completely removed in an earlier stage.

Gasoline commercial specifications:

Table 10: Commercial specifications gasoline.[58]

Property	Limits
Octane number	87 – 94 <
Flash point (°C)	-23
Kinematic viscosity (mm^{2}s^{-1} at 40 °C)	0.72
Density (kgm^{-3})	715-770
Lead (gL^{-1})	Max 0.013
Sulfur (%wt)	Max 0.0080
Benzene (%vol)	Max 3.5
Oxygen content (%vol)	Max 5.5-11.0

The gasoline produced from the biomass will have a high octane number. The sulfur and lead concentrations will be extremely low and the same holds for the oxygen and benzene content. Oxygen and benzene rich molecules will be mixed in by other refineries.

3.7.3 Location:

As is clear from the introduction the plant will be based in the Netherlands. Most of the pyrolysis oil production is in Hengelo, the eastern part of the country. Almost all the refineries in the Netherlands are near the port of Rotterdam. Also, the new Haringvliet hybrid park will be situated in de Van Pallandtpolder in South-Holland, which is also very close to the coast and very close to Rotterdam. The logical choice is thus the choice of Rotterdam Harbour. It is close to the hybrid renewable energy park, it is an industrial area full of refineries, it is very accessible by land, rivers and the sea. Fortunately, the Netherlands is not a big country, around 200 km separate the bio-oil production site and the plant. This distance can be travelled in a short amount of type by most types of transportation.

3.7.4 In and out streams

Just as for the block diagram, the in- and out-streams will be discussed in more detail in the next chapter.

3.8 Economic margin

In the BoD phase the calculation of the margins is a very simplified and best-case scenario process. It is the amount of product produced per year times its selling price from which the costs of the raw material and its price are subtracted. The fixed factor is the 5000 $kg \cdot hr^{-1}$ of bio-oil. Its price is €250$\cdot ton^{-1}$.[15] The class IV water is basically demineralized water, so that price will be taken.[59] The flowrate of the water is based preliminary calculations performed and assuming an electrolyser efficiency of 80%. No data could be found on the price of the specific produced diesel and gasoline. The price at the pump of renewable diesel and standard gasoline from Shell was taken as reference. [60, 61] To find the proceeds price per unit the excise duty and taxes, where removed from the pump price. To find the price per ton the densities of diesel and gasoline from tables 9 and 10 were used. The flowrate of diesel and gasoline combined will be taken as 60% of the biomass flowrate, divided equally. Later on, it will be seen that production of them both is not the same. The preliminary costs look as follows:

Table 11: Economic margin calculations.

Feedstock incoming				Product leaving			
Chemicals	**Flowrate (t/yr)**	**Price (€/t)**	**Cost (M€/yr)**	**Chemicals**	**Flowrate (t/yr)**	**Price (€/t)**	**Proceeds (M€/yr)**
Bio-oil	40.000	250	10.00	Diesel	12000	1293	15.516
Water	36.040	1	0.036	Gasoline	12000	932	11.184
Total costs			10.036 (M€/yr)	Total sales			26.700
Margin							16.7 (M€/yr)

An annual maximum profit of 16.66 million euro is possible.

Chapter 4

The model

This chapter will present the model that was designed to simulate the process. The program AspenPlus version 8.8 was used towards this goal. Process simulation is a very powerful engineering tool. The performance and operation of a complicated chemical process can be studied, without the cost and time needed for pilot plants and laboratory experiments respectively. Nowadays powerful process simulation packages and programs exist, which simulate reality closely. The engineer can acquire information about the mass and energy balances, try different unit sequences and use sensitivity analyses to see how differing certain parameters influence the process, all from his or her laptop. Even though the kinetics and thermodynamics of real-life are sometimes hard to capture, or even unknown, a solid first estimate can be found. The accuracy depends on many factors, the most important ones however are the property data used and the thermodynamic model chosen. Process modelling can even be applied to existing processes, to find areas of improvement and try different configurations.

After the extensive literature review in chapter 2 and the preliminary design specifications of chapter 3, the proper foundation was set for the design of the model. The model needs to integrate three main components in this thesis. The renewable electricity powered electrolyser, the gasifier and the upgrading of the syngas to the desired prodcuts. The model is distributed in 5 sections. These are the gasifier and cleaning, the electrolyser, the Fischer Tropsch reactor, the refinery and the turbine. Each of the sections will have a similar structure. First the specific type of reactor or unit will be chosen and justified, based on the options presented in the literature review. After that, a magnified section of the respective unit will be presented and after this the streams, model inputs and considerations will be explained. Assumptions made during the modelling will be presented where needed. Some sections of the model are supported by Excel or Matlab calculations. When this is the case, these will also be explained.

Figure 15 shows a screenshot of the entire process, made in AspenPlus. As can be seen, the simulation is divided into blocks, the squares with hierarchy written inside. This is done to have a better overview of each section and have an overall better overview.

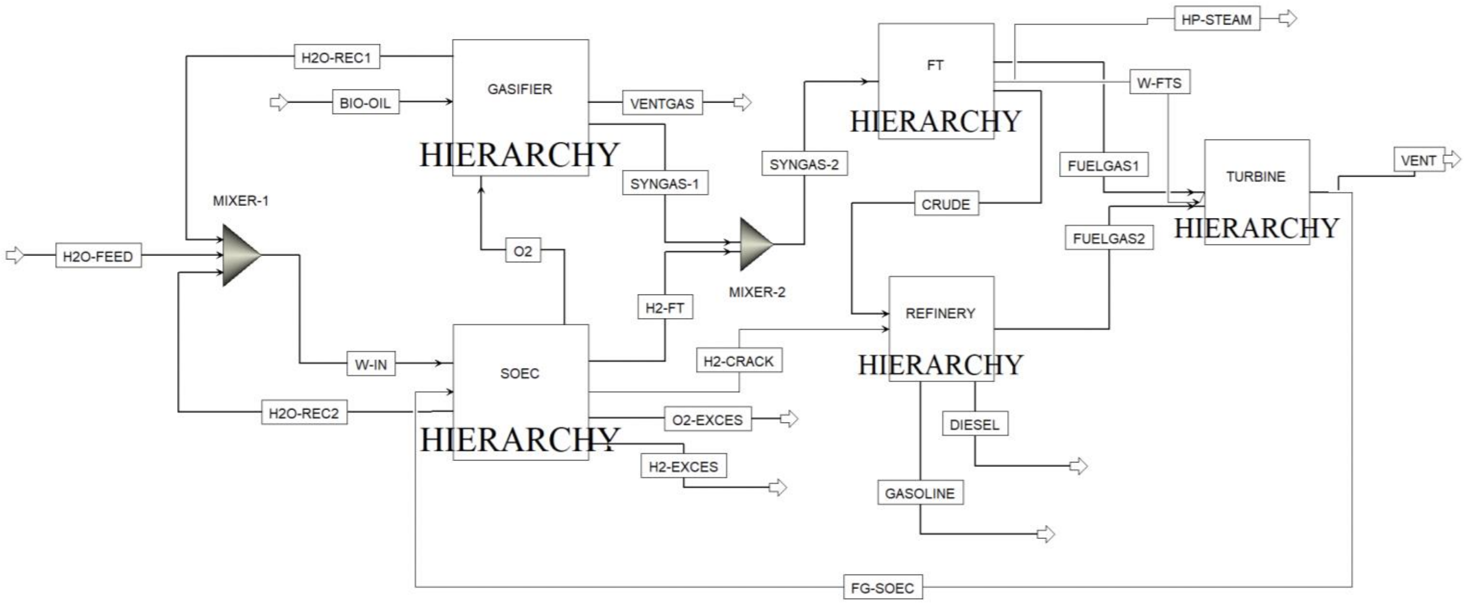

Figure 15: Screenshot entire model.

4.1 Gasifier section:

The first unit that is being modelled is the gasifier. The gasifier is the recipient of the fast pyrolysis oil, which forms the basis of this process.

Based on the information in section 2.1 in the literature review, the choice has been made to use an Entrained Flow (EF) gasifier. This has the following arguments.

- Used for large capacity operation.

In this thesis the operating capacity is equal to roughly 24MW_{th}, but the EF gasifier has the potential for even larger operating capacity >> 100 MW_{th}. The demand for the products will remain very high in the upcoming decades, if the process is to grow, the EF gasifier can easily handle the throughput for the new demand. The large scales also allow for more economical production of biofuels.

- Little pre-treatment needed.

The bio-oil feed can be considered a semi slurry. Consisting of different solid hydrocarbons suspended in the moisture present in the biomass, with small amounts of ash. This can directly be supplied to the EF gasifier.

- Good heat integration with the process.

The EF gasifier will operate semi-adiabatically. The combustion reactions provide large amounts of high-quality heat, which can be integrated with the heat demanded by the SOEC electrolyser or other parts of the process.

- Little tar production.

The FT process is very sensitive to any type of contaminant. Tars are one of the most difficult and costly ones to clean from the syngas. The relatively high temperatures reached, due to the semi-adiabatic operation in the EF, promotes the disintegration of the tar molecules. Meaning that most of the molecules that would be considered tar are already converted to either CO or CO_2 and will not cause the damaging effects of tars in the downstream equipment.

Figure 16 displays a screenshot of the gasifier section as modelled in AspenPlus, it will be explained step by step.

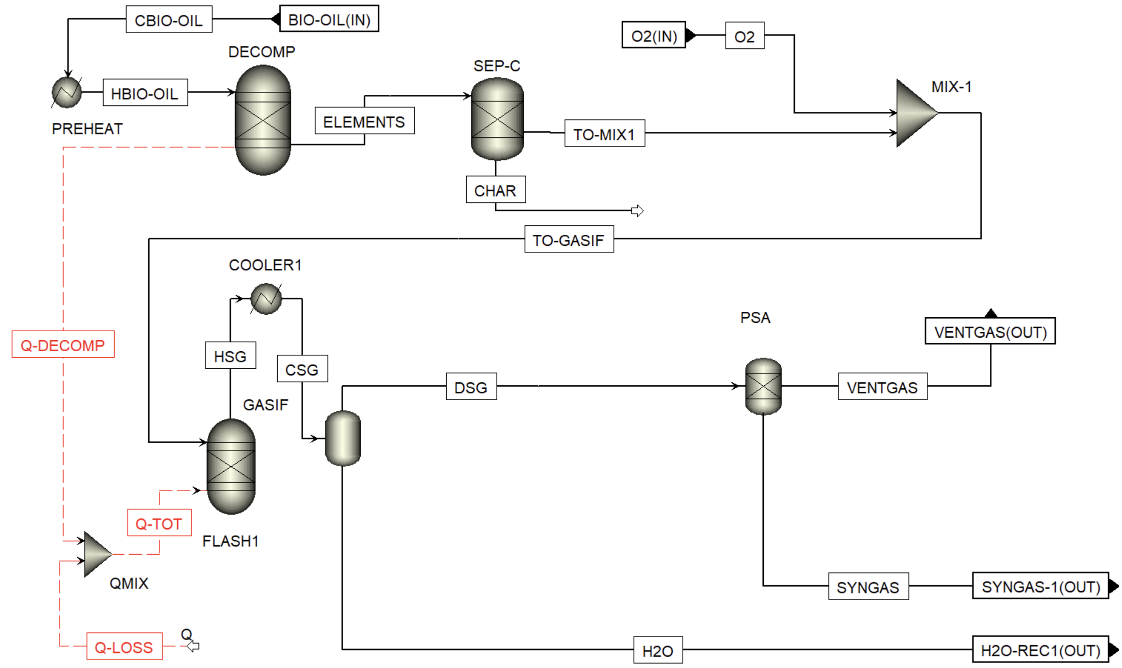

Figure 16: Screenshot model gasifier section.

As could be read in chapter 3 the pyrolysis oil is derived from pinewood. The composition of the bio-oil was retrieved from experimental data of Leijenhorst et al. They conducted the proximate and ultimate analysis on bio-oil received from the BTG fast pyrolysis plant, the results were displayed in tables 6 and 7 in section 3.7. The bio-oil received, comes from 7 different containers, the average values of these were taken, for highest data accuracy. Firstly, the bio-oil composition and its input into Aspen will be explained. Secondly, the gasifier modelling process and simplifications applied. Lastly the cleaning of the syngas will be addressed.

4.1.1 Defining and estimating properties of bio-oil

One of the main powers behind the software of Aspen Plus is that it has an enormous database of thermodynamic properties for chemical molecules. It are these properties that allow for detailed mass and energy balance calculations and identifying chemical behavior. Inputting the molecules that one expects to have present in the model is the starting point, the program will now identify the molecule and will access its properties from the database.

Bio-oil is a very general term for a product retrieved from the fast pyrolysis of biomass. Since the biomass source differs greatly and so does the resulting bio-oil, no fixed configuration of bio-oil is available in Aspen. To be able to use properties, the bio-oil will have to be defined manually.
It could be seen from the proximate analysis, that the bio-oil is roughly 21.1 wt% water and very small amounts of solids and ash are present. The rest is made up of volatile matter, which is composed of a large number of different hydrocarbon molecules. All of these come from

the decomposition of lignin, hemicellulose and cellulose. Since the gasifier operating conditions will be able to break down the majority of these molecules to only CO_2, CO and H_2, the main concern to get right is the amount of carbon, oxygen, hydrogen and the contaminants present in the bio-oil, since these will dominate the properties. These amounts can be found from the ultimate analysis.

Properties section

The starting point is defining the bio-oil in the properties. By classifying its type as a "non-conventional" it becomes available to the system. All the other relevant molecules are added as well, an important one is to define carbon in the solid phase as well. In the "components specifications", bio-oil is once again defined as non-conventional. Next up is the selection of the "methods" in the properties part. The "PR-BM" method is chosen, which stands for the Peng-Robinson equation of state with Boston-Mathias modifications. The PR-BM method works well with ideal hydrocarbon gas mixtures.

The last step in the properties part is to define the properties of the non-conventional component, which only is bio-oil. The enthalpy is set to "HCOALGEN", the density is set to "DCOALIGT". This asks for three datasets, the "PROXANAL, ULTANAL and SULFANAL". Which are all available for the bio-oil used. Now the properties section can be run, to fixate all of the selected options. Next up is the simulation section.

Simulation section

In the first part of the simulation section, under the "setup" map "specifications" can be selected. Here the stream class is changed to "MCINCPSD". Now the program can recognize and work with three different types of stream classes. "MIXED" has all of the molecules that are in the vapor or liquid phase. "CIPSD" holds all the molecules present in the solid phase. Lastly "NCPSD" contains all the non-conventional molecules. This step is needed for the program to be able to mix and process these streams together.
Now the stream BIO-OIL can be drawn in the flowsheet. By clicking on the stream, the input of the stream can be provided to the program. Under the "NC", non-conventional tab, finally the composition of the stream can be defined. Like was said earlier the proximate and ultimate analyses are used to do this. In the "component attribute" section, the following data is inputted for the PROXANAL, ULTANAL and SULFANAL:

Table 12: PROXANAL input.

PROXANAL	Moisture	Fixed Carbon (FC)	Volatile matter (VM)	Ash
	21.1	0.01	99.99	0

Table 13: ULTANAL input.

ULTANAL	Ash	Carbon	Hydrogen	Nitrogen	Chlorine	Sulfur	Oxygen
	0	57.49	6.6	0.1	0	0.0046	35.8

Table 14: SULFANAL input.

SULFANAL	Pyritic	Sulfate	Organic
	0.0046	0	0

The oxygen for the ULTANAL is the remainder of 1-sum(all other components). The ash content found in the original proximate analysis is added to carbon, to keep the 100 wt%. Lastly the Particle Size Distribution is needed as input. It was assumed that all the particles fell under the first category, which is between 0-20 µm. The reason is that varying the particle size had zero effect on the results of the gasifier. Now it has been achieved to fully define the bio-oil in the form of sub-stream "NCPSD", but to be able to use its properties in combination with the other molecules it has to be converted in terms of "MIXED" and "CIPSD"**.**

In figure 16, incoming stream CBIO-OIL is now defined. This stream firstly comes across a heat exchanger. This heat exchanger will heat up the cold bio-oil, to 52 °C. [15]This is done to reach a viscosity of the bio-oil of 20 $mm^2 \cdot s^{-1}$. This is generally considered as the desired maximum viscosity, found for example for atomization in diesel engines. This makes the oil flow better and easier to handle. After that, the now hot bio-oil, HBIO-OIL, encounters a Ryield reactor. This Ryield reactor will be used to achieve the previously described goal of transferring the molecules from the NCPSD stream to the MIXED and CIPSD stream, where it can react with the other molecules and its properties can be used.

RYield reactor: DECOMP

This unit is used for modelling purposes. The molecules in the bio-oil are present in the NCPSD stream-class. To be able to use the thermodynamic properties of the bio-oil molecules and let them react, the atoms have to be transferred to the MIXED and CIPSD stream calls. The first thing that needs to be specified are the temperature and pressure of the reactor. These are chosen to be 500 °C at a pressure of 1 bar. The ash content was set to 0. The goal is to define the concentrations for water, hydrogen, oxygen, nitrogen, sulfur and solid carbon, the atoms come from the NCPSD stream and have the values fixed by the PROXANAL, ULTANAL and SULFANAL input. The determination of these in an ultimate analysis set-up ends at around 500 °C, that is why that temperature was chosen.

The ultimate analysis determines the weight fractions on a dry basis, but these are not the correct weight fractions for the bio-oil that enters the system, which still has its moisture. Since the moisture content is equal to 21.1 wt%, the values that were displayed in the ULTANAL table will have to be corrected with a factor 0.789. These corrected values will be the yields of the previously mentioned target molecules and are inputted in the yield reactor as basis yield.

Table 15: Input Ryield DECOMP.

	water	hydrogen	Oxygen	Nitrogen	Sulfur	Carbon (s)
Basis yield (wt fraction)	0.211	0.052074	0.282505	0.000789	$3.629 \cdot 10^{-5}$	0.453596

Water, hydrogen, oxygen, nitrogen and sulfur will be transferred to the MIXED stream and solid carbon to the CIPSD stream. The original flowrate of 5000 $kg \cdot hr^{-1}$ is now 0 for the NCPSD stream and divided over the other two streams.

Lastly the PSD tab is used to change the particle size distribution to a fraction of 0.5 in the first range of 0-20 μm and a 0.5 fraction of 20-40 μm. Which is closer to reality at this temperature but does not matter for the final amounts of the molecules transferred.

Sep C metal removal and gasifier carbon conversion

The stream "ELEMENTS" now encounters a separator. Which separates a fraction of 0.04 of C(s) from the CIPSD substream, which leaves the reactor as stream CHAR. This value is the amount of carbon that does not react in the gasifier and is found in literature[15], so 96% of the original carbon present in the bio-oil will go to the gasifier. This step is for modelling purposes only. The gasifier is modelled to consume all the carbon, meaning that separating the unreacted carbon after the gasifier unit cannot be done downstream. It has already been mentioned that the metals also need to be separated from the system. This could be achieved by for example a metal or ceramic filter or a rotating particle separator. Since modelling such a unit has no effect on the energy balances in the system, it is assumed that the metals and particulate matter present in the bio-oil, are also completely removed in **SEP-C**. All the other molecules remain in the stream and pass through the separator. The stream is now labeled as TO-MIX1.

MIX-1

Is a very simple unit, that does not require any specifications, it mixes the oxygen from the electrolyser with stream TO-MIX1, creating the final stream, which will enter the gasifier. This stream is called TO-GASIF.

Gasifier

The most important unit in this section, the gasifier. As could be seen in the literature section, three different reaction zones can be identified inside an EF gasifier. The droplet evaporation zone, the partial oxidation zone and the thermal reforming zone. Each of these zones has different kinetics, reaction rates and behavior. Modelling these three zones independently based on kinetics, which differ per biomass source, is beyond the scope of this thesis. That is why the gasifier will be modelled as a Gibbs reactor RGIBBS, just like in real life it is only one reactor, in Aspen. A few assumptions are necessary to justify this way of modelling it:

1. The gasification process is assumed to occur at steady state under quasi-adiabatic and thermodynamic equilibrium conditions.
2. Pyrolysis oil gasification occurs instantaneously, and the volatile products formed mainly consist of H_2, CO, CO_2, CH_4, H_2S, N_2, H_2O and C(s).
3. All gases are ideal and uniformly distributed in the gas phase.

The following options were used for the gasifier reactor:

- The calculation option was set to "*calculate phase equilibrium and chemical equilibrium".*
- The operating pressure was set to 7 bar, because the downstream PSA unit will operate at this pressure.
- For the phases the maximum number of solid solution phases was set to 0, the "*include vapor phase*" and "*merge all CISOLID species into the first CISOLID substream*", where ticked
- In the products tab, the "identify possible products" dot was ticked, and the hydrate check was set to rigorous. The products listed in point 2 of the assumptions were presented as possible products.
- To operate the gasifier under adiabatic conditions the heat duty was set to 0.
- In figure 16 two heat streams going to the gasifier can be seen. These represent the heat loss inside the gasifier and will quantitively be described in the next chapter. Because of the addition of these streams the reactor is modelled as quasi-adiabatic.

Two things are achieved at this point. All of the solid carbon from the CIPSD stream is converted to CO or CO_2 in the MIXED stream, every molecule is now in the same stream class and can react with the other molecules. Raw syngas is made, which consists mainly of water, CO, CO_2 and hydrogen gas.

Between gasifier and pressure swing adsorber

This part of the model can be discussed quicker and without too many details. The syngas leaves the gasifier as stream HSG, hot syngas. **COOLER1,** is a heat exchanger that will extract the heat from the hot syngas. The temperature drops 35 °C and close to all of the water is removed from the syngas in **FLASH1**, operating at 7 bars as well**.** The dehydrated syngas is sent to the next unit, the pressure swing adsorber as stream DSG. The water removed by **FLASH1** will be recycled to the SOEC electrolyser, it leaves the gasifier section as stream H2O-REC1.

Pressure swing adsorber (PSA):

The PSA unit is used to remove the H_2S, N_2 and CO_2 from the syngas. In industry this cannot be done by only one unit, but different PSA unit would be required. Nevertheless, it was modelled in this way, as a SEP unit in AspenPlus. Since the goal is to make clear that the syngas is cleaned this part of the model is not done in a lot of detail, the exact operation is assumed to be beyond the scope of this thesis. It is operated as a separator unit, called PSA. The fractions of H_2S, N_2 and CO_2 are completely removed from sub-stream MIXED by setting the value of "split fraction" to 1. These contaminant gasses leave the system as **VENTGAS.**

The now clean syngas stream, leaves **PSA** at the bottom and is ready for upgrading in the Fischer Tropsch section. The H_2 : CO ratio at this point is 0.69 : 1.

4.2 Electrolyser section

In this section the model of another integral part of the system will be explained, namely the electrolyser. The choice has been made to use a SOEC electrolyser. First the choice for this type of electrolyser will be explained. After that, the model and simulation in Aspen Plus will be explained and what assumptions were made.

Why SOEC electrolyser?

- Good thermal integration with BtL processes

The first reason for choosing a SOEC electrolyser is its capability to be integrated in this biomass to liquid process. Not only the gasifier, but the FT reactor and hydrocracking unit, create high-quality heat. The SOEC electrolyser requires high heat to operate properly. Meaning that this high-quality heat can be used to heat up the steam that will enter the electrolyser, instead of wasting it. The operation at high temperatures is the second very important reason for choosing the SOEC electrolyser.

- Due to the high operating temperatures, very favorable thermodynamics and reaction kinetics are achieved. This results in unrivaled conversion efficiencies.

High current densities can be achieved with relatively cheap electrodes, due to the favorable kinetics. Favorable thermodynamics result in overall higher efficiencies. The last argument for the SOEC has to do with higher electrical efficiencies.

- High electrical efficiencies, since heat also aids in the breaking down of the water. This results in favorable OPEX costs, which are expected to be price determining in the future. [28]

Electrolysis is the splitting of water into its constituents, hydrogen and oxygen gas, using electrical energy. Electricity is a valuable energy carrier. Thermolysis is the splitting of a substance using heat. This high temperature achieved with large amounts of heat, will assist the electricity in breaking down the water. Less electricity is required for the same production, lowering the operating cost of the SOEC electrolyser.

- Co-electrolysis with CO_2

It is not applied in this thesis, but CO_2 can be cofed with the steam in the SOEC electrolyser, directly producing syngas, this is called co-firing.[62] There are some CO_2 waste streams in this process, more on this will be seen in chapter 7 on further recommendations.

Now that it is clear why the SOEC electrolyser is chosen, it will be seen how this is modelled using Aspen Plus. On the next page a screenshot of the SOEC-electrolyser section is shown, all the streams and units will be discussed. The important units will be discussed in detail, while the less important units will be mentioned to complete the flow cycle.

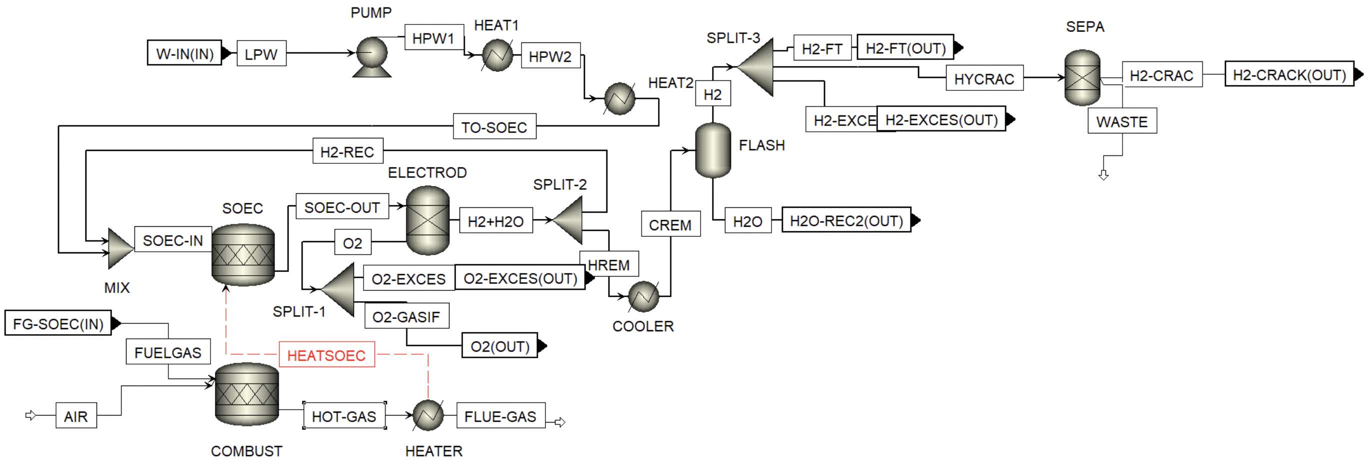

Figure 17: Screenshot Electrolyser section of model.

The electrolysis reaction of water is quite simple. The anode- and cathode reactions have been presented in the literature part. In basic terms the model must be able to separate water into hydrogen and oxygen gas.

From water to the electrolyser:

The starting point is the low-pressure water, called stream LPW. As was said in chapter three, this is already demineralized water. It enters at ambient temperature and a pressure of 1 bar. The LPW stream encounters the first unit, **PUMP**, which will pressurize the stream to 20.1 bar. High pressure inside the electrolyser further improves performance and the syngas will also be used under pressure downstream. Pressurizing a liquid is significantly less energy taxing than a gas, so the pressurization is the first action performed. The pressure of stream HPW1 is equal to 20.1 bar. After this the stream HPW1 encounters two heat exchangers. The water needs to be heat up to 700 °C, the operating conditions of the electrolyser. Two heat exchangers are used, to account for the varying CP of liquid and vaporized water. Both use the "ELECNRTL" property method, which is useful for polar mixtures and especially in electrolysis context, this property method will be used in the whole section. The input for **HEAT1** is 700 °C and 20.1 bar for the flash specifications, with a vapor fraction of 1. The input for **HEAT2** is the same except the vapor fraction specification, which is left blank. The stream leaving **HEAT2** is called TO-SOEC and meets **MIX**, where it is mixed with a recycle stream, that will be discussed shortly. No pressure drop is assumed for **MIX**, so the input is only a 0, for pressure. The valid phases remain vapor and liquid. The stream SOEC-IN, enters the SOEC electrolyser unit.

The SOEC electrolyser

The electrolyser is modelled as a stoichiometric reactor, Rstoic. The operating conditions were already said to be 700 °C and 20.1 bar, with vapor-liquid as the valid phases. The stoichiometric reactor will model only one simple reaction:

$$2\,H_2O \;\rightarrow 2\,H_2 + O_2 \qquad \text{Eq. (4.1)}$$

This is put in the reaction tab of the setup of the stoichiometric reactor. The specification type is a fractional conversion of 0.8. This is the efficiency of the electrolyser based on previous literature on the modelling of SOEC electrolysers. The intricate resistances and the effect they have on the electrolyser performance, as well as pressures are assumed to be negligible, to simplify the modelling of the reactor. In the scope of this thesis, it is important to find a value for the power consumption for the production rate and integrate the oxygen and hydrogen stream in the other units. To aid in this, the heat of reaction for water at 25 ° and 1 atm, as reference, has been specified as well. This heat of reaction equals $2.86 \cdot 10^5$ kJ·mol^{-1} and is supplied in the heat of reaction tab, the reference phase chosen is vapor.

The stoichiometric block now converts 80% of the incoming water to hydrogen and oxygen gas. The stream exiting the Gibbs reactor is called SOEC out, and contains the hydrogen and oxygen products and the unreacted water. In reality these gases would never mix and hydrogen would leave the electrolyser at the cathode and oxygen at the anode. To simulate these electrodes a separator block is used.

Separator block ELECTRODE:

The separator block lets all of the molecules present, water and hydrogen mainly, leave the separator with stream H2+H2O, except oxygen. The split fraction for oxygen is set at 0 and it leaves the separator as stream O2. The oxygen stream is fed to **SPLIT-1**, which separates the oxygen stream in a part that is used in the gasifier and another part considered as excess, streams O2-GASIF and O2-EXCES respectively. The oxygen meant for the gasifier is not cooled, since it will help to pre-heat the bio-oil stream going to the gasifier.

Heat supply to the electrolyser:

To operate the electrolyser below thermoneutral voltage, heat needs to be supplied. This heat will come from the combustion of the by-product fuel gas, of which a part is split off for the SOEC unit, more on this in section 4.5. Stream AIR and FG-SOEC are combust in unit COMBUST, the exiting stream HOT-GAS carries the heat from the combustion to unit HEATER, which in its turn supplies the heat to the electrolyser via heat stream HEATSOEC. The cooled down HOT-GAS is now called stream FLUE-GAS and exits the system as a waste stream.

Separating water from hydrogen:

The final step that needs to be modelled is the separation of the hydrogen and the water. Before this is done however, the stream is led to **SPLIT-2**. This splitter recycles 20% of the water and hydrogen mixture back to the electrolyser. This is done maintain reducing conditions and avoid oxidation of the nickel in the hydrogen electrode. [] The other 80% of the steam and hydrogen mixture is sent to **COOLER. COOLER** cools down the HREM stream to 25 °C, condensing most of the water. The now cold stream CREM is sent to **FLASH,** this unit separates the water and the hydrogen. The last block is **SPLIT-3,** which divides the hydrogen in three streams. One hydrogen stream goes to the FT unit to upgrade the syngas, the second stream to the hydrocracker and the last stream is considered excess hydrogen. Adding heat to the electrolyser:

The last part that of the SOEC-electrolyser model constitutes the supply of heat to the electrolyser. In addition to electric power, heat will also be supplied to the electrolyser. This heat comes from the combustion of the by-product fuel gas. In the next two sections 4.3 and 4.4 the origin of the fuel gas will further be discussed.

Stream FG-SOEC enters the unit and carries the fuel gas. Stream AIR contains the air needed for the combustion of the fuel gas. The unit COMBUST is a Rstoic and the settings are set to a heat duty of 0 and a pressure of 0 bar. The bocks “generate combustion reactions” is ticked, which models the complete combustion of the molecules that make up the fuel gas. The heat generated is retrieved in unit HEATER, which cools down stream HOT-GAS, coming from the COMBUSTOR, to 35 °C. The products of the combustion reaction leave the system as stream FLUE-GAS. The heat retrieved by HEATER is supplied to the SOEC electrolyser by stream HEATSOEC. In chapter 5 the amount of heat needed for the electrolyser is calculated.

4.3 Fischer tropsch synthesis section

Based on the extensive literature review and the target products, the choice has been made to use a LTFT process with a cobalt catalyst inside of a slurry bubble column reactor.
The choices for the combination of LTFT and cobalt catalyst are:

- Diesel and gasoline product

Diesel and gasoline are both considered middle distillates. Since the main goal is to produce diesel, paraffinic chains are desired. A cobalt catalyst and the LTFT conditions have a large selectivity to longer hydrocarbon chains and middle distillates. The cobalt catalyst also has a very high selectivity towards paraffins, as explained in chapter 2.

- Low water gas shift activity

The cobalt catalyst has a very low reaction rate in both ways for the water gas shift (WGS) reaction. The benefit is that the CO_2 is very limited and the available carbon is used to lengthen the chains.

- Cobalt catalyst is little affected by the presence of water

The main by-product during the FTS is water. Since the activity for the WGS reaction is very low and the active sites of the cobalt catalyst do not get de-activated or occupied by water, it is a better choice than an iron catalyst.

There are also several reasons for choosing a slurry bubble column reactor, which are:

- Large production capacity

Same reasoning as was seen for the EF gasifier is applied here. If the process were to grow to a large capacity, which is to be expected, the slurry bubble column can immediately meet the larger demand production.

- Selectivity towards longer hydrocarbon chains, large α achievable

The liquid medium makes sure that fouling particles or large chains do not de-activate catalysts, which allows for the production of large hydrocarbon chains when the conditions are tuned towards a larger α.

- Good heat and mass transfer

The FT process is very exothermic, good heat transfer is needed to keep the process safe and allow for the desired isothermal conditions to be maintained. The good mass transfer ensures high enough production per reactor volume, which is also important for the last point.

- Higher cost efficiency than the other reactors

The FT unit is used to upgrade the syngas into a mixture of different length hydrocarbon chains, called syncrude. The goal is to have operating conditions for a high selectivity towards long chains. All of the streams and units will be discussed, important parts of the model will be discussed in more detail and the assumptions used to simplify the model will be presented. Figure x shows a screenshot of the model of the FTS. The property method chosen for the FT section is again PR-BM, since the molecules involved are mainly hydrocarbons.

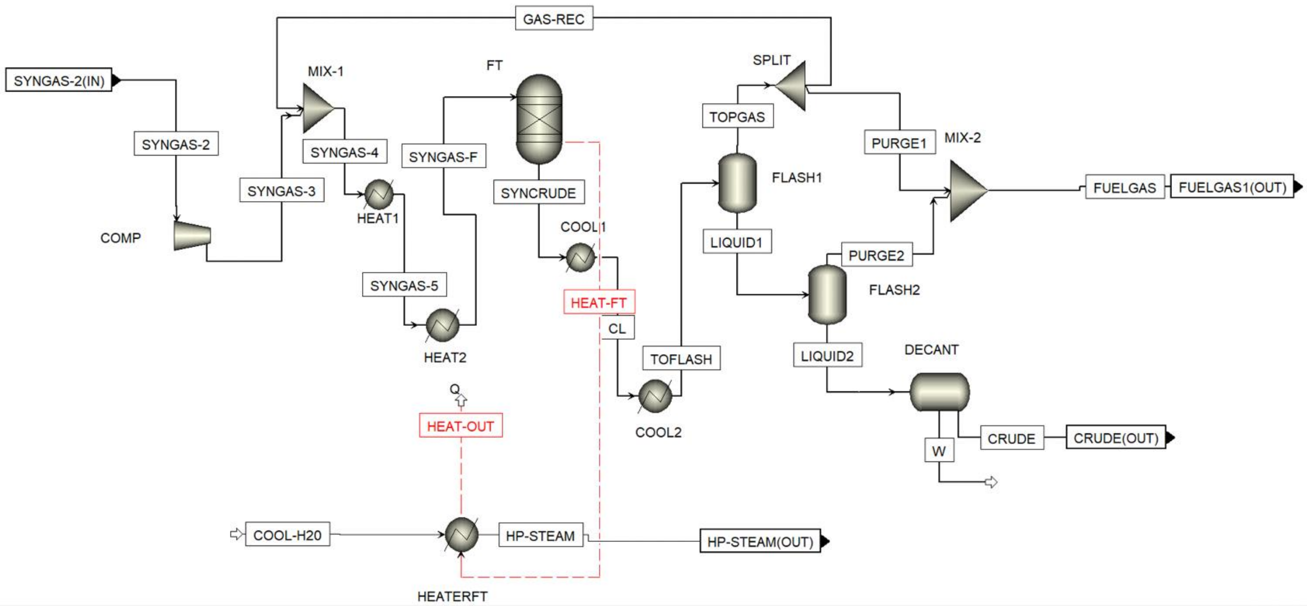

Figure x: screenshot FT section

In the main flowsheet, displayed in figure x, it could be seen that the syngas from the gasifier and the hydrogen from the electrolyser are mixed in **MIX-2,** the operating pressure inside the FT reactor is higher than for both the streams, so to only have to use one compressor, the streams are mixed beforehand. The mixed stream SYNGAS-2 is the starting point of this section. It first encounters a compressor, COMP, which will compress the stream up to 25 bar. The isentropic efficiency is set to be 75%, based on literature. Stream SYNGAS-3 encounters unit **MIX-1,** where it is mixed with a recycle stream that will be discussed shortly. **HEAT1** and **HEAT2** to heat up the syngas to reactor conditions. Stream SYNGAS-F is the final and ready version of the syngas, which will enter the FT reactor.

FT reactor:

Finding and developing a kinetic based FT model proved to be a very hard task, due to time limitations the choice was made to model the CO conversion using the standard ASF distribution.

$$\alpha = (0.2332\,\frac{\gamma CO}{\gamma CO\ +\ \gamma H_2} + 0.633)[1 - 0.0039(T - 533)]$$

Equation x was already presented in the literature section. it can be used to find the chain growth probability factor α. This correlation takes into account the effects of the H_2 : CO ratio and the temperature, which are the two most important effects on the chain growth probability. Thus varying these two in excel could give the best operating conditions for the reactor. This was done in the following way. The first term with the partial pressures of CO and H_2 can be isolated and looks as:

$$\frac{CO}{CO\ +\ H_2}$$

By calling the H_2 : CO ratio x, the following expression for H_2 is obtained. $H_2 = CO \cdot x$. substituting this into the isolated form and rewriting gives:

$$\frac{CO}{CO + CO\ \cdot x} = \frac{CO}{CO(1+x)} = 1 + (1+x)^{-1}$$

This form represents how the influence of different x values on α can easily be checked. The temperature is already in a variable form. In literature the best conditions for LTFT cobalt catalyst are between 220-240 °C, with a ratio of 2.15. Inputting 220 °C and 2.15 for x gives an α around 0.82. α increases for this ratio, when the temperature is lowered to 200 °C, to 0.8734. Since the cobalt catalyst can function optimally with the 2.15 : 1 ratio, this will be the reactor inlet ratio. The temperature however was chosen to be 200 °C, since this gave the highest α.

$$Mc_n = \ \alpha^{n-1}(\alpha - 1)$$

This equation for the ASF distribution was also already presented in chapter 2. With the now optimal α fixed, the distribution for the different carbon numbers can be calculated. n represents the carbon number. So for methane, by filling in n = 1 and the value for α, the molar fraction of methane is found. This can be done for all the molecules up to carbon number 30. Every molecule predicted by the ASF, that is larger than C_{30}, is added in the molar fraction of C_{30}. In other words MC_n is calculated for C_1-C_{29} and C_{30} is equal to 1-sum(MC_n(n=1-29)). This is done to have a total molar fraction of 1 for the ASF spectrum.

Since a cobalt catalyst is used, the products are assumed to only be paraffinic. The archetype equation for every carbon number looks as:

$$n\ CO + (2n+1)H_2 \rightarrow\ C_nH_{2n+2} + nH_2O$$

The goal now is to combine the results from the ASF distribution with this archetype equation to find the how much CO is converted towards the production of hydrocarbon n. To do this, the number found for MC_n, is multiplied by n. Doing this finds how much CO is converted per mole of hydrocarbon n formed.

By doing this for every hydrocarbon from C_1-C_{30} and adding this, the total number of CO needed to produce 1 mol of syncrude with respect to each molar fraction of the C_1-C_{30} hydrocarbons is found, for this α.

Now the final step can be done. By dividing the CO needed for hydrocarbon n by the CO needed for the total range, so 1 mol syncrude, one finds the fractional conversion of CO that has reacted towards the formation of hydrocarbon n. The following block diagram with propane n=3 as example will make it clearer.

Step 1:

Calculate M_{C_3}. this is the molar fraction of propane in the syncrude. If MC_3 = 0.15, in 1 mol of syncrude 0.15 mol propane will be present.

Step 2:

Calculate how much CO is needed for propane. So if MC_3 = 0.15, the amount of CO needed to produce the amount of propane in 1 mol syncrude is $0.15 \cdot 3 = 0.45$ mol CO

Step 3:

Find the total amount of CO needed per 1 mol syncrude. Now divide the amount of CO of propane (0.45) by the total amount of CO per mol syncrude. This is the fractional conversion of CO for propane.

The last step before this can be entered into the model is taking the overall conversion of CO into account. In chapter 3 it was found that based on preliminary kinetics calculations and literature the overall CO conversion in the FT reactor is equal to 80%.

To enter all of this information in Aspen a stoichiometric reactor was used. The temperature and pressure were set at 200 °C and 25 bar. In the next tab, the reactions tab, the previously described process in incorporated.

First the reaction equation must be put into Aspen for every n. As said before every reaction equation has the “archetype” form as presented in equation x. In step 3 the fractional equation of CO for molecule n is found, multiplying this by 0.8 takes the overall CO conversion into account. Now by selecting in the Aspen “fractional conversion” under “specification type”, the fractional conversion in terms of CO can be inputted and the syncrude composition can be calculated by the reactor.

Splitting the small unwanted molecules and left-over permanent gases:

The stream leaving the stoichiometric reactor is called SYNCRUDE. COOL1 and COOL2, cool down the syncrude to 35 °C. The goal of cooling down the syncrude is to separate the hydrocarbon products from the small permanent gases like CO and H_2 and smaller hydrocarbon products, up to C_4 from the other, now condensed hydrocarbon molecules. The cooled stream TOFLASH now enters flash separator **FLASH1,** where the previously described separation is done at 25 bar. The stream with the undesired light molecules TOPGAS meets **SPLIT,** 98% of the stream is sent to **MIX-1**, where it is mixed with the fresh syngas for another round in the reactor. This is done to increase the CO conversion and get as much syncrude as possible. The other 2% leaving SPLIT as PURGE1 is sent to **MIX-2.** This 2% is purged off to prevent buildup of the heavier hydrocarbons. Even though they are only present in very small concentrations, in the order of ppm, they can negatively affect the FT process. The second stream exiting **FLASH1** is stream LIQUID1. LIQUID 1 contains all of the desired products and a large amount of the by-product water, also a minute fraction of the previously mentioned small molecules. To get rid of these completely, **FLASH2** does the same as **FLASH1**, but the pressure in **FLASH2** is 1 bar, opposed to the pressure of 25 bar in **FLASH1**. Lowering the pressure makes the small molecules even more volatile and the concentration of them in brought down even more. The small gases leave **FLASH2** as stream PURGE2 and meet with stream PURGE1 in **MIX-2**, they leave the FT-section as one stream FUELGAS, full of small combustible molecules.

Separating the hydrocarbons from water

The last part of the FT section is the separation of the hydrocarbon mixture from the water. **FLASH2** was the second unit that already removed all of the small and permanent gases. The bottom stream leaving **FLASH2** is called LIQUID2. LIQUID2 is sent to a decanter.

Decanter:

The decanter unit is used to separate two liquids. At the specifications tab of the decanter, during the set-up, first the conditions are chosen. These are kept at 35 °C and 1 bar, just like **FLASH2**. For the key components to identify the second liquid phase only water is chosen, all the other components remain is the first liquid phase. The key component threshold for the 2nd phase was set to be a mole fraction of 0.5. This is only achieved by water. So the unit **DECANT** removes more than 99.9% of the water.

Stream CRUDE is the product of the Fischer Tropsch section. Now in the next unit, the desired products need to be extracted. The next unit is the hydrocracker.

Cooling down the FT reactor:

It was already mentioned that the FTS is a very exothermic process. To keep the reactor isothermal, it needs to be cooled, by using water. The water runs through tubes going through the reactor. These tubes can withstand high pressures. Raising the temperature of the water will cause the water to evaporate and produce steam. With increasing temperature and a constant volume, since the pipes do not expand, the pressure of the steam will also rise. In this way high pressure steam can be formed with the heat of the FT reactor.

Stream COOL-H_2O contains the cooling water. It is supplied to unit HEATERFT. Stream HEAT-FT is the stream that carries the heat duty of the FT reactor, to HEATERFT. The temperature of HEATERFT is set to 200 °C and a vapor fraction of 1 is also set. The heat from the FT reactor is thus now used to heat up the entering cooling water to 200 °C, also increasing the pressure. This high pressure steam is also an end product that will be sold of.

4.4 refinery section

In this section the crude hydrocarbon mixture produced in the FT reactor is going to be separated into the desired fractions, as is done in the refining industry. Since oil-refining is a whole industry in and of itself, most inspiration will be taken from existing, commercially well-developed processes. First the choice of the reactor type for the hydrocracker will be given and its operating conditions. After that the model will be presented.

The choice has been made to use a fixed bed reactor and a NiMo/[γ- Al_2O_3 + (Ni)/USY] catalyst. The operating conditions are set to be 360 °C and 35 bar. The arguments are as follows:

- The fixed bed reactor type hystorically most used in industry
- The fixed bed type reactor cheaper, because of easier design and operation than slurry reactor
- The fixed bed reactor large enough capacity for current process
- Feed clean enough for fixed bed

The considerations for choosing between the different types of reactors are the same as presented in part 2.4.3, where the strong and weak points of each reactor type were discussed. Since only a small amount of the crude will be sent to the hydrocracker, the heat production will not be excessive and mass transfer limitations are manageable even with the larger catalyst particles. Another requirement for fixed bed hydrocracking specifically is that the feed must be free of nickel and vanadium, which it is since it is not traditional crude oil. All these factors considered guide the choice towards the simple operating and low-cost fixed bed reactor. The operating conditions are taken from Shell, which uses a fixed bed hydrocracker towards the production of middle-distillates.

The feed for the hydrocracker are long chains of C_{21+}, with the largest fraction of C_{30}, due to the previously described correction for the ASF distribution. $C_{30}H_{62}$ is also called squalene. It was found by Saab et al. that for the chosen operating conditions and middle distillates as main yield, the chosen catalyst, NiMo/[γ- Al_2O_3 + (Ni)/USY], is the best choice.

The hydrocracker and its parameters have now been specified. But only a fraction of the crude will ever meet the hydrocracker unit. The first few separations of the stream CRUDE are done by distillation columns. The specifications for the distillation columns are found with Aspen. On the next page a screenshot of the hydrocracker section is presented in figure x.

The core of the refinery section are distillation columns to separate the crude oil and a hydrocracker unit to increase the yield of the desired products. Figure x shows a screenshot of the hydrocracker section.

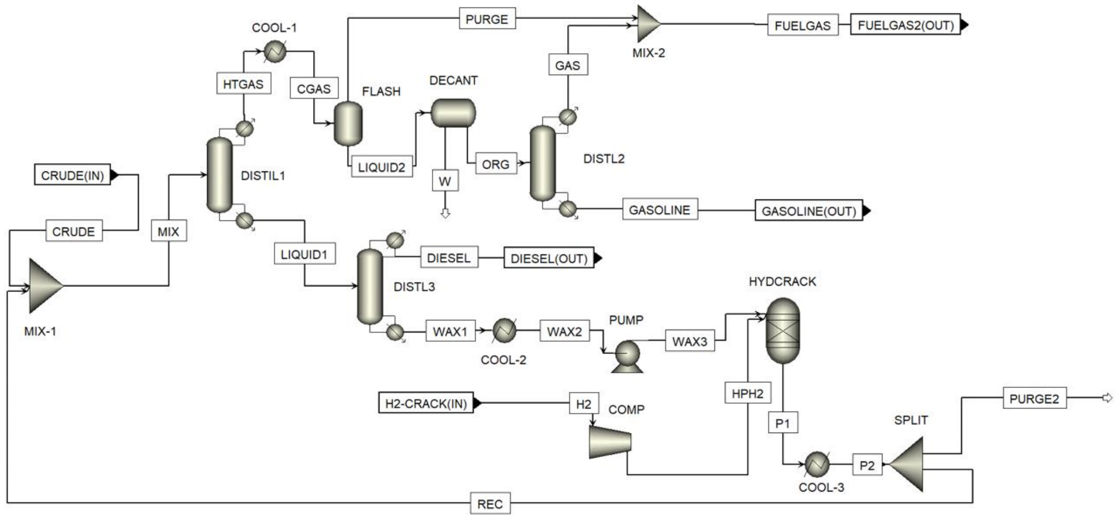

Figure x: screenshot of the entire refining section.

The starting point is stream CRUDE, which comes from the FT unit. As was already said it is a mixture of all the hydrocarbons produced. 4 different ranges of hydrocarbons will be specified, that are present in the crude, these are presented in table x:

Group	Fuelgas	Gasoline	Diesel	Wax
Hydrocarbon range	$C_2 – C_4$	$C_5 – C_{10}$	$C_{11} – C_{21}$	$C_{22} – C_{30}$

Table x: hydrocarbon ranges.

The distillation columns are present to separate the fractions presented in table x. The hydrocracker will convert the wax range to middle distillates. Stream CRUDE firstly encounters unit **MIX-1**. The recycle stream that enters **MIX-1,** will be explained in a later stage. The stream leaving **MIX-1**, first encounters **DISTIL-1**. An extensive explanation will be provided on the modelling of column **DISTIL-1**. The other two columns are modelled in the same way, their specifications will be displayed.

DISTIL-1:

DISTIL-1 is modelled as a radfrac column in Aspen. Since there is water present in stream CRUDE and the assumption is made that this is considered free water, this needs to be made available in the setup section of properties. Free water is considered as pure water, no significant amount of contaminants is dissolved in it and it is a clean waste stream. This is a valid assumption, since the other molecules involved are small concentrations of small permanent gases and hydrophobic, apolar paraffinic hydrocarbon chains.

The radfrac unit needs several input units. The first model run will use educated guesses for the radfrac unit. After that, sensitivity analysis will be used to find the optimum input values. In the configuration section the following options are chosen. The calculation type is “equilibrium”, the number of stages “15”, the condenser is set to “partial vapor”, the reboiler is a “kettle”, the valid phases are set to “Vapor-Liquid-FreeWaterCondenser” and the conversion is set to “standard”. The valid phase including free water has already been explained. The other choice that requires explanation is the condenser setting. “partial vapor” is chosen since only vapor phase distillate is assumed.

The initial guess for the reflux ratio was 1 and the distillate rate was set to around 70% of the feed rate. The initial guess for the feed stage was in the middle, stage 8. The distillate was assumed to be completely vapor and the bottom product completely liquid. lastly the pressure inside the column was chosen to be 1 bar. Running this will provide an initial separation. Now the choice must be made which groups DISTIL-1 needs to separate. The choice is made that the fuelgas and gasoline will leave the column as the distillate and diesel and wax as the bottom product. The light key is going to be C_{10}, since this is the largest molecule in the gasoline range. The heavy key is chosen to be C_{11}, since this is the lightest molecule in the diesel range.

Sensitivity analysis on the DISTIL-1 unit will be used to find more accurate estimates for the following parameters that needed to be put in the program. These are the:

- Reflux ratio
- Feed stage
- Distillate to feed ratio

These three are the variables to be manipulated. But to see the effect, a reference needs to be chosen. This reference is going to be the mole fraction of the light key, C_{10}, in the top stream of DISTIL-1, called HTGAS in the model. The optimum values for the manipulated variables are those that yield the highest mole fraction of the light key in the distillate stream.

For the reflux ratio the “MOLE-RR” function was used. The reflux ratio was varied between 0 and 3 and it had little influence on the outcome of the separation.

For the feed stage the “FEED-STAGE”, function was used. As long as the feed was above stage 13, considering 15 stages, little effect was observed.

For the distillate to feed ratio the “D:F”, function was used. This had a very strong effect on the mole frac in the distillate and a clear optimum could be chosen for the distillate to feed ratio, to achieve the desired separation. The results section will go deeper into the exact values.

Lastly all three factors where run together and this reinforced the individually observed effects. The distillate to feed ratio is the dominant determining factor.

This is the working principle used for all three distillation columns. After the third distillation column a table will provide all the specifications for all three columns.

Now the top part of the flowsheet will be discussed, following the distillate stream exiting **DISTIL-1**, called HTGAS. HTGAS contains fuelgas and gasoline, which need to be separated. To achieve this the stream is firstly cooled in COOL-1.

This cooling of the stream will remove the majority of the water, which will leave separator **FLASH**, as a part of stream LIQUID2. The imposed conditions allow a vapor-liquid equilibrium, that already makes a premature separation between the fuelgas and gasoline. But this is not on the desired level of separation. The top stream of the **FLASH** unit, called PURGE, contains all the left-over permanent gases and the majority of ethane. The PURGE stream has a very low water content and this is necessary for it to be used as a combustible stream. The PURGE stream will encounter **MIX-2,** more on this shortly.

The bottom part of the **FLASH** unit is called stream LIQUID2, which contains the water and is free of the small gases and rich in the hydrocarbons of the gasoline range. LIQUID2 is sent to the **DECANT** unit, which removes enough water to lower the volumetric water content of the gasoline below 0.5%, it is operated at 10 °C . The water leaves the system as stream W. Stream ORG is sent to distillation column 2, called **DISTIL-2**.

DISTIL-2:

DISTIL-2 is again modelled as a radfrac unit. The idea and logic behind the modelling has already been explained in the **DISTIL-1** section. The important factors to note are that the cut-off molecules are C_4 for the light key and C_5 for the heavy key. Also the condenser pressure was set at 5 bar, otherwise the mass-balance was not achieved in the column. The top stream leaving **DISTIL-2** is called GAS. It is made up of close to 70% propane and notable fractions of butane and pentane. Stream GAS flows to the earlier mentioned **MIX-2**, where it meets with the top stream of the **FLASH** unit, **PURGE**. Together they form stream **FUELGAS**, with a vapor fraction of 1, ready to be sent to the turbine unit to be combusted and produce steam in this way.

The bottom stream leaving **DISTIL-2** is GASOLINE. The shares of the hydrocarbons in the specified gasoline range is roughly equal, with cetane having the largest share. This is considered one of the end products of this thesis. High octane number, sulfur-free, paraffin rich gasoline. The liquid fraction is 1, it is ready for transportation.

This covers the top stream of the process and has explained the way towards two of the four identified parts of the crude-oil produced in the FT unit. The bottom part of the process focusses on the separation of diesel and wax. The bottom part of the process starts at the bottom product of **DISTIL-1,** stream LIQUID1. It is important to note that the fraction of water in LIQUID 1 is negligible, a mass fraction of around 10^{-9}. Stream LIQUID1 flows to the third and final distillation column, **DISTIL-3**.

Distil-3:

The last distillation column is also a radfrac column. This time the parameters distillate to feed ratio, reflux ratio and feed stage, were optimized towards separation of diesel and wax. The light key is considered to be C_{21}, while the heavy key is C_{22}. The important things to note here are that both streams are targeted to leave the column as liquids. This is done to avoid unnecessary heat loss due to overheating. Also the wax will be further processed in the hydrocracker at a temperature that is reached in the distillation column and lets the wax remain in the liquid phase. Since the amount of water is so minute and both the distillate and bottom products will be liquid, the condenser is set to “total” in the configuration section. The top product, leaving as stream DIESEL, is the second and mostly desired product, diesel. It is a very high-quality diesel, with high cetane number, sulfur free, only paraffinic hydrocarbons and ready for blending. The bottom product leaving **DISTIL-3** is the wax, leaving as stream WAX-1, contains the long hydrocarbon chains, exceeding the desired product range, which will be sent to the hydrocracker.

Before heading to the hydrocracker section, all of the relevant distillation column parameters will be presented in table x.

Column / Parameter	DISTIL-1	DISTIL-2	DISTIL-3
Condenser temp (°C)	114.9	56.5	240.8
Reboiler temp (°C)	250.9	76.7	399.8
Reflux ratio	1	0.05	2
Distillate : Feed	0.57	0.151	0.82
Feed stage	10	2	10
Number of stages	15	15	15
Distillate phase	Vapor	Vapor	Liquid
Bottom phase	Liquid	Liquid	Liquid
Free water present	yes	yes	No

Table x: overview distillation column specifications.

WAX-1 is sent to unit **COOL-2,** which will cool the stream down to the reactor temperature of 360 °C of the hydrocracker. It is now called stream WAX-2. Stream WAX-2 is sent to unit **PUMP**, which will raise the pressure of the liquid stream to that of the hydrocracker reactor, 35 bar. The efficiency of unit **PUMP** is assumed to be 80%. The stream is now called WAX-3 and will enter the hydrocracker unit, **HYDRCRACK**. The other requirement for a hydrocracking process is the presence of hydrogen. Stream H2 is the amount of hydrogen produced in the electrolyser, to be used for the hydrocracking. It is compressed by unit **COMP**, to 35 bar, which are the reactor conditions. **COMP** has an isentropic efficiency of 75%. The streams leaves **COMP** as HPH2. The hydrogen is not preheated, since in terms of mass flow it is around 120 times smaller than the WAX3 stream, so it will heat up almost instantly when entering the reactor. A unit is safed in this way and the compression also raises the temperature.

HYDCRACK:

The hydrocracking is a process that does not speak for itself. The molecules present in the wax will be catalytically split and the free radicals will be filled by the hydrogen molecules present. Two factors need to be determined to model the hydrocracker unit.

1. What is the product distribution of the hydrocracking process at the conditions used?

This first part can be found in literature. Article [] reports that at 35 bar and 360 °C, the mass yields of propane, octane, cetane and C_{23+} are known, presented in figure x. It is an assumption that only these molecules are formed, but these are the relevant molecules for this process and will be the dominant products, since the operating conditions are chosen in this way. These molecules are selected as being the "representatives" of the yields for the hydrocarbon ranges given in figure x.

Table 2. Hydrocracking of Iron-Catalyzed FT Slurry Bed Reactor Wax at 3.5 and 7.0 MPa Using a 0.55 h^{-1} LHSV and a H_2/Wax Ratio of 1500/1 L_n/L

	run no.					
	2/1	2/2	2/3	2/4	2/5	2/6
pressure, MPa	7.0	7.0	7.0	3.5	3.5	3.5
T, °C	360	365	370	350	355	360
C_{23+} conversion, wt %	26	37	56	34	50	84
yields, wt %						
C_1-C_4	1.6	2.2	3.6	2.3	3.8	11
C_5-C_9	2.1	3.5	8.4	3.4	6.7	13
$C_{10}-C_{22}$	22	31	44	27	40	63
C_{23+}	74	63	44	66	49	13
selectivity, wt %						
C_1-C_4	6.1	6.2	6.3	6.9	7.5	10
C_5-C_9	8.1	9.4	15	10	12	15
$C_{10}-C_{22}$	85	84	79	82	80	75

Figure x: mass yields hydrocracking.

2. Finding how much hydrogen needs to be supplied to the hydrocracker unit.

This part of the hydrocracker unit is more difficult and will be explained step by step. The eventual goal is to solve the following equation for 1 gram of wax:

$$wax + \boldsymbol{u}\, H_2 \rightarrow \boldsymbol{w}\, C_3H_8 + \boldsymbol{w}\, C_8H_{18} + \boldsymbol{w}\, C_{16}H_{34} + \boldsymbol{w}\, C_{26}H_{54}$$

u and ***w*** are the variables that need to be found.

Step 1: Defining wax

The starting point is defining what "wax" is. Stream WAX-3 is made up of different molecules. First of all the assumption is made that all the carbon present in stream WAX-3 will be converted to the 4 representatives. Since the consistency of stream WAX-3 is known in Aspen, all of the mol-fractions of the different molecules are copied into an excel file.

By multiplying the mol-fraction of each molecule with the amount of carbon atoms the molecule has and adding this up, the amount of total carbon present in 1 mol of WAX-3 can be found. The same can be done for hydrogen. The next step is to multiply the respective mol-fractions of each molecule with the molar mass of the respective molecule. Adding this up yields an average molecular weight for the molecules in WAX-3.

A fictive molecule is now created, that simplifies the consistency of stream WAX-3 into one molecule, whose molecular formula and weight is known. This molecule will be called wax, just like in equation x.

Step 2: converting 1 gram of wax

Since the yields of the four representatives are mass yields, the mass of the wax molecule will have to be used, to eventually find the molar yields. The starting point will be 1 gram of wax. Since the molar mass of wax is found in step 1, the amount of moles of wax in 1 gram is known.

To find the molar fractions the molar mass of the 4 representatives can be used, combined with the assumption that all the carbon of the wax molecule is converted. From figure x it is known that of the 1 gram of wax, 0.11 grams will be propane, 0.13 grams gasoline, 0.63 grams diesel and 0.13 grams of cerane is formed. By dividing these masses by the respective molar masses, the amount of moles of each of the representatives resulting from the conversion of 1 gram of wax is found. The mole fractions can be found by dividing the respective amount of mole of the molecules by the total amount of mole. Combining this knowledge with equation x, the following table can be set up:

		Mole	Carbon	Hydrogen
Reagents	Wax	0.002694 [1*]	26.32072[2*]	54.64144[2*]
	Hydrogen	***u***	0	2
Products	C_3H_8	0.36851 ***w***	3	8
	C_8H_{18}	0.16812 ***w***	8	18
	$C_{16}H_{34}$	0.411 ***w***	16	34
	$C_{26}H_{26}$	0.05237 ***w***	26	54

Table x: processing 1 gram of wax.

2* is the result of step 1, differs with changing wax composition. 1* is found by dividing 1 gram by the molar mass of molecule wax.

Step 3: finding the values of ***u*** and ***w***

To find the values of ***u*** and ***w*** the atom balance on carbon and hydrogen needs to be set up. From table x it can be read that on the left-hand side of equation x, only wax contains carbon. The amount of carbon is 0.002694 mole x 26.32072 C atoms per molecule is 0.0709056. By doing the same step for the 4 representatives on the right-hand side of equation x, the atom balance of carbon is found and looks as follows:

$$Carbon\ balance:\ 0.0709056 = 10.3881\ \mathrm{w}$$

w can now easily be found. The next step is setting up the atom balance for hydrogen. On the left-hand side hydrogen is present in both the hydrogen molecule and wax. Again the amount of hydrogen can be found from table x for the left hand side of equation x. The same can be done for the right hand side and the atom balance of hydrogen looks as follows:

$$Hydrogen\ balance: 0.147199 + 2u = 22.7762w$$

Since w is known, the value of u is easily found. Everything needed for equation x is now known and a varying weight amount of wax can directly be related to the amount of moles of hydrogen needed to be produced by the electrolyser and the mass yields of the representatives. The power of this will be demonstrated in the next chapter, where sensitivity analyses will be applied.

So the amount of hydrogen in stream HPH2 is now known, through the calculation of factor 2.

The **HYDCRACK** unit is modelled as a yield reactor. The operating conditions where earlier justified and were set to 360 °C and 35 bar. In the yield tab the four representative molecules were listed as product options and the conversions on mass basis of figure x were used. Adding the mol-fractions, provided by Aspen, of stream WAX-3 together did not yield 1. A correction was made by multiplying the sum of the molar fractions, with the yields in figure x. In this way no warnings were issued by Aspen.

The stream leaving **HYDCRACK** is called P1, firstly it encounters **COOL-3.** The stream is now called P2 and enters unit **SPLIT**. Unit **SPLIT** recycles 99% of P2 back to the earlier encountered **MIX-1,** where it is mixed with the incoming crude from the FT section and in this way the overall yield of the desired molecules is increased. The last stream in the section if the PURGE stream, leaving P2. In reality, the produced molecules of P2 are not strictly the 4 representatives. To avoid buildup of these unwanted molecules, the PURGE stream is used. This is also why **COOL-3** is used, to not release hot gas into the atmosphere.

This covers the refinery section of the model. The last section if the turbine section, which follows stream FUELGAS from this section.

4.5 Turbine section

Since one of the main targets of the model integration was the overall energy efficiency, the unused fuel-gases will be combusted to drive a turbine. The turbine and generator combination will produce electricity, that can be supplied to the electrolyser unit. The working principles of the reaction turbine and generator have been discussed in section 2.5. No further specification of the turbine and generator choice will be provided, since that level of detail is outside the scope of this thesis, that is why the model will immediately be explained. A screenshot of the model of the turbine section shown in figure x.

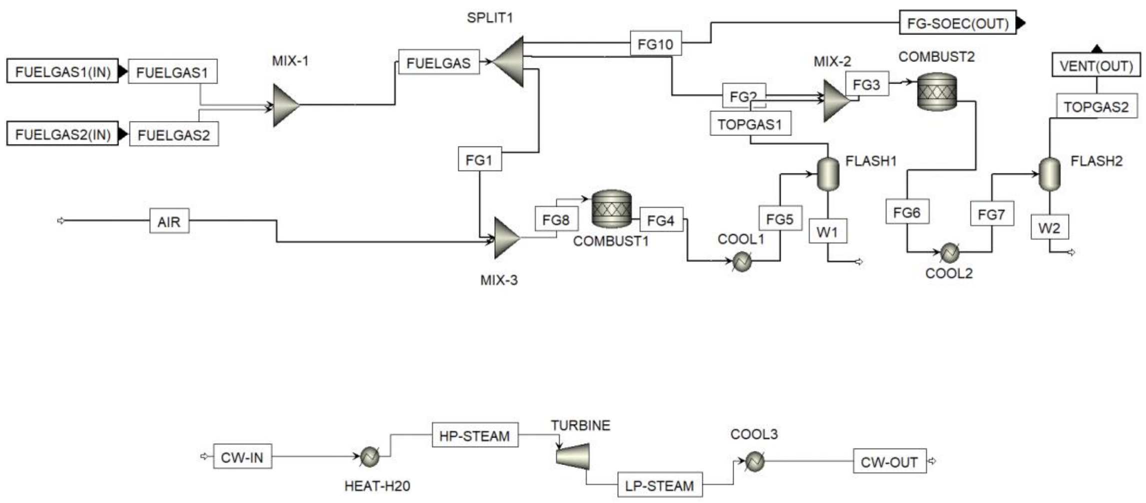

Figure x: screenshot Aspen turbine section.

This part of the model will be discussed in three sections. The first section is on the combustion of the fuel-gases which where a by-product in the FT and refinery unit. The second section covers the combustion of char, produced in the gasifier section. These two are responsible for the heating of the cold water to produce the steam used to drive the turbine. The third section is therefore the process of the actual electricity generation.

Section 1: combustion of fuel gas 1 and fuel gas 2

The composition of FUELGAS1 and FUELGAS2, have been discussed in their respective sections. Both enter the system at 1 bar and slightly above 30°C. **MIX-1** is the first unit in which both are mixed together and leave the system as FUELGAS. FUELGAS proceeds to unit **SPLIT1**, where the stream is split into FG1, FG2 and FG10. Stream FG-10 is equal 10 198.5 $kg \cdot hr^{-1}$, this fuel gas leaves the turbine section to the SOEC unit, where it is combusted to provide heat to the SOEC electrolyser. The reason forsplitting stream FUELGAS will be explained by describing how the combustion is modelled. The combustion is modelled in the units named **COMBUST-1** and **COMBUST-2** respectively. All are modelled in the same way as stoichiometric reactors.

COMBUST:

The starting point of the combustors is a stochiometric reactor. The first input Aspen needs can be found under the “specifications” tab, where the operating conditions and valid phases are chosen. The flash type is selected to be pressure and a duty input is also required. The pressure is set a 1 bar and the duty to 0 MW. The valid phases are chosen as vapor-liquid. The property method is again PR-BM, since the hydrocarbon chains are still dominant and present.

The second tab is the “reactions” tab. No reactions are put in and the tab is left at its default settings. This is done because Aspen itself provides the option of combustion in its next “combustion” tab. In the combustion tab “generate combustion reactions” is ticked and NO_x combustion product is chosen to be nitrogen dioxide, NO_2.

By running this block with the reactant and an oxidizing agent as input, the hydrocarbons will be combusted and completely converted to water and carbon dioxide.

Now that the working principles and settings of the combustion block are known, the explanation of the fuel gas combustion continues. SPLIT-1 divides the FUELGAS stream in three streams. A fraction of 0.25 of the original stream continues as FG1, 0.25 of the original stream continues as FG2 and the remaining 0.5 as FG10. There are three reasons for splitting the FUELGAS stream in three parts.

- Heat exchangers have a maximum operating temperature

If the stream is run as a whole with the described settings, the temperature of the product stream is raised to more than 1700 °C. This is too high for most commercial heat exchangers. [bron in favorieten] by dividing it in three, the temperature of the outlet streams varies between 800-900 °C.

- Little to no formation of NO_2

The second reason also has to do with keeping the temperature limited to the 800-900 °C range. Significant amounts of the polluting NO_x molecules are formed at temperatures exceeding 1204 °C. By limiting the maximum temperature this problem is also eliminated and no extra cleaning unit is needed.

- Intermediate water removal

After the heat from the product stream is extracted by the heat exchanger, the water content of the air used for further combustion is reduced. Enhancing the combustion performance in the next combustor unit.

The combusting agent is air. The composition of air is imputed according to [bron]. Table x shows the input. The minute mol fractions of argon, neon, helium and krypton have been added to the mol fraction of N_2, since these are also inerts.

Component	Mol fraction
N_2	0.79012113
O_2	0.20946
CO_2	0.000417
CH_4	$1.87 \cdot 10^{-6}$

Table x: composition of air

The air enters as stream AIR, at 25 °C and 1 bar pressure, to make the calculation simpler and since the combustors operate at 1 bar. The total amount of air needed could be found by running the fuel gas through one combustor unit and see how much the difference of the amount of O_2 was between the inlet and outlet stream. FG1 and stream AIR are both supplied to **COMBUST1**. The total combustion of all the hydrocarbons takes place. The stream exiting **COMBUST1**, FG4, contains the reaction products CO_2 and H_2O, the inert N_2 and unreacted O_2. Stream FG4 is sent to **COOL1**, where the heat is extracted and the stream is cooled down to 35 °C. After this, now named stream FG5, is fed to unit **FLASH1**. Unit **FLASH1** is operated at 25 °C and 1 bar of pressure. More than half of the water present in stream FG5 is removed and leaves **FLASH1** as liquid water called stream W1. The top stream of FLASH1 is called TOPGAS1 and contains the oxygen needed for the next combustion unit.

TOPGAS1 and stream FG2 are mixed together in MIX-3 and sent to **COMBUST2** as stream FG3. The same full combustion of all the hydrocarbons takes place in **COMBUST2** and raises the temperature of the inlet stream above 800 °C. The exiting stream, FG6, has its heat extracted in **COOL2,** which again cools it down to 35 °C. The resulting stream, FG7, is fed to **FLASH2**. **FLASH2** operating at 25 °C and 1 bar, removes almost 70% of the water, leaving as stream W2. The top stream leaving **FLASH2** is called TOPGAS2 and contains the amount of oxygen needed for the combustion of the last part of the original stream FUELGAS.

Stream TOPGAS2 and stream FG10 are mixed in **MIX-3**. The resulting stream FG11 is combusted in **COMBUST3**. The temperature reached is close to 900 °C and the stream leaves **COMBUST3** as FG8. Unit **COOL3** extracts the heat from FG8, stream FG9 leaves the system.

By running the model and investigating the results from all three cooler units, **COOL1,2,3,** the total heat duty can be found. Or in other words, the heat generated by the total combustion of the fuel gas.

Section 3: Electricity generation

Now that it is known how much heat is generated, this heat can be supplied to the cold water that will be turned into steam. The cold water enters the system as stream CW-IN. The temperature of the water is 25 °C and the pressure is 1 bar. To drive a turbine the steam needs to be pressurized. Pressurizing the liquid water is much less energy intensive than firstly heating the water, that is why stream CW-IN is supplied to unit **PUMP**. The discharge pressure of **PUMP** is 5 bar, the pump has an efficiency of 80%. The stream leaving **PUMP** is now called HPCW.

HPCW enters unit **HEAT1**. The specifications for the heater unit are called flash specifications. The valid phases for **HEAT1** are “Vapor-Liquid-FreeWater”. The property method for **HEAT1** is set to STEAM-TA, since the only molecule involved is water being converted to steam. The “flash type” option is set to duty. The duty has to be specified and is equal to the total heat duty found by adding the heat duties of the coolers. By determining the target temperature for the turbine operation, the water flowrate of CW-IN can be perfectly determined. The turbine will process the steam at 5 bar and a temperature of 300 °C. The flowrate of CW-IN is thus a function of the target temperature of 300 °C and the heat produced by the combustion reactions. Stream HPSTEAM leaves unit **HEAT1** at 300 °C and 5 bar.

Unit **HEAT2** is set to 1 bar and a heat duty of 0 MW. The difference with **HEAT1** is that the valid phases are now set at “Vapor-Liquid”. This again corrects for the difference in cp value for liquid and vaporized water. The stream leaving **HEAT2** is called TOTURBIN.

Stream TOTURBIN is sent to unit **TURBINE3**. In the specifications tab of a compressor block, the “model” option is set to “turbine”. The “type” is set to isentropic. The discharge pressure is set to 1 bar and the isentropic efficiency is assumed to be 75%. The stream exiting **TURBINE3** is called LPSTEAM. LPSTEAM is sent to unit **COOL6**, where it is cooled down to 35 °C, so that it can be safely released into the environment as a waste stream. By running the model and checking the results of **TURBINE3**, it can be found that almost 5 MW is produced in the turbine.

This concludes the model set-up. In the next chapter the results of the model, model verification and sensitivity analyses on sections of the model will be applied.

Chapter 5

Results & Discussion

This chapter presents the results obtained for the model. Sensitivity analysis was applied to obtain the optimum conditions, where needed this is presented. The model is also verified, where it was possible, relative to literature. The obtained results are discussed as well.

5.1 gasifier

This section will cover the results obtained in the gasifier unit. The first part that will be discussed are the (red dotted) heat streams, which could be seen in section 4.1, leading to the gasifier. The reason why they are present and how they have been calculated will be explained. After this the variables OER and SC, will be explained regarding the model and how the final input values have been obtained. Lastly the found syngas composition will be compared to the experimental work of Leijenhorst et al.

Heat streams:

In the model three heat streams are present. QDECOMP, QLOSS and QTOTAL. Each will be explained separately. Starting with QDECOMP.

QDECOMP:

As was explained in section 4.1 the DECOMP unit is solely present for modelling purposes. In real life the bio-oil would immediately flow to the gasifier unit, where it will come in contact with the oxygen and steam. The decomp unit was used to convert the non-conventionally defined bio-oil, into parts of the MIXED and CIPSD substreams, in which all the other molecules of the system are as well.
The bio-oil was heated from 52 to 500 °C, this costs energy. Since this step does not occur in reality and this heat should not have to be added, it is considered a heat loss. To compensate for this added energy, the heat added will be removed from the gasifier. This is done via stream QDECOMP. The value of stream QDECOMP is determined by the temperature rise and mass flowrate and is calculated by Aspen.

QLOSS:

The gasifier is modelled quasi-adiabatically, its net heat duty is modelled as equal to 0. Heat integration is an important part of this thesis and will be discussed in the following chapter. Not all of the heat released in the gasifier can be captured for heat exchange purposes. That is why a 5% heat loss is assumed in the gasifier. This 5% can be calculated by using the LHV value of 17.2 $MJ \cdot kg^{-1}$, found by leijenhorst et al. The calculation of QLOSS is therefore as follows:

$$QLOSS = \frac{17.2\ MJ \cdot kg^{-1}\ * 5000\ kg \cdot hr^{-1}}{3600\ s \cdot hr^{-1}} * 5\% = \ 1.19444\ MW$$

QTOTAL:

QDECOMP and QLOSS meet in unit QMIX and continue as QTOTAL. QTOTAL is fed to the gasifier and thus embodies the heat losses in the gasifier section. Since the calculation method for the gasifier gibbs reactor was chosen to be “Calculate phase equilibrium and chemical equilibrium”, the heat duty is kept 0. All of the energy formed by the reactions inside the gasifier is now supplied as heat to the outgoing stream. So the heat formed and useable for heat exchange is stored inside the outlet stream HSG of the gasifier.
The final values of the heat streams are presented in table x:

Stream	Heat (MW)
QDECOMP	-7.16519
QLOSS	-1.19444
QTOTAL	-8.35963

Table x: heat streams.

With the heat losses fixed and the value of QTOTAL calculated by Aspen, the gasifier model can almost be run. The gasifier uses oxygen, coming from the SOEC electrolyser, as gasifying agent. Steam is also usually added to gasification reactions, to increase the H_2 yield and control the temperature inside the gasifier. That is why in the first run a stream supplying steam to the gasifier was also present. First the OER will be explained and after that the effect of the addition of steam.

OER

The oxygen equivalence ratio was already mentioned in section 2.1. For clearer visualization purposes the equation will again be shown.

$$\lambda = \frac{external\ O_2\ supply\ /fuel\ supply}{stoichiomeric\ O_2\ requirement/\ unit\ of\ fuel\ input}$$

The main question was to find a way to determine the stoichiometric O_2 requirement. Since the biomass has a unique composition and contains many different molecules. The starting point was to identify the atoms/molecules in the biomass that will react with oxygen. These where hydrogen, carbon and nitrogen. To find the amount these three present in the bio-oil, the mass fractions on dry basis and flow-stream of the bio-oil are used. Three equations can be made for the reactions of the three identified molecules with oxygen. Next to them are three equations to find the amount of mass of the respective atom in the bio-oil stream:

$C(s) + O_2(g) \rightarrow CO_2(g)$ $\qquad$ $C_{mass} = \ 0.453596\ \cdot \left(1 - \frac{CHAR}{CTOTAL}\right)\ \cdot OIL$

$H_2(g) + \frac{1}{2}O_2(g) \rightarrow H_2O(g)$ $\qquad H_{mass} = 0.052074 \cdot OIL$

$\frac{1}{2}N_2(g) + O_2(g) \rightarrow NO_2(g)$ $\qquad N_{mass} = 0.000789 \cdot OIL$

From the equations on the left side it can be seen that per C- and N-atom, two oxygen atoms are consumed. For H the opposite is true, two H atoms are consumed per oxygen atom. On the right hand side the mass flowrate of the atoms are found in kg·hr^{-1} since OIL is the bio-oil stream of 5000 kg·hr^{-1}. By combining this information and using the molecular weights of the molecules, the amount of mass of oxygen needed for the stoichiometric combustion can be found. The following three equations can be made:

$$O_{massC} = \frac{C_{mass}}{Mw_C} \cdot 2 \cdot Mw_O \qquad O_{massH} = \frac{H_{mass}}{Mw_H} \cdot \frac{1}{2} \cdot Mw_O \qquad O_{massN} = \frac{N_{mass}}{Mw_N} \cdot 2 \cdot Mw_O$$

Mw_C, Mw_H, Mw_N, Mw_O, being the molecular weights of carbon, hydrogen, nitrogen and oxygen respectively. The values were taken as:

Mw_C = 12 kg·kmol^{-1} $\qquad$ Mw_O = 16 kg·kmol^{-1},
Mw_H = 1 kg·kmol^{-1} $\qquad$ Mw_N = 14 kg·kmol^{-1},

Adding the O_{mass} values of the three seems like the answer to the stoichiometric O_2 requirement, but one last important aspects need to be taken into account. The biomass itself also contains free oxygen molecules and water, both contributing oxygen atoms to the mixture. These oxygen atoms need to be removed from the sum of the O_{mass} to find the stoichiometric O_2 requirement for the bio-oil fuel. The amount of oxygen in the bio-oil can be found with:

$$O_{mass\ bio-oil} = (0.282505 + \left(0.211 \cdot \frac{Mw_O}{Mw_{H_2O}}\right)) \cdot OIL$$

The stoichiometric oxygen requirement, O_{2_stoich}, is now equal to:

$O_{2\_stoich} = O_{massC} + O_{massH} + O_{massN} - O_{mass\ bio-oil}$, in kg·hr^{-1}.

With the help of Aspen O_{2_stoich} was found to be equal to 5538.69 kg·hr^{-1}. The oxygen input, stream O2 in the model can be varied. Equation x is now transformed to the form:

$$\lambda = \frac{external\ O_2\ supply\ /fuel\ supply}{stoichiomeric\ O_2\ requirement/\ unit\ of\ fuel\ input} = \frac{stream\ O2\ (x\ kg{\cdot}hr^{-1})}{O_{2\_stoich}\ (5538.69\ kg{\cdot}hr^{-1})}$$

The equation used for the sensitivity analysis in Aspen looked as:

$$O2 = \lambda \cdot O_{2\_stoich}$$

Before demonstrating the sensitivity analysis performed to find the optimal OER, the other important variable, SC need to be discussed.

SC:

SC refers to the steam to carbon ratio. As the name says it is the molar ratio between moles of steam supplied and moles of carbon in the fuel. It is not shown in figure x of the gasification flowsheet, but a stream STEAM was modelled, to supply the gasifier with steam. The equation used in Aspen to model the molar flowrate of STEAM was:

$$STEAM = SC \cdot C_1$$

, where $SC = \frac{mol\ H_2O}{mol\ C}$ and C_1 is the mol amount of carbon in stream TO-GASIF.

Now that the OER and SC are explained and a way to vary them is provided the most important part of the gasifier section will be discussed, which is "what is the goal of the gasifier?"

The gasifier produces syngas, which is supplemented by the hydrogen stream from the electrolyser. The only carbon-source entering the system is the bio-oil. The gasifier is modelled to convert the carbon into either CO, CO_2, CH_4 or C(s). As will be seen shortly the amount of C(s) and CH_4 formed is negligible.
Since no WGS reactor is used and the cobalt catalyst has very low activity for the WGS, the goal is to immediately get an as high as possible CO : CO_2 ratio. Since this means that the highest possible amount of CO is obtained. The amount of hydrogen formed is of lesser secondary concern. Since the gasifying agent is pure oxygen from the electrolyser, this means that a double amount of hydrogen molecules is also produced in the electrolyser, as will be seen in section 5.2, this is more than enough to upgrade the produced syngas to the desired H_2:CO ratio of 2.15. The sensitivity analyses where thus performed, to obtain the highest CO : CO_2 ratio.

To do this, the model analysis tool in Aspen was used, the sensitivity function to be more precise. Two variables were made, which varied λ and SC. First the influence of varying OEC

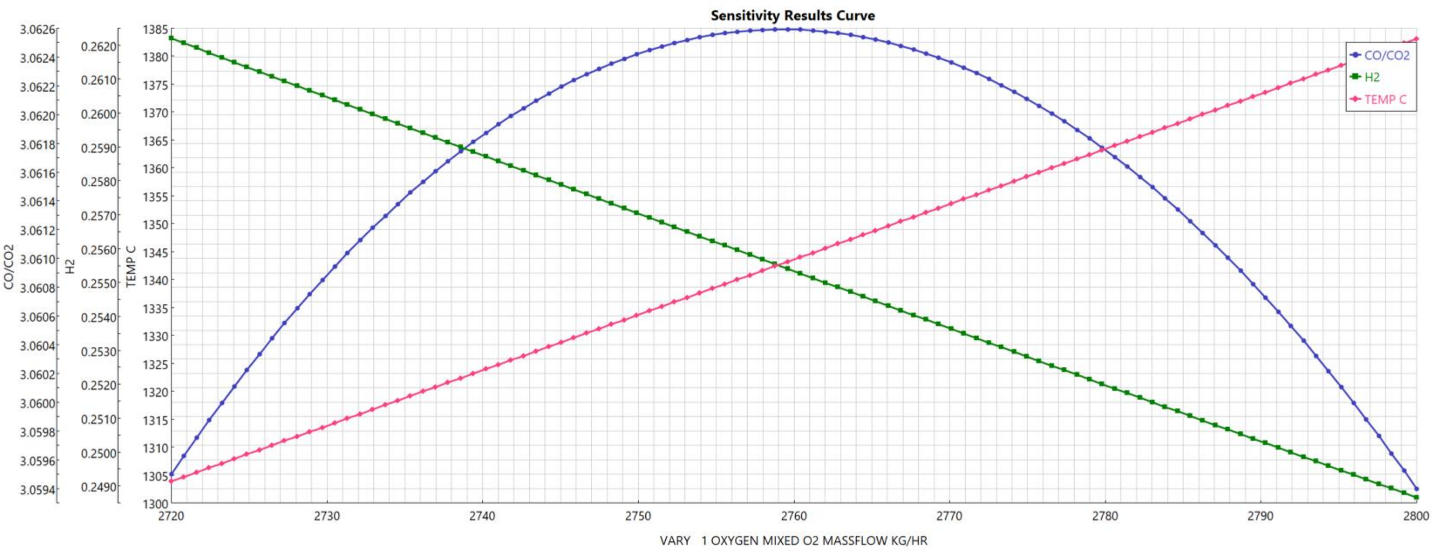

and SC separately was tested. The final plot for the influence of the OEC, without a steam input to the gasifier is shown in figure x.

The OER is varied between 0.491 and 0.506. It was observed from earlier variable limits that the top of CO/CO_2 could be found in this interval. It can be seen that the maximum value for CO/CO_2 is at 2760 kg·hr^{-1}, which is equal to an OER of 0.498. Further it can be seen that the reactor temperature increases with increasing OER and the H_2 yield decreases, as expected. The final OER value is therefore chosen to be 0.498.

With this OER value in fixed, the effect of adding steam to the gasifier was observed via sensitivity analysis. This can be seen in figure x on the next page.

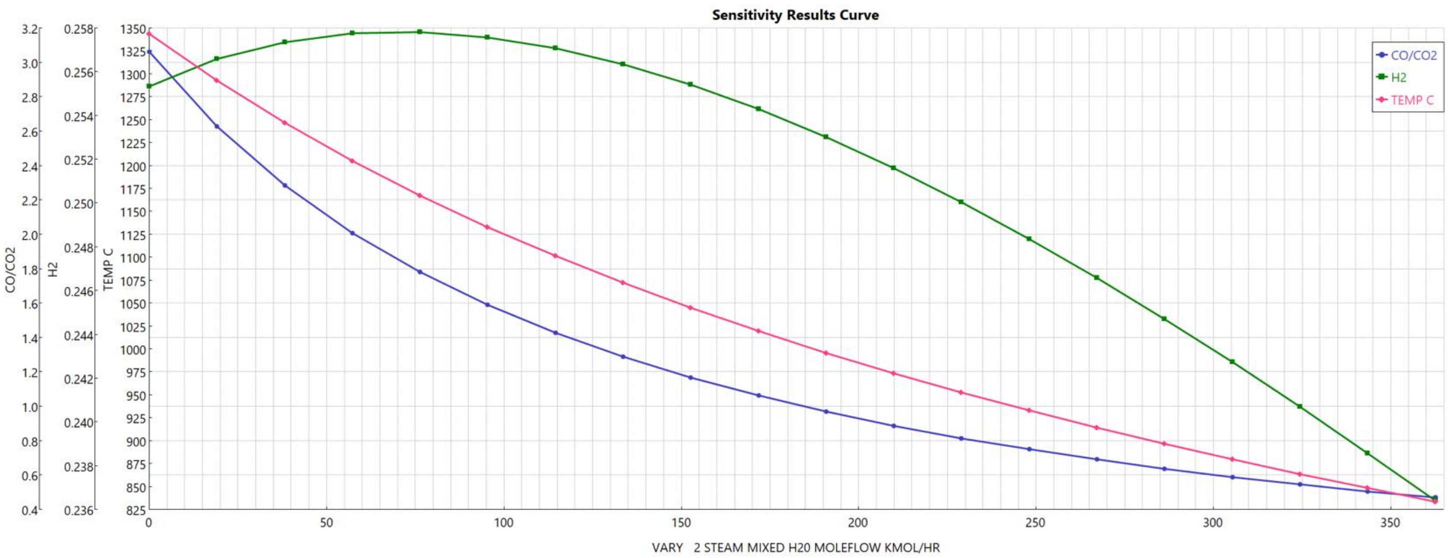

Figure x: sensitivity analysis SC

The SC was varied between 0 and 2. It can immediately be seen from the blue line, which represents the CO/CO_2, that the maximum value is obtained at SC = 0. With increasing the SC, the ratio keeps dropping. The temperature of the outlet stream HSG, drops with increasing SC. The only advantage of adding steam is that around 80 kmol·hr^{-1} a peak hydrogen fraction is reached. These observations have been observed for combining the results of OER 0.3-0.8 and SC 0-7.
Since the goal was maximizing the CO/CO_2 ratio, it is decided that no steam will be supplied to the gasifier. By running the gasifier with the optimal OER, which was specified by a “calculator” block in Aspen plus under the “Flowsheeting options” map, and the previously described heat losses the final syngas composition leaving the gasifier for the specified products is obtained and looks as presented in table x. Next to table x, table x shows the final gasifier conditions.

Syngas composition leaving gasifier	
Component	Mol fraction
CO	0.3701973
CO_2	0.1208772
H_2O	0.2531919
H_2	0.2553367
C(s)	$3.2132 \cdot 10^{-19}$
CH_4	$2.8417 \cdot 10^{-8}$
H_2S	$1.53312 \cdot 10^{-5}$
NO_2	$5.4948 \cdot 10^{-17}$
N_2	0.000381501

Table x: syngas compostion.

Gasifier operating conditions	
Temperature	1343.62 °C
Pressure	1 bar
λ	0.498
SC	0

Table x: gasifier conditions

Model verification:

The composition on dry basis can be obtained by removing the water fraction and is presented in table x. Table x also displays the experimental results obtained by Leijenhorst et al, where the fractions of the gases are presented as volume fractions. Since the assumptions was made that the gases behave as ideal, the mol-fraction is equal to these volume fractions. The final column represents the relative error, between the first two columns.

Gas composition (dry, N_2 free)	Aspen values	Experimental values	Relative error (%)
CO	49.5 %	45.6 %	8.6 %
CO_2	16.2 %	22.5 %	28 %
H_2	34.3 %	30.1 %	13.9 %
H_2 : CO	0.690	0.660	4.5 %

Table x: comparison Aspen model and experimental values.

Since the bio-oil composition was taken from the Leijenhorst et al. article and the literature on experiments of direct EF bio-oil gasification is scarce, the obtained values were firstly compared with the experimental values of Leijenhorst et al. It can be seen that the errors vary in magnitude, but the CO_2 and H_2 concentrations differ the most.

Reasons for the deviation can be the pressure difference in the operating conditions of the gasifier, which usually increases the H_2 concentration with increasing pressure. The OER also differed significantly. By running the model with the pressure and OER of the article, values closer to the experimental values where obtained.
The maximum temperature obtained in the experiment was 1321 °C. Meaning that the model achieved a relative error of just 1.71 %.

With the OER of 0.498 and no steam addition, sensitivity analysis on the pressure of the reactor was performed. The pressure range was tested from 1 bar up to 100 bar and the influence on the CO/CO_2 ratio was negligible. This is not congruent with reality. A reason could be the way in which the gasifier unit is modelled. The DECOMP step raises the amount of moles in the reagent stream dramatically. The reactions for the specified products from the gasifier unit all have less moles on the right-hand side. Around 120 $kmol \cdot hr^{-1}$ is the difference between stream TO-GASIF and stream HSG.

Gas cleaning unit PSA:

The gas cleaning unit was captured entirely in the separator block PSA. In reality three different units are needed to remove the H_2S, CO_2, N_2 and the excess water. As was said earlier, this is a national level project and many peers have already worked on it, who made a more thorough gas cleaning unit. The focus of this thesis is on the FT and refinery units. That is why an detailed gas cleaning unit was considered beyond the scope of this thesis and full separation of the mentioned contaminants is assumed.

5.2 SOEC

In this section the results of the SOEC electrolyser model will be presented and discussed. Two main questions need to be answered.

- How much feed water is needed to meet the oxygen and hydrogen demands for the downstream units?
- How much electricity does the SOEC electrolyser consume?

These questions will be answered separately. The electricity requirement and operating conditions for the SOEC electrolyser will also be compared to literature for the model verification.

H_2O feed:

In figure x of section 4.2, where the model of for the SOEC electrolyser was presented, it could be seen that a recycle stream is present back to the electrolyser. The explanation for this was provided in section 4.2 and it has a fixed value of fraction 0.2 of the stream leaving the SOEC unit. This stream recycles back water and hydrogen. The other recycling stream that supplies water to the electrolyser comes from the gasifier unit. A feed unit H2O-FEED, in the main flowsheet, is the last part responsible for the electrolyser's water supply. The electrolyser conversion is fixed at 80%, so the only variable that dictates the hydrogen and oxygen production is H2O-FEED. The flowrate of this stream was varies in a sensitivity analysis, which is shown for the two gases below.

O_2 – requirement:

The required flowrate of the gasifying agent oxygen was established in the previous section and equates to 2760 kg·hr^{-1} or 86.2532 kmol·hr^{-1}. A sensitivity analysis was performed to see how large H2O-FEED must be to meet this oxygen output. The result is seen in figure x below.

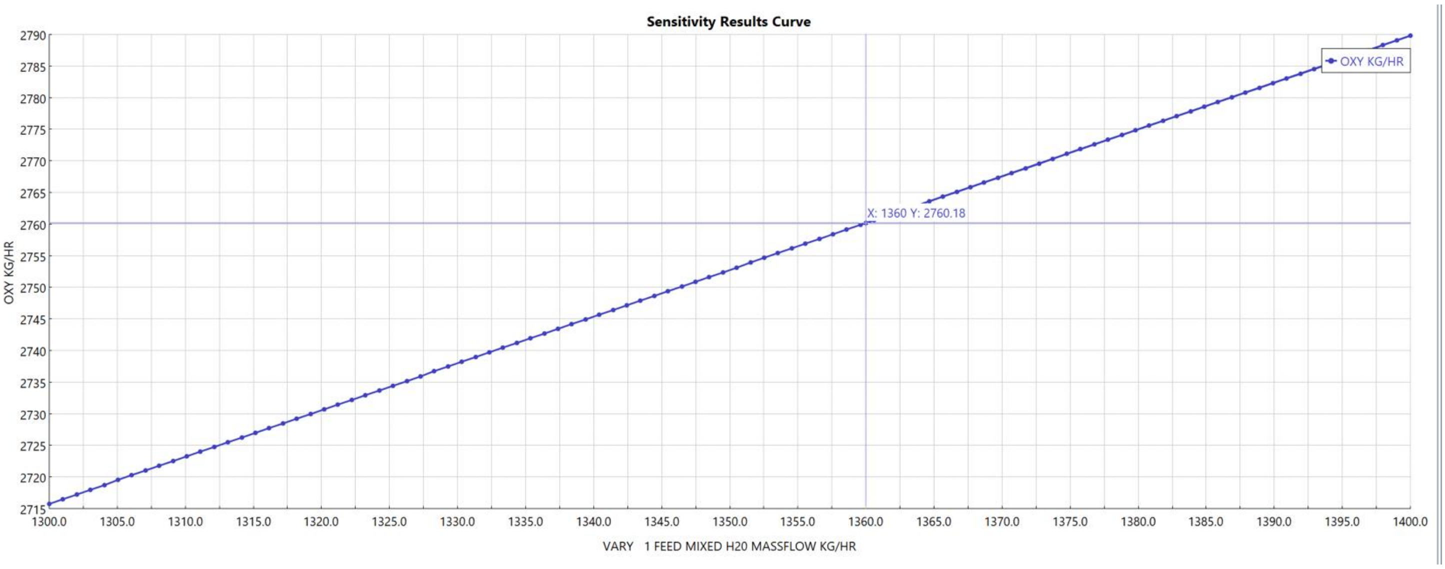

Figure x: required feed rate for oxygen.

The tracker in figure x displays that a feed-rate of 1360 kg·hr^{-1} of water is needed for an oxygen production of 2760 kg·hr^{-1}.

H_2-requirement:

In the previous section the syngas composition coming out of the gasifier could be found. The H_2:CO ratio was found to be 0.6897. This ratio needs to be upgraded to 2.15:1. The CO molar flowrate in the syngas was found to be 136.653 kmol·hr^{-1}. Meaning that a hydrogen flowrate of 293.804 kmol·hr^{-1} needs to achieved. The hydrogen flowrate in the syngas is already 94.253 kmol·hr^{-1}. Meaning that the electrolyser needs to produce the 199.551 kmol·hr^{-1} to upgrade the syngas for the FT unit. There is another hydrogen requirement for the hydrocracker unit as was explained previously. By using the calculation method as explained in section 4.4, this amount is less than 2 kmol·hr^{-1}. Meaning that the sensitivity analysis will determine at which water feed rate, 201.551 kmol·hr^{-1} of hydrogen is produced. The results are shown below in figure x:

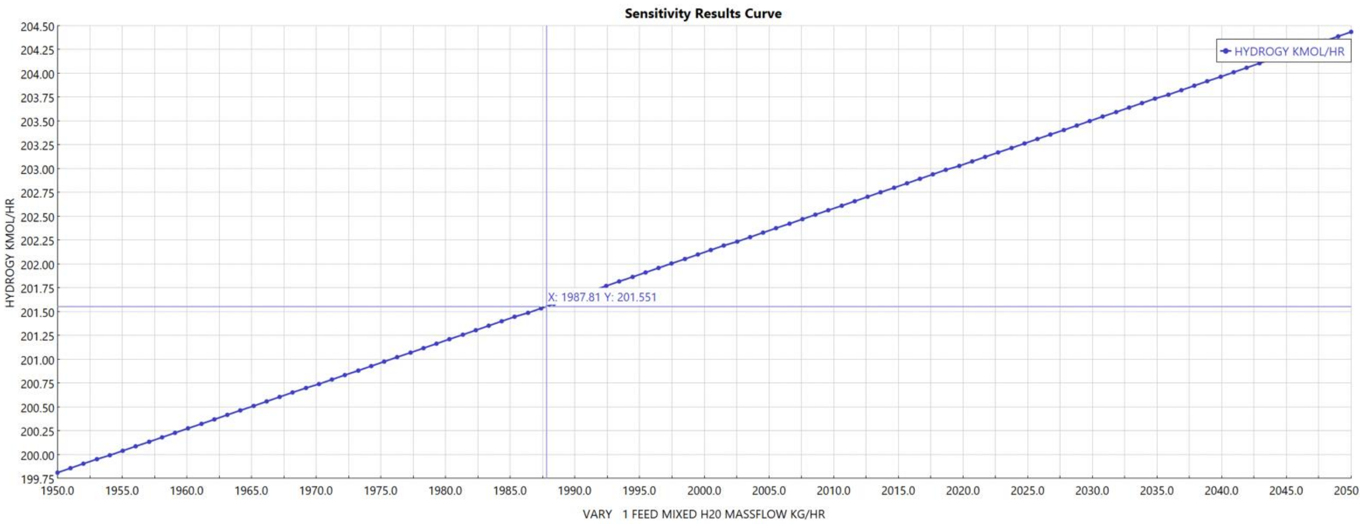

Figure x: required feed rate hydrogen

As can be seen in figure x, demonstrated with the marker, the required feed flow rate of water is equal to 1987.81 kg·hr^{-1}. Since this number is much larger than the number found for the oxygen requirement it is concluded that the hydrogen demand dictates the feed flowrate of water. The final feed input was chosen to be 2000 kg·hr^{-1}, to leave some room to spare for both molecules.

Now that the feed rate of water is known the second question can be answered.

The straightforward way would be to find the operating voltage and the current running through the cell. By finding the current density, the amount of active surface area needed can be found, as well as the amount of SOEC's needed.

The operating voltage:

The standard cell potential of water electrolysis at 25 °C, 1 atm and 1 molarity for the molecules is equal to 1.23 V. For different conditions the value of the standard cell potential changes. The standard cell potential ε^0_{cell} is connected to the Gibbs free energy for the formation of the water, the relationship is as follows:

$$\varepsilon^0_{cell} = \frac{\Delta G_f}{n \cdot F}$$

- ΔG_f is the Gibbs free energy for the formation of water.
- F is the Faraday constant, equal to 96485 $C \cdot mol^{-1}$.
- n is the number of electrons transferred in the reaction, which is 2.

The operating conditions for the SOEC electrolyser are 20.1 bar and 700 °C. The influence of the applied pressure and the steady state concentrations on the voltage will be tested. To do this, the standard cell potential at 973.15 K and 1 bar needs to be calculated. Since Aspen has a large thermodynamic properties database it can be used to obtain the Gibbs free energy value at these conditions. Thermodynamic tables online like [nist.gov] also have values for different temperatures at 1 bar. The closest value is available for 1000 K at 1 atm. The value found with Aspen is equal to -216.920 $kJ \cdot mol^{-1}$, the value according to [nist.gov] is equal to -192.590 $kJ \cdot mol^{-1}$. To correct for the slight offset in temperature and pressure for the literature values, the average of these two values will be taken and is equal to -204.755 $kJ \cdot mol^{-1}$. Using equation x, the value of ε^0_{cell} at 700 °C and 1 bar is found to be 1.061 V. To test the effect of the increased pressure and the steady state concentrations the Nernst equation can be used:

$$\varepsilon_{cell} = \varepsilon^0_{cell} - \frac{R \cdot T}{n \cdot F} \cdot \ln Q$$

- ε_{cell} is the instantaneous cell voltage at the specified conditions
- ε^0_{cell} is the standard cell potential, equal to 1.061 V.
- T is the temperature in Kelvin, equal to 973.15 K.
- R is the universal gas constant equal to 8.314 $J \cdot K^{-1} \cdot mol^{-1}$.
- Q is the reaction quotient, which measures the concentrations of the molecules at a given time.

The reaction quotient Q is a transient variable, changing the cell voltage constantly. It is expressed in terms of partial pressures or concentration. For the electrolysis of water Q looks as follows:

$$Q = \frac{[H_2]^2 \cdot [O_2]}{[H_2O]^2} \cdot (\frac{P_{SOEC}}{P_{sc}})$$

- The term in the square brackets represent the concentrations of the molecules. Since the ideal gas law is assumed, these equal the mole fractions and thus are unitless.
- P_{SOEC} is the pressure of the SOEC electrolyser, equal to 20.1 bar.
- P_{SC} is the pressure at standard conditions, equal to 1.013 bar.

The concentration of the molecules times the pressure term, represents its partial pressure. The pressure term is needed since the gasses exert a different pressure than at standard conditions. By combining equations x and x, the cell voltage can be found. The last remaining input are which concentrations to use. After running the model, the recycle streams are taken into account and the system is assumed to operate at steady state. Three different concentrations can be considered. These are the input concentrations to the electrolyser when the extent of reaction is 0, the output concentrations of the electrolyser when the extent of reaction is 1 and the values in between these concentrations. For the latter the halfway point will be taken, when the extent of reaction is equal to 0.5. These concentrations are the mole fractions found in Aspen and this looks as follows, presented in table x.

molecules	ξ = 0	ξ = 0.5	ξ = 1
H_2O	0.833	0.479	0.125
H_2	0.167	0.396	0.625
O_2	0	0.125	0.250

The cell potential will be the highest at ξ = 0 and the lowest at ξ = 1, to obtain the most accurate estimate of the cell operating potential the ξ = 0.5 values will be used.
By filling everything in, in equation x, ε_{cell} is found to be 1.039 V and will from now on be referred to as the operating voltage. As expected, it is lower than at standard cell conditions, since the operating conditions of the cell enable better operation. When using Aspen to find the Gibbs free energy of the water at 700 °C and 20.1 bar a value of -191.145 kJ·mol^{-1} is found, equaling a reversible, V_{rev}, or open circuit voltage of 0.991 V. This value is very close to that found by [gibbsyy]. The thermoneutral voltage is equal to 1.285 V, since the enthalpy value at 1000 K is equal to -247.955 kJ·mol^{-1} [nist.gov]. In literature the thermoneutral voltage for most SOEC electrolyser is listed as 1.29 V, but no temperature is specified. The value found is thus in line with literature.
Since heat integration is an important aspect of this thesis and as will be seen in the next chapter, enough heat is available, it is decided that the SOEC is able to perform beneath the thermoneutral voltage. Meaning that the electricity efficiency increases. The operating voltage of the cell, V_o, will be chosen as that found by the Nernst-equation, 1.039 V.

The next step to find the power requirements of the SOEC electrolyser is finding the current at which it will operate. The Faradaic current for the reaction can be determined with the following equation:

$$I_F = n_{H_2O} \cdot n_e \cdot F \cdot \frac{1}{3600}$$

- I_f is the faradaic current in Ampère.
- n_{H2O} is the amount of mol per hour of steam consumed in steady state.
- n_e is the number of electrons consumed per mole of steam reacting.
- F is again the faradaic constant.
- The last term converts the hour term to seconds, to get Ampère's.

Filling everything in looks as follows:

$$I_F = \frac{201.7321\ kmol\ steam}{hour} \cdot \frac{2\ mol\ e^-}{mol\ steam} \cdot \frac{96485\ Coulomb}{mol\ e^-} \cdot \frac{1}{3600} = 1.0813\ \cdot 10^7\ A$$

Power consumption of the electrolyser:

Now that the operating voltage and the current are known the power can easily be found with:

$$P_{SOEC} = V_o \cdot I_F$$

P_{SOEC} is equal to 11.23 MW. Assuming power losses of 5% due to the other electrical components, like the cabling, inverter and other internal resistances, the power requirement is raised to 11.82 MW.

Current density calculation:

To find the amount of electrolysers necessary to meet the demand, the last variable needed is the current density. The following relation can be used:

$$J = \frac{V_o - V_{rev}}{ASR}$$

The only unknown is the ASR, which stands for area specific resistance. Finding the ASR for the electrodes at the specified conditions can be achieved by the following empirical relationship:

$$ASR(P, T) = D \cdot \exp\,(-B \cdot T) \cdot \exp\,(-C \cdot P)$$

- D, B and C are constants, T is the temperature in K and P the pressure in bar. The values are estimations based on experimental data in the 750-850 °C range. It is assumed that it also holds for 700 °C.
- D equals 35.71 $\Omega \cdot cm^{-2}$

- B equals 0.0057 K^{-1}
- C equals 0.0217 bar^{-1}

The ASR is found to be 0.090 $\Omega \cdot cm^{-2}$. Using this value to find the current density results in J = 0.533 $A \cdot cm^{-2}$. This is a fairly low current density. It can be made higher, by increasing the operating voltage of the cell. The trade-off is between increased power consumption by the electrolyser with increasing operating voltage, but with lower capital costs, due to less surface area needed. Since it is clear from the beginning of this thesis that the energy efficiency is the primary goal, the low current density will be used. The degradation of the electrolyser is also slowed down by the lower current density.

By dividing the current needed, by the current density, the total active surface area can be found and is equal to 2135 m^2. State of the art SOEC's have active electrode areas around 100 cm^2, however cells with active electrode areas as high as 550 cm^2 have been produced and demonstrated. Currently cell stacks of up to 100 cells are becoming commonplace [soec promotion] and designs for stacks with 350 cells have been proposed. When taking the current values for the amount of cells per stack and active surface area per cell, 2135 stacks are needed. In early 2020, a SOEC demonstration plant in Salzgitter, Germany, had 48 stacks per SOEC module. Meaning that 45 SOEC electrolysers are needed. When using the most optimistic numbers for the active electrode area per cell and number of cells per stack, only 111 stacks are needed, which could be held by only 3 SOEC modules.

Table x summarizes the previously discussed characteristics of the SOEC and provides a clearer overview.

Parameter	
n_{H2O} ($kmol \cdot h^{-1}$)	201.7321
V_{tn} (V)	1.285
V_o (V)	1.039
I_F (A)	$1.0813 \cdot 10^7$
J ($A \cdot cm^{-2}$)	0.553
ASR ($\Omega \cdot cm^{-2}$)	0.090
P_{SOEC} (MW)	11.82
Area (m^2)	2135
# SOEC electrolysers	3-45

The current design uses the least amount of electricity and can have a high enough production with three electrolysers. In reality the operating voltage would be significantly higher, to increase the current density as well. Operating a thermoneutral voltage for example, while keeping the ASR the same, would result in a current density of 3.27 $A \cdot cm^{-2}$. This is slightly above the current densities found by [deense artikel ref 37], where the electrode microstructure and test conditions were optimized. The ASR is also on the very low side, these are typically more in the order of 0.3 $\Omega \cdot cm^{-2}$. The reason for the deviation could be that the extrapolation used by [] is invalid. The pressure is also assumed to have an effect on the ASR, it lowers it. This is not yet fully disclosed.

Heat supply:

The observant reader would have notice a flaw in the energy requirements proposed so far. Since the operating voltage is beneath the thermoneutral voltage, the reaction would draw heat from the electrolyser environment, up to a point where the reaction can no longer proceed. That is why external heat needs to be provided to the electrolyser. Before calculating this heat a short explanation about the buildup of the energy demand is given. The total energy demand for the conversion of the steam is equal to the enthalpy of formation at the specified temperature, this is demonstrated in the equations below:

$$\Delta H_{tot} = \Delta G + T \cdot \Delta S$$

$$total\ energy = electric\ energy + heat\ energy$$

As can be seen in figure x, the total energy demand rises with increasing temperature, but the heat demand is rising at a steeper angle. The latter depends entirely on the entropy term, since it rises quicker than the enthalpy term, the Gibbs free energy and thus the electricity demand is dropping with increasing temperature.

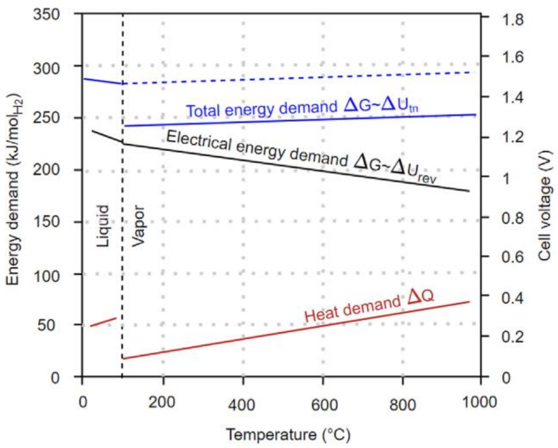

At 700 °C and 20.1 bar the Gibbs free energy found with Aspen is equal to -191.145 kJ·mol^{-1}, while the enthalpy value is equal to -247.955 kJ·mol-1. Meaning that according to equation x the heat energy demand is -56.81 kJ·mol-1. But since the operating voltage was found to be 1.039 V, the Gibbs free energy provided by the electricity is -200.495 kJ·mol^{-1}.
Meaning that 47.46 kJ·mol-1 of heat is required to keep the reaction going. This is on top of the heat required to heat the steam up to 700 °C. The heat required to maintain the operating voltage below the thermoneutral voltage is equal to 2.695 MW.

The heat needed to heat up the water, starting from 32 °C to 700 °C can be found with the following equation:

$$Q = \dot{m}_{H_2O} \cdot Cp_{liq} \cdot \left(\Delta T_{liq}\right) + \dot{m}_{H_2O} \cdot Cp_{vap} \cdot \left(\Delta T_{vap}\right) + \dot{m}_{H_2O} \cdot \Delta H_{vaporization}$$

- Q is het heat supplied
- $\dot{m}_{H2O}$ is the mass flowrate of the water in kg·s^{-1}
- Cp_{liq} is the specific heat capacity of liquid water, it equals 4.182 kJ·kg^{-1}·K^{-1}
- ΔT_{liq} is the temperature range in which the water remains liquid. The boiling point of water at 20.1 bar is equal to 212.4 °C, so ΔT_{liq} equals 180.4 °K.
- Cp_{vap} is the specific heat capacity of vaporised water, it equals 3.025 kJ·kg^{-1}·K^{-1}
- ΔT_{vap} is the temperature range in which the water remains is vapor. So ΔT_{liq} equals 487.6 °K.
- $\Delta H_{vaporization}$ is the latent heat of vaporization of the water and equals 1888.65 kJ·kg^{-1}.

Q is found to be 4.157 MW. Meaning that the total energy requirements are 11.82 MW of electric energy and 6.852 MW of heat, to run the SOEC electrolyser.

5.3 Fischer Tropsch

This section will present the results of the Fischer Tropsch section. Since the chain growth probability factor is directly related to the pressure and temperature, also translating into a fixed ASF distribution, varying the operating conditions of the reactor is not possible. Since the gasifier unit was already optimized towards maximum CO production and the SOEC electrolyser produces enough hydrogen for the (optimum) 2.15 : 1 ratio, these values are also fixed. This section will give an insight in the composition of the syncrude formed in the FT reactor. The composition of the fuel gasses will also be highlighted.

Syncrude to crude composition:

As described in section 4.3 the stream entering the FT section in the model is called SYNGAS-2, this stream is the result of the gasifier and the electrolyser. The final stream entering the FT reactor is called SYNGAS-F. SYNGAS-F is comprised of the syngas entering the FT section in the model and the recycle stream GAS-REC. The stream leaving the FT reactor is called SYNCRUDE. In table x the relevant mol concentrations of these streams are given:

Stream	CO ($kmol \cdot hr^{-1}$)	H_2 ($kmol \cdot hr^{-1}$)	H_2O ($kmol \cdot hr^{-1}$)	H_2 : CO
SYNGAS-2	136.653	294.661	0.33227	2.156
SYNGAS-F	169.888	500.321	1.3572	2.945
SYNCRUDE	33.9741	210.064	137.271	6.183
REC-GAS	33.235	205.66	1.02493	6.188
(SYNGAS-F) - SYNCRUDE	135.9139	290.257		2.136

At first glance it can seem that the ratio of the syngas entering the FT reactor is not the optimal 2.15 : 1. But when the amount of CO reacting and H_2 reacting, which can be found by subtracting stream SYNCRUDE from SYNGAS-F, is divided the ratio is again found to be 2.14, as seen in the last row of table x. The latter also shows the amounts reacting per hour. The slight decrease is caused by the small amount of CO and H_2 being removed by stream PURGE-1.
Now that the streams and working principles around the FT reactor are shown the molar and mass fractions of the produced syncrude will be shown. The produced molecules are combined according to the previously classified carbon ranges, fuelgas, gasoline, diesel and wax.

Class	Mol frac	Mass frac
CO	0.0587421	0.090945
H_2O	0.237341	0.2363327
H_2	0.3604248	0.0401596
Methane (CH_4)	0.174198	0.1557089
Fuelgas ($C_2 – C_4$)	0.144411	0.2937544
Gasoline ($C_5 – C_{10}$)	0.01584434	0.08194666
Diesel ($C_{11} – C_{21}$)	0.00601166	0.06894028
Wax ($C_{22} – C_{30}$)	0.001561626	0.03216419

The results are as the ASF distribution predicted. The next table shows the fractions of the methane, fuelgas, gasoline, diesel and wax again, but now without taking CO, water and hydrogen into account.

Class	Mol frac	Mass frac
Methane (CH_4)	0.509	0.246
Fuelgas ($C_2 – C_4$)	0.422	0.464
Gasoline ($C_5 – C_{10}$)	0.046	0.130
Diesel ($C_{11} – C_{21}$)	0.018	0.109
Wax ($C_{22} – C_{30}$)	0.0046	0.051

Since the yield of the desired products is low after just one pass, 98% of the methane and fuelgas are recycled back to the FT reactor, via stream REC-GAS. In section 4.3 the water removal process was explained and the effect of the recycle stream can be seen when looking at the composition of the stream leaving the FT model section, CRUDE. Just like in table x, only the relative hydrocarbon fractions will be shown. The final mass flowrate, temperature and pressure of stream CRUDE are also presented.

Class	Mol frac	Mass frac
Methane (CH_4)	0.000521018	5.45461E-05
Fuelgas ($C_2 – C_4$)	0.088084	0.029995
Gasoline ($C_5 – C_{10}$)	0.48947	0.333007
Diesel ($C_{11} – C_{21}$)	0.320144	0.432687
Wax ($C_{22} – C_{30}$)	0.083094	0.202063

As can be seen in table x, the yield of the has dramatically increased. Comprising close to 77% of the weight of the CRUDE stream. As was told in the in the previous chapter, this yield will further be increased in the refinery section, where the waxes will be converted.
The final mass flowrate, temperature and pressure of stream CRUDE are also presented in table x.

Parameter	
Flowrate ($kg \cdot hr^{-1}$)	1665.58
Temperature (°C)	35
Pressure (bar)	1

The other by-product, that will be further processed, is the separated fuel gas, leaving the FT model section as stream FUELGAS. The composition and other relevant parameters of the fuel gas is provided in table x on the next page.

Component	Mol fraction
CO	0.0563021
H_2	0.3352981

CH_4	0.1873015
C_2H_6	0.1564353
C_3H_8	0.1204277
C_4H_{10}	0.0743284
C_5H_{12}	0.0338123
Other parameters	
Flowrate ($kg \cdot hr^{-1}$)	315.949
Temperature (°C)	31.15
Pressure (bar)	1
LHV ($MJ \cdot kg^{-1}$)	45.77

Since the energy integration is a key aspect in this thesis and the Fischer Tropsch reaction is very exothermic, the heat released will be presented and compared with literature. Aspen has the heat duty of the FT-reactor calculated as -6.237 MW or $-2.24541 \cdot 10^7$ $kJ \cdot hr^{-1}$. In table x it was shown that 135.9139 $kmol \cdot hr^{-1}$ of CO is converted. De Klerk [] states that the energy release is in the order of −160 $kJ \cdot mol^{-1}$ CO converted. Using this number to multiply the CO reacting, gives a heat duty of $-2.1746224 \cdot 10^7$ $kJ \cdot hr^{-1}$ or equivalently -6.041 MW. The values are very close.

5.4 Refinery

This section will present de results obtained in the refinery section. For all three distillation columns the degree of separation achieved will be summarized in tables. The FLASH unit also performs a rough separation and the same will be done as for the distillation columns. Next, the hydrocracker reactor will be examined, showing the results of the method explained in section 4.4 on acquiring the hydrogen demand. The heat duty of the hydrocracker will also be presented. Lastly the characteristics of the diesel and gasoline obtained will be presented.

Distillation column 1:

The first distillation column separates the fuel gas and gasoline from the diesel and wax. To quantify the level of separation the composition of the top and bottom streams, exiting DISTIL-1, will be given. Again the molar and mass fractions will be shown. Since the yield of the hydrocracker is recycled back, to mix with the incoming crude, the starting composition of the refinery feed is changed, once the plant is running. The stream entering DISTIL-1 is called MIX, its composition is as given in table x.

Class	Mol frac	Mass frac
Methane (CH_4)	$4.21 \cdot 10^{-4}$	$4.44 \cdot 10^{-5}$
Fuelgas ($C_2 - C_4$)	0.142	0.045
Gasoline ($C_5 - C_{10}$)	0.428	0.295
Diesel ($C_{11} - C_{21}$)	0.338	0.469
Wax ($C_{22} - C_{30}$)	0.077	0.189

It can be seen that the mass fraction of diesel has increased, because of the hydrocracker unit. The streams exiting DISTIL-1 are HT-GAS as top product and LIQUID-1 as bottom product. The number of moles of the different compounds, relative to the original amount of moles of the respective compound in stream MIX are given in table x. Next to that, in table

Class	Transferred to HT-GAS	Transferred to LIQUID-1
Methane	100 %	0 %
Fuelgas	100 %	0 %
Gasoline	96.4 %	3.6 %
Diesel	0.02%	99.8%
Wax	0 %	100 %

Class	Mole frac in HT-GAS	Mole frac in LIQUID-1
Methane	$7.4 \cdot 10^{-4}$	0
Fuelgas	0.249	$4.67 \cdot 10^{-11}$
Gasoline	0.724	0.035
Diesel	$1.22 \cdot 10^{-4}$	0.785
Wax	0	0.179

As is evident from these two tables the desired separation is performed well, the distillation column settings as presented in section 4.4 were correct. All of the water that was still present in the CRUDE after the FT unit, has left DISTIL-1 with stream HT-GAS. Since this water cannot be present in the final gasoline and fuel gas, it has to be removed by the

combination of units FLASH and DECANT. The performance of these two units is summarized in the following two tables x and x on the next page.
Stream HT-GAS is the incoming stream for FLASH and the top stream is PURGE and the bottom stream is called LIQUID2. LIQUID2 is the incoming stream for DECANT and the two exiting streams are W and ORG.

Class	transferred to PURGE	transferred to LIQUID2
Methane	97.6 %	2.4 %
Water	23.6 %	76.4 %
Fuelgas	53.4 %	46.6 %
Gasoline	3.2 %	96.8 %

Class	Transferred to W	Transferred to ORG
Methane	0 %	100 %
Water	55.7 %	44.3 %
Fuelgas	0 %	100 %
Gasoline	0 %	100 %

As was said in section 4.4, the decanter removes enough water to bring the volumetric water content down to the limit of 0.5 vol%. The flash separator already separates most of the gasoline from the fuel gas, but a significant amount of fuel gas is still present in the gasoline, which needs to be removed. This is done in DISTIL-2

Distillation column 2:

The incoming stream for the distillation column is stream ORG, which comes out of the decanter. The exiting top stream is GAS and the bottom product is stream GASOLINE. Table x displays the results of the separation. Table x next top it breaks down the molar composition of both streams.

Class	transferred to GAS	transferred to GASOLINE
Methane	100 %	0 %
Water	33.5 %	66.5 %
Fuelgas	91.7 %	8.3 %
Gasoline	2.2 %	97.8 %

Class	Mole frac in GAS	Mole frac in GASOLINE
Methane	$1.44\cdot10^{-4}$	$1.53\cdot10^{-30}$
Water	0.024	0.00847
Fuelgas	0.852	0.0138
Gasoline	0.124	0.978

Again it is evident that the separation level achieved by the distillation column is very high. The gasoline consists of almost 98% of only molecules in the gasoline range. Since gasoline is the desired product and the fuel gas a useable by-product their relevant characteristics will be presented next.

Characteristic	
Mass flow rate ($kg\cdot h^{-1}$)	557.5
Temperature (°C)	76.7
Octane number	
Density ($kg\cdot m^{-3}$)	630.3
Water content (% vol)	0.847
Sulfur (%wt)	$5.065\cdot10^{-20}$
LHV ($MJ\cdot kg^{-1}$)	44.81

Comparing the gasoline to table x in section 3.6 to the gasoline produced is not a good measurement to test the gasoline produced, since it is not the same product. The gasoline produced will be mixed in with conventional gasoline from a refinery. This mixing will also lower its volumetric water content to be under the threshold value.

Characteristic	
Temperature (°C)	36.6
Mass flow rate ($kg\cdot h^{-1}$)	111.9
LHV ($MJ\cdot kg^{-1}$)	45.44

Distillation column 3:

Now the results of the top part of the refinery model section are presented. The separation of the diesel and wax is performed in DISTIL-3, the entering stream comes from DISTIL-1, LIQUID 1. The exiting streams are DIESEL on top and WAX-1 at the bottom.

Class	transferred to DIESEL	transferred to WAX-1
Gasoline	100 %	0 %
Diesel	99.3 %	0.7 %
Wax	97.3 %	2.7 %

Class	Mole frac in DIESEL	Mole frac in WAX-1
Gasoline	0.043	$1.45\cdot10^{-9}$
Diesel	0.951	0.029
Wax	0.0058	0.971

A very high separation is again reached. The diesel produced has the following characteristics, shown is table x.

Characteristic	
Mass flow rate ($kg\cdot h^{-1}$)	989.9
Temperature (°C)	240.8
Cetane number	
Density ($kg\cdot m^{-3}$)	537.9
Water content (% vol)	$1.84\cdot10^{-9}$
LHV ($MJ\cdot kg^{-1}$)	30.41

Hydrocracker:

The fictive wax molecule was found to have the following molecular formula and weight, $C_{26.32}H_{54.64}$ and 371.21 $g\cdot mol^{-1}$. U in equation x was found to be 0.00413, meaning that for the flowrate of 386.55 $kg\cdot h^{-1}$ for stream WAX-3, 1.597 $kmol\cdot h^{-1}$ of hydrogen is needed to be supplied. Since the Ryield was set to use the mass yields, the mass flows of propane, octane, cetane and hexacosane are known at this inflow. The effect of the hydrocracker was already incorporated at the beginning of this section, mostly increasing the diesel yield. The reactions inside are net exothermic, which can also be seen in the heat duty of -0.014 MW. Since a Ryield was used, varying the pressure, temperature or increasing the H_2 flow beyond the stoichiometric limit had no effect on the yield of the four products.

Total carbon conversion to the desired products:

Since the flowrates of gasoline and diesel are now known, the total carbon conversion of the process can be found. Since only paraffins were assumed to be products, it is clear that for every C atom, the amount of H atoms is equal to $2 \cdot C + 2$. But the weight fraction of the carbon differs for every molecule. That is why excel was used, as described in section 4.4 for the wax, to find the total amount of carbon and hydrogen in the gasoline and diesel.
The gasoline has 0.821 kg of water in the stream, the weight fraction of carbon was found to be 0.839768. Meaning that if the amount of water is subtracted from the gasoline flowrate and multiplied by the carbon weight fraction, the amount of carbon that ended up in the gasoline is equal to 467.5 kg·hr^{-1}. All of the diesel mass is in the hydrocarbons, the weight fraction of carbon was found to be 0.848026, meaning that 839.5 kg·hr^{-1} of carbon is present in the diesel stream. Adding this up results in 1307 kg·hr^{-1} of carbon in the desired molecules. The bio-oil delivers 2268 kg·hr^{-1} of carbon. Yielding a carbon conversion efficiency of 57.6 %.

5.5 turbine

The goal of the turbine section was to use the by-product fuel gas to drive a turbine and improve the energy efficiency of the process. The fuel gas from the FT section and the refinery section together form stream FUELGAS in the turbine section. Whose characteristics are summarized in table x.

Characteristic	
Temperature (°C)	32.3
Mass flow rate (kg·h^{-1})	427.8
Pressure (bar)	1
Vapor fraction	1
LHV (MJ·kg^{-1})	45.7
HHV (MJ·kg^{-1})	49.9

The intermediate coolers cool down the streams to 35 °C, as explained in section 4.5. the vapor fraction of the fuelgas is at this temperature still almost 0.99. That is why the LHV will give a more accurate idea of the energy that can be extracted from the fuel gas. The function used to obtain the LHV is called LHVMS-15, which calculates the lower heating value at 15 °C.

With the mass flow rate and LHV value it can be found that 5.427 MW of energy is created. When adding the heat duties of the COOLERS1,-2,-3, the number 5.738 MW is found. The reason that its higher is the temperature difference between 35 °C and 15 °C at which the

LHV is referenced. More water would have condensed at the lower temperature, lowering the LHV. That is why the second number will be used as the potential for creating steam.

The liquid water's pressure is raised to 5 bar and heated to 300 °C hot steam, to be used to drive the turbine. Via a sensitivity analysis in Aspen varying the CW-IN flowrate and finding the net heat duty of HEAT-1, it was found that 6750 kg·h^{-1} of cold water can be converted to high pressure steam. The TURBINE3 section has as result a production of -0.491 MW of electricity. Which can be fed to the electrolyser.

The outlet temperature of the steam that has passed through TURBINE takes the isentropic efficiency into account. By using steam tables and the steady flow energy equation the obtained result for the electricity production can be checked.
The potential energy term in the steady flow energy equation is negligible, since the elevation between the inlet and outlet of the turbine is the same. The kinetic energy term is negligible as well. The kinetic energy gained by the steam during its time inside the turbine comes from the internal energy term. No heat loss is assumed as well in the turbine and the steady flow energy equation reduces to:

$$\dot{W} = \dot{m}(h_2 - h_1)$$

- Where $\dot{W}$ is the work performed in MW
- $\dot{m}$ is the mass flowrate in kg·s^{-1}
- h_2 the specific enthalpy in MJ·kg^{-1} at the outlet of the turbine
- h_1 the specific enthalpy in MJ·kg^{-1} at the inlet of the turbine

The input for the inlet and outlet stream is displayed in table x.

Parameter	Inlet stream TOTURBIN	Outlet stream LPSTEAM
$\dot{m}$ (kg·s^{-1})	1.875	1.875
T (°C)	300	161.107
P (bar)	5	1
h (MJ·kg^{-1})	3.064	2.795

Filling in equation x yields 0.504 MW. Which is very close to the value found with Aspen.

The power output of the turbine due to the combustion of the by-product fuel gas is found in this section. The next chapter will solely focus on the heat exchange and energy efficiency of the entire plant. Other hot streams with high quality heat could also be used to create the steam, once the primary heat requirements are met. Meaning that the amount of power produced by the turbine could be higher.

This concludes the result section. Due to the way of modelling and optimizing based on literature values, the degree of variability for this integrated process is on the low side. But it must be stated that the constraints all flow over into each other, creating a very efficient process, with minimal feed requirements. The chain looks as follows:

Since the bio-oil feed is fixed, the minimum amount of oxygen as gasifying agent required, with the aim for as much CO production as possible is found. This in its turn fixes the amount of hydrogen needed to upgrade the syngas to the optimal ratio for FTS. Together with the hydrocracker demand this fixes the amount of hydrogen the electrolyser must produce. Since the FT product distribution is modelled with only the ASF distribution, α is again a fixed value. The yield of the FT reactor is in its turn fixed. The refinery has optimized distillation columns for maximum separation, but again a fixed, literature based, product yield and operating conditions. Lastly this fixes the yield of fuel gas, which if air is supplied in the perfect stoichiometric amount, also fixes the amount of electric power generated in the turbine.

Since the aim was to produce an as energy efficient process as possible, while maximizing the diesel and gasoline yield, using these optimum literature values is a good way to achieve this. The next chapter will go deeper in the overall energy efficiency of the process.

Chapter 6

Energy efficiency analysis

This chapter will analyze the energy efficiency of the entire process. First a heat integration will be applied to the process. There are several heat sources and heat sinks that can be used as efficiently as possible. After the heat exchange network is formed and taken into account, the final efficiency can be determined. Section 6.1 will start with the design of a heat exchanger network. Section 6.2 will show all the energy sources and demands. Lastly section 6.3 will combine these findings.

Heat

This section will be dedicated to making the process as energy efficient as possible, mainly by designing a heat exchanger network. The presented process has two large heat sources, the gasifier and the FT section. The SOEC and turbine sections are heat sinks. Three different aspects will be discussed. First meeting the heat duties of the SOEC electrolyser and the FT reactor will be discussed. Secondly a heat exchanger network will be designed between the hot and cold streams of the process. Lastly the stand-alone heat duties will also be tried to combine as efficiently as possible, these will be different flash units and the distillation columns.

6.1.1 Heat duties of the FT reactor and SOEC electrolyser

Fischer Tropsch reactor:

It was found in section 5.3 that the heat duty of the FT reactor is -6.237 MW, to be operated at isothermal operating conditions. The way in which this heat will be used was the creation of high-pressure steam, as explained in section 4.3.

The cooling water enters the section at 1 bar and 20 °C. Since the FT reactor operates at 200 °C, the water cannot exceed a temperature of 200 °C. This and fixating the vapor fraction as 1, allows unit HEATERFT to use all the energy to heat up a specified flowrate of water. This flowrate was determined by using the “design-specs” tool in Aspen Plus. The other heat stream attached to unit HEATERFT was HEAT-OUT. By starting with a relatively low flowrate, which is sure to be completely heated to 200 °C and then running the model, it could be found how much of the heat leaves with stream HEAT-OUT. This heat can be used to heat up more water. The design specs block was used to find the flowrate of water to make stream HEAT-OUT equal to 0 MW.
This flowrate of water was found to be 7884.44 kg·hr^{-1}, thus creating 7884.44 kg·hr^{-1} of high-pressure steam. The pressure of the steam reached was found to be equal to 15.59 bar.

The slurry bubble column reactor allows for heat transfer that is good enough to assume that the full heat produced in the FT reactor is used for the heating of the water.

The SOEC electrolyser:

In section 5.2 it was determined that in order to operate the SOEC-electrolyser below its thermoneutral voltage, external heat must be supplied, which minimizes the amount of electricity needed. The heat needed was found to be 2.695 MW. As explained is section 4.2 the heat will come from the combustion of the by-product fuel gas, obtained in the FT and refinery units. To reach this amount of heat it was found through sensitivity analysis, varying the mass flow of stream of FG-SOEC and checking the net heat duty of unit HEATER in the SOEC section, that 198.5 kg·hr^{-1} of the fuel gas must be combusted. In the process 3035 kg·hr^{-1} of air is consumed as well.

This covers the two most important heat duties. The next step is to make a heat exchanger network between the hot and cold streams. The streams of the high-pressure steam produced and the combustion of the fuel gas do not participate in this network, since their goal is already established.

Heat integration of the streams:

The pinch analysis method will be applied to find the optimum heat exchanger network between the streams. All the hot streams and cold streams that are eligible for heat exchange are considered. The reboilers and condensers of the distillation columns are in practice often heat exchanger, their heat demands are also taken into account. Using Aspen plus to analyze the distillation column results, under the section “profiles” the vapor and liquid streams of each stage are given, as well as the temperature at that stage. For the condensers, the temperature of the second top stage was chosen as the hot temperature of the stream that needs to be cooled down. The mass flowrate was equal to the vapor flowrate of this same stage going to the top stage. For the reboilers it was the opposite, the stage, one above the last stage, was used to find the cold temperature. The liquid flowrate from this stage to the bottom stage, was equal to the flowrate of the stream. The streams selected and all their relevant properties are shown in table x.

No.	Stream	Block in As	Condition	Fm (kg/s)	Cp (kJ/kgC)	Fm*Cp (kW	*Tin* (C)	*Tout* (C)	*ΔT* (C)	P (bar)	*ΔH* (kW)
H1	syngas cooling	gasifier	Hot	2,13	2,11431	4,50349	1343,62	35	-1308,62	1	-5893,35
H1-1				2,13	1,76392	3,75715	1343,62	67,2	-1276,42	1	-4795,7
H1-2				2,13	16,004	34,0885	67,2	35	-32,2	1	-1097,65
H3	H2 + H2O cooling	SOEC	Hot	0,32	8,72509	2,79203	700	25	-675	20,1	-1884,62
H3-1				0,32	6,53128	2,09001	700	136	-564	20,1	-1178,77
H3-2				0,32	19,872	6,35905	136	25	-111	20,1	-705,854
H4	FT Syncrude cooling	FT	Hot	2,91	5,98403	17,4135	200	35	-165	25	-2873,23
H4-1				2,91	2,49129	7,24966	200	155	-45	25	-326
H4-2				2,91	7,2938	21,225	155	35	-120	25	-2547
H5	Distil-1 Top cooling	Refinery	Hot	0,186	5,50669	1,02424	114,867	25	-89,867	1	-92,0457
H6	Distil-1 condenser	Refinery	Hot	0,45	9,91527	4,46187	138,025	114,867	-23,158	1	-103,328
H7	Distil-3 condenser	Refinery	Hot	0,825	8,33428	6,87578	283,806	240,802	-43,004	1	-295,686
H8	Distil-3 Bottom cooling	Refinery	Hot	0,107	3,35501	0,35899	399,767	360	-39,767	1	-14,2758
H9	Hydrocracker product cooling	Refinery	Hot	0,108	2,81736	0,30428	360	35	-325	35	-98,8894
H10	Fluegas-1 cooling	Turbine	Hot	1	1,24508	1,24508	1168,14	35	-1133,14	1	-1410,85
H10-1				1	1,18992	1,18992	1168,14	45,5	-1122,64	1	-1335,85
H10-2				1	7,14286	7,14286	45,5	35	-10,5	1	-75
H11	Fluegas-2 cooling	Turbine	Hot	1	1,32348	1,32348	1289	35	-1254	1	-1659,65
H11-1				1	1,23218	1,23218	1289	52	-1237	1	-1524,21
H11-2				1	7,96706	7,96706	52	35	-17	1	-135,44
C1	Heating water to steam for SOEC	SOEC	Cold	1,21	5,81909	7,0411	32,6042	700	667,396	20,1	4699,2
C1-1				1,21	4,81968	5,83181	32,6042	212,6	179,996	20,1	1049,7
C1-2				1,21	1957,68	2368,79	212,6	213,6	1	20,1	2368,79
C1-3				1,21	2,17607	2,63304	213,6	700	486,4	20,1	1280,71
C2	Preheating of bio-oil	gasifier	Cold	1,39	2,30726	3,20709	25	52	27	1	86,5915
C3	Heating syngas	FT	Cold	2,91	2,98129	8,67556	108,395	200	91,605	25	794,725
C4	Reboiler Distil-1	Refinery	Cold	1,41	7,7616	10,9439	214,123	250,868	36,745	1	402,132
C5	Reboiler Distil-2	Refinery	Cold	0,21	6,97689	1,46515	56,953	76,693	19,74	5	28,922
C6	Reboiler Distil-3	Refinery	Cold	1,61	17,8809	28,7883	388,037	399,771	11,734	1	337,802

As can be seen some of the streams are split. For each individual potential hot or cold stream a temperature-enthalpy (T,H) diagram was made in Aspen over its temperature range. The slope in a T,H-diagram is equal to the reciprocal CP. By looking at the constructed T,H-diagram, different regions, with different CP values, can be distinguished. To keep the stream behavior as realistic as possible the streams who have this starkly different CP-value regions are split, otherwise stream could be coupled who do not match on CP. The phase transitions are also modelled as separate streams, since these are a very distinct region, this is the best way to incorporate their contribution.

Pinch analysis:

First of all an explanation of the pinch will be provided. The pinch is a point between all the streams in which the heat transfer is the most constrained or lowest. The pinch divides the system into two thermodynamic regions. The region above the pinch is a heat sink, where the heat from the hot streams is utilized as much as possible to heat up the cold streams above the pinch, if more heat is needed a hot utility can be used. The region above the pinch is the other way around. Heat transfer across the pinch is unwanted, it does not provide the most energy efficient solution, since it increases both the cold and hot utility with the amount of heat transferred across the pinch.

To find the pinch the problem table method is used. Which consists of several steps:

1. A minimum temperature difference, ΔT_{min}, is chosen. The actual temperatures of the hot streams are subtracted with half ΔT_{min} to create interval temperatures. For the cold stream half ΔT_{min} is added. In this way there is always a temperature difference assured, since if the temperatures are equal, no heat would flow.
2. All of the interval temperatures found are ranked in order of magnitude from high to low, so the highest temperatures on top all the way to the lowest interval temperature. Values that appear more than once are only listed once.
3. Each stream has a starting and an end temperature. For each of the found intervals a heat balance can be set up by determining which streams are present in that interval. This is represented by formula x.

$$\Delta H_n = (\sum CP_c - \sum CP_h) \cdot \Delta T_n$$

Where,

- ΔH_n = net heat required in the nth interval
- ΣCP_c = sum of the heat capacities of all the cold streams in the interval
- ΣCP_h = sum of the heat capacities of all the hot streams in the interval
- ΔTn = interval temperature difference = $(T_{n-1} - T_n)$
- The heat capacity is the heat capacity flowrate in $kJ \cdot °C^{-1}$

4. The net heat of each interval is 'cascaded' to the interval below. This implies that a temperature difference is upheld, in which the heat can be transferred between the hot and cold streams. If this net value is negative in a respective interval, this means that the gradient is in the wrong direction, meaning that thermodynamically heat exchange is not possible.
5. Find the most negative value and add this value on the top of the interval. By introducing this heat and letting it cascade again. All the values will be positive, the most negative value is now 0 and this interval equals the pinch. The heat introduced

is the hot utility. Heat left on in the bottom interval needs to be cooled down by a cold utility.

These steps have been performed on the streams of table x in Excel. In Appendix x screenshots of this process can be found. The results of the table problem method are visualized in two different ways. Figure x shows the composite curves of the hot and cold stream.

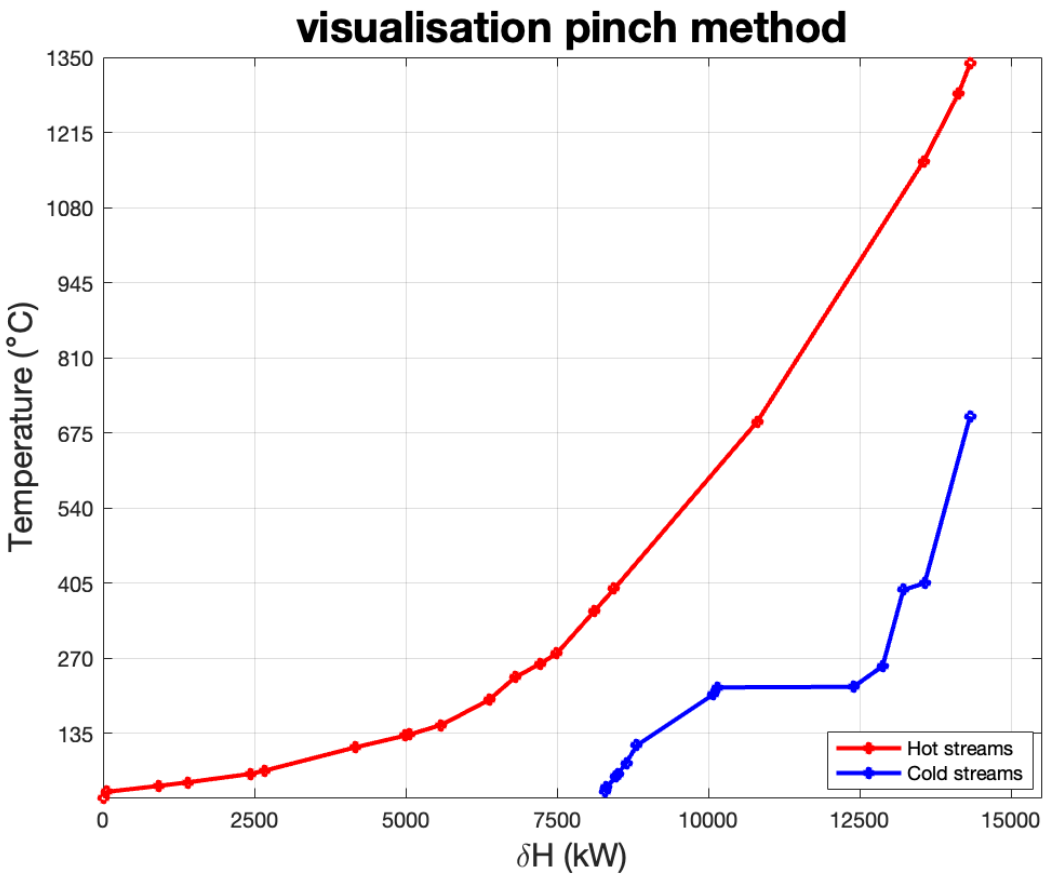

Since the x-axis is in ΔH, the curves can be shifted horizontally. This has been done for the cold composite curve, so that on the right side the highest point for both curves is at the exact same x-coordinate. This eliminates the need for a hot utility. Since it can be seen that the entire cold composite curve is underneath the hot composite curve and heat the red line has a part on the x-axis without the company of the blue line. This is a so-called threshold problem. There are two types of threshold problems. The first type has the closest temperature, the pinch, at the side of the non-utility and from there the curves diverge. The second type has the pinch in a region between the two ends, the closest point is called a pseudo pinch.

The figures are made using Matlab. As can be seen the pinch is located, where the curves are the closest to each other. This can be seen clearer in the next figure, which shows the grand composite curve (GCC). The GCC displays the net ΔH for each interval. It is shown in figure x.

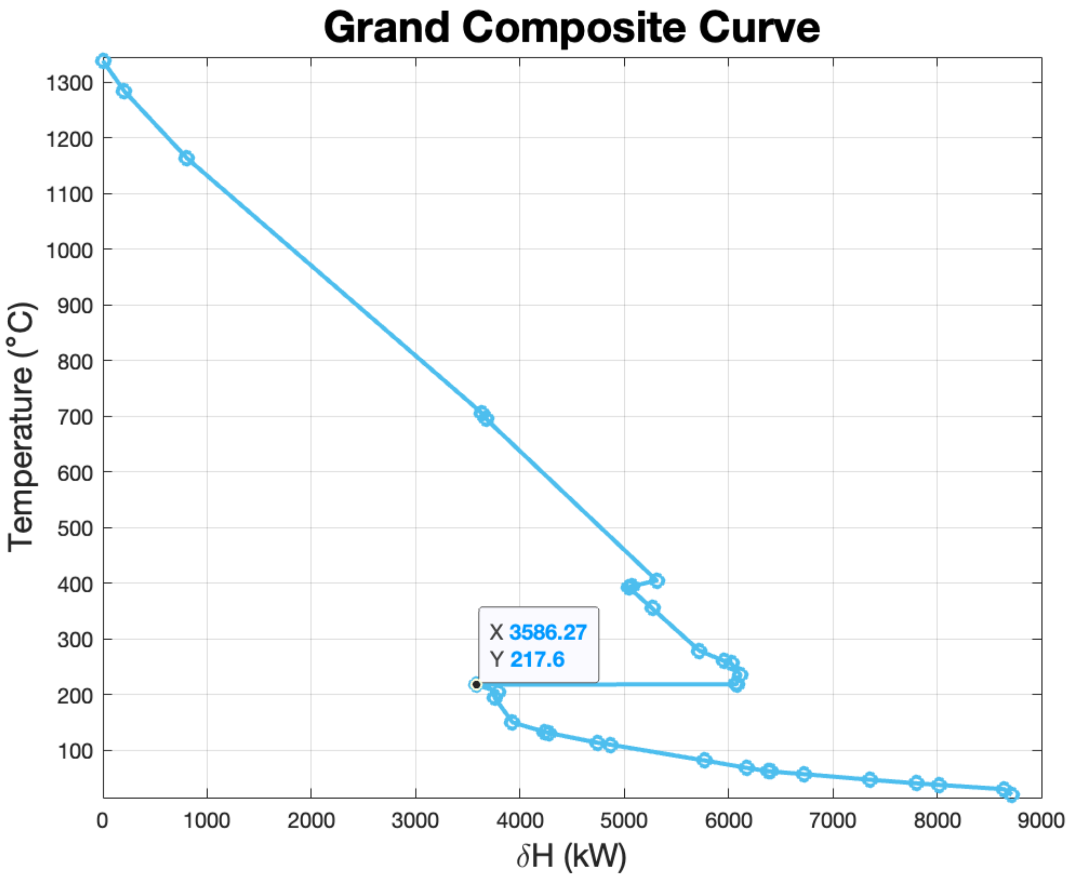

As can be seen the pinch is not exactly 0, meaning that for each interval the net heat duty was above 0. The pseudo pinch is at 217.6 °C. It is very important to note that heat does flow at the pseudo-pinch. It was said earlier that heat transfer across the pinch should be avoided as much as possible, but it is different for the pseudo pinch. As can be seen from figure x, the amount of heat that will be transferred from the hot to the cold region is equal to 3586.27 kW. This heat does not perform any work above the pinch. It is very important to note that unlike a 'normal' pinch, the pseudo pinch is a zone where heat flows, as seen in figure x. Other than this the pseudo pinch 'acts' as a 'normal' pinch. Since the pinch temperature of 217.6 °C is an interval temperature, the pinch for the hot streams occurs at 222.6 °C and for the cold streams as 212.6 °C, this is basically adding back the ΔT_{min} values.

To design a heat exchanger network for maximum heat recovery a few steps are again used.

First of all the network will be drawn as a grid. The middle of the grid contains two vertical lines. The hot streams are drawn above the cold streams. The region above the pinch is drawn on the left side of these vertical lines, with the hot streams flowing from left to right, descending in temperature until they reach the hot stream pinch temperature of 222.6 °C. If the stream is also present below the pinch temperatures, it starts on the left at 222.6 °C and continues to the right until its final temperature. The cold streams above the pinch are also drawn from left to right, but their temperature at the vertical lines is 212.6°C. If the cold stream continues or starts below the pinch, it starts at 212.6 °C. All of the CP values of the streams are written on the right-hand side of the grid.

6.1.3 Heat exchanger network

To combine the streams in the two regions a few rules are important. Since the region above the pinch was considered a heat sink, the maximum energy recovery is obtained if no cooling is needed. The network design starts at the pinch, to ensure the maximum temperature difference the following rule is most important above the pinch.

$$CP_h \leq CP_c$$

Meaning that the CP of the hot stream must be lower than the CP of the cold stream. Because if the CP_h would be larger than CP_c the lines would converge above the pinch, since the slope of the T,H-diagram is equal to the reciprocal of CP.

The opposite is true for the region below the pinch. Here the following must be true.

$$CP_h \geq CP_c$$

This shows the power of separating the streams based on their CP, as was said earlier. More flexibility in combining streams is received in this way.

Actual heat exchanger network:

Now that the theory behind designing a heat exchanger network is clear the actual case design for this model will be given. As was said earlier, this is a threshold problem. Meaning that only one utility is required. In this case only a cold utility will be required. The goal is to minimize this cold utility as well.
When adding up the ΔH of the hot and cold streams above the pseudo pinch the values are 7976.37 kW and 4389.4 kW respectively. The difference is 3586.97 kW, as found in figure x, which showed the GCC. The difference in these values is 0.7 kW, but this comes from rounding off in between the calculations. This means that this heat sur plus is carried through the pinch to the cold part by the different hot streams. This also means that not all the hot heat streams will be connected to cold streams, since the cold streams are already completely warmed up by the streams that do participate.
Below the pinch the situation is the same, much more heat is available in the hot streams, than needed by the cold streams. The sum of ΔH for the hot streams below the pinch is 6350 kW and for the cold streams it is equal to 1959.4 kW. A surplus of 4390.6 kW, this is without the heat transferred across the pinch.

As was explained before the pinch analysis is designed to maximize the heat energy that can be retrieved between hot and cold streams. Since the surplus of heat in the hot streams is so significant, the choice is made to take a more logical approach to heating up the cold streams. This means that the number of heat exchangers will be kept to a minimum and streams will high value heat, high temperatures, will be tried to be saved. Because the high-quality heat can again be used for the production of high-pressure steam to drive the turbine.

Above the pinch:

An overview in table form of the streams present above the pinch, their temperatures, CP's and ΔH values is provided in appendix x .By applying the logical approach as described above the following matches have been made:

	Hot stream	Cold stream	ΔH exchanged (kW)	Temperature hot stream (°C)	Temperature cold stream (°C)
Heat exchanger 1	H1-1	C1-1 + C1-2	3649.5	372.23	700
Heat exchanger 2	H3-1	C6	337.8	538.4	399.8
Heat exchanger 3	H1-1	C4	402.1	265.2	250.9

The green boxes indicate that the cold stream has reached its final temperature. Heat exchanger one firstly takes on two parts of the the most important cold stream, the heating of the water to steam for the electrolyser. C1-1 is the heating of the steam from 212.6 °C to 700 °C and C1-2 is the energy needed for the vaporization of the liquid water to steam. Since C1-1 and C1-2 are part of the same stream, they can be combined as one with stream H1-1, which is the hot syngas stream, starting at 1343.6 °C. The CP rule is also maintained, since the combination of the cold CP's greatly exceeds the hot CP. After this heat exchange stream H1-1 is cooled down to 372.23 °C and still carries 562.17 kW of heat. This part is sent to heat exchanger 3, where the reboiler of DISTIL-1 is supplied with enough heat to be heated to its end temperature of 250.9 °C. The stream H1-1 still has heat left, which is carried over across the pinch. Stream H3-1, carrying the hot hydrogen and water from the SOEC at 700 °C, is used to meet the heat duty of the reboiler from DISTIL-3, stream C6. Stream H3-1 is only cooled down to 538.4 °C.
This means that all the cold streams are completely heated up to their final temperature, the CP rule is maintained and only two hot streams are used.

Meaning that streams H2-1,H7,H8,H9,H10-1,H11-1, from above the pinch can be used to heat up the cold streams below the pinch.
Before identifying which hot streams could be used for steam generation, the cold part, below the pinch, will also be covered.

	Hot stream	Cold stream	ΔH exchanged (kW)	Temperature hot stream (°C)	Temperature cold stream (°C)
Heat exchanger 4	H4-1 + H4-2	C1-1	976.3	143.9	200
Heat exchanger 5	H7	C1-1	73.4	273.1	212.6

Heat exchanger 6	H4-2	C2	86.6	138.9	52
Heat exchanger 7	H6	C5	28.9	131.5	76.7
Heat exchanger 8	H7	C3	222.3	240.8	134
Heat exchanger 9	H3-1	C3	572.4	264.5	200

To heat the four cold streams and keep the valuable hot streams in mind, 6 heat exchangers are needed for the cold part. Stream H4, cooling of the syncrude, has a high enough CP to heat up stream C1-1, which is heating up the water to its boiling point. Since stream H4 starts at 200 °C, it cannot heat up stream C1-1 completely to 212.6 °C. The missing heat is supplied by the condenser of DISTIL-3. The preheating of the bio-oil, stream C2, and the reboiler duty of DISTIL-2, C5, both have small heat requirements at low temperatures and are therefore easily satisfied by low quality heat streams. Lastly the heating up of the syngas from 108.4 to 200 °C, stream C3, needs to be done. Stream H7 has 222.3 kW left, which it can transfer to C3, heating it up to 134 °C. The remainder of the heat is supplied by stream H3-1. This is the only CP violation, since $CP_h < CP_c$, but since it can be seen that H3-1 is cooled down to 264.5 °C it is clear that the delta T remains high enough and stream C3 can completely be heated up to its target of 200 °C.

This means that all the cold streams of the system are completely heated up to their final temperature, but as said before much heat is left in the hot streams. A process flow diagram is produced using the program visual paradigm, it has all the important streams and products with the 9 heat exchangers highlighted in red.

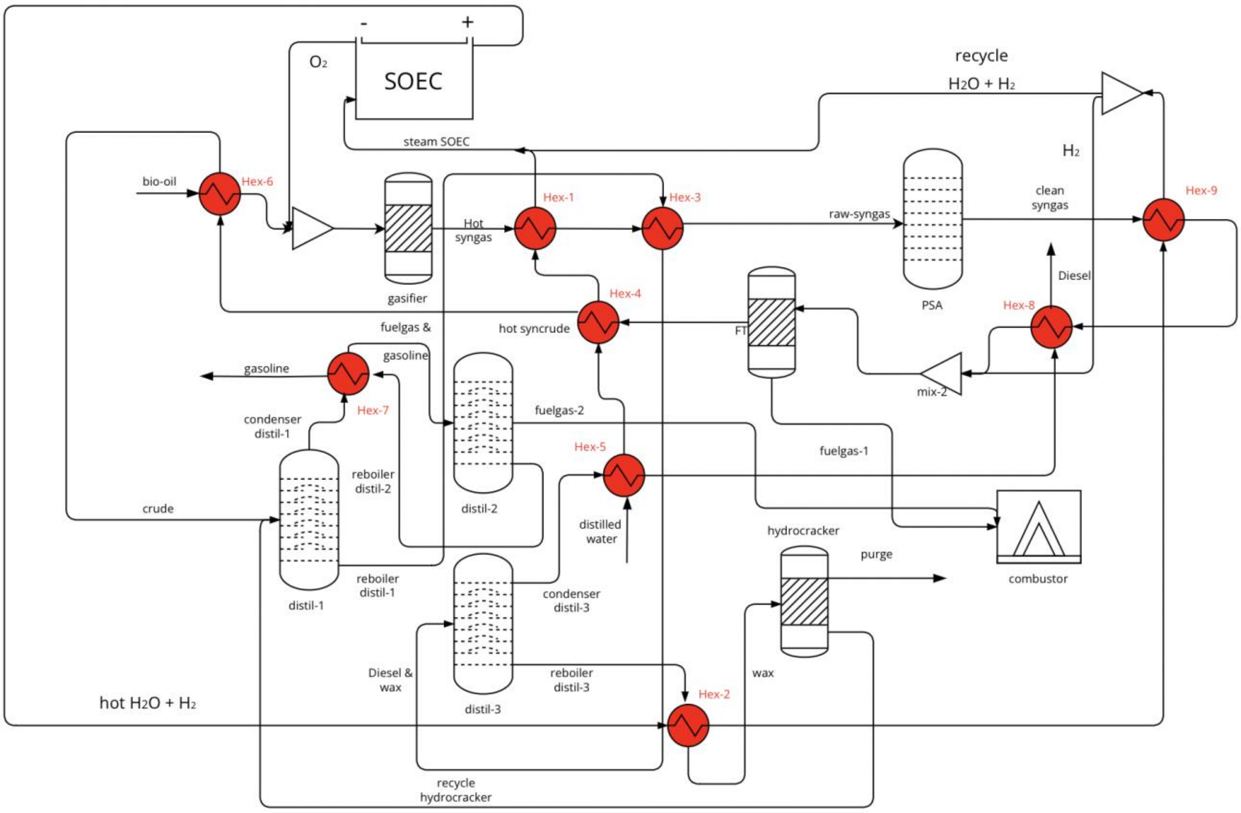

Producing high pressure steam:

Table x gave an overview of all the streams involved. By looking at the temperature of the streams and the heat left, it can be seen that the only reasonable streams for steam production are H10 and H11, the combustion of the by-product fuel gas. The other streams have either to little heat left, to make investing in a heat exchanger worth it, or the temperature of the streams is too low to create high pressure steam.
Thus the results remain the same as presented in section 5.5, since, the combustion of the fuel gas and the power produced by the turbine have already been discussed there.

The final heat duties left are relatively small and are summarized in table x.

Unit	Model section	Heat duty kW
PSA	gasifier	-22.2
Flash 1	FT	-149.6
Flash 2	FT	17.9
Decant	refinery	-5.9
Hydrocracker	refinery	-14.0
Flash 2	turbine	-49.8

The heat duty of Flash 2 will be met by using electricity, a total of 17.9 kW. The heat released by the other units is released into the surroundings and considered a heat loss, it equals 241.5 kW.

Final heat balance:

The final heat balance is based on the overview of the hot and cold streams, presented in table x and the heat exchanger network, combined with the measures for the heating duties of the other units. The total amount of heat present in the hot streams is equal to 14.33 MW, including the energy produced by the combustion of the fuel gasses. The cold streams combined needed 6.35 MW, which was fully provided by the hot streams, maintaining the correct minimum temperature difference and adhering to the CP rules. The difference between these two numbers is 7.98 MW. Since the fuel gas streams where not used for heat transfer and their purpose is to be used for the production of electricity in the turbine, their heat duties will be subtracted from this number. The amount of heat present in the fuel gas streams was 3.07 MW. Meaning that the hot streams still contain 4.91 MW of energy, at varying temperatures, which will need to be cooled by a cold utility, since the streams need to be cooled down for a reason in the process. The cooling of the low-pressure steam coming from the turbine, produces 2.45 MW. This stream leaves the turbine at a temperature of 253.5 °C. According to Fortman et al, the Carnot efficiency of this heat to produce more power is around 2 %, meaning that 0.05 MW of additional electricity could be produced. This is an extremely low number, that is why the best use for this waste heat is to make it available in the municipal sector for heating applications, where efficiencies close to 100 % can be achieved, via different thermal energy storage techniques.

6.2
Energy analysis of the entire process:

In this section the final energy analysis of the process will be analyzed. As is known the energy efficiency is equal to the energy flowing out of the process, divided by the energy put into the process. In formula form and already taking filling in the relevant components this looks as follows:

$$\eta = \frac{\dot{m}_{Diesel} \cdot H_{Diesel} + \dot{m}_{gasoline} \cdot H_{gasoline}}{\dot{m}_{bio-oil} \cdot H_{bio-oil} + P_{SOEC} + P_{el}} \cdot 100\%$$

Where,

- η = the efficiency of the process in %
- $\dot{m}_i$ = the mass flowrate of component i in kg·h^{-1}
- H_i = the heating value of component I in MJ·kg^{-1}
- P_{soec} = the electric energy consumed by the electrolyser
- P_{el} = the electric energy consumed for pumps, compressors and heating

The values are summarized in table x, the results of the heat integration are also included in the table:

Class	Energy carrier	Energy (MW)
Feedstock	Bio-oil (5000 kg·h^{-1})	23.89 (LHV)
(by) Products	Diesel (990 kg·h^{-1})	8.36 (LHV)
	Gasoline (557.5 kg·h^{-1})	6.94 (LHV)
	HP steam (7884.4 kg·hr^{-1})	6.24
	Municipal heat	2.45
Electricity SOEC	SOEC power	11.82
Electricity other	SOEC unit PUMP	0.0034
	FT unit COMP	0.623
	FT unit FLASH2	0.0179
	Refinery unit PUMP	$9.29 \cdot 10^{-4}$
	Refinery unit COMP	$8.93 \cdot 10^{-4}$
	Turbine unit Turbine	-0.616
	Cold utility	4.91
Balance without heat integration	**Total out**	15.3
	Total in	36.3 + 4.91
Balance with heat integration	**Total out**	23.99
	Total in	41.21

Now applying formula x, results in an energy efficiency of 37.1 %. This is the number obtained when not taking the heat integration into account, except the cold utility requirement, since this is an inherent energy cost.
If the heat integration would be taken into account, the products would now be the diesel, gasoline, municipal heat and the 200 °C, 16.5 bar steam produced with the heat of the FT reactor. The steam captured the heat of the FT reactor and is an export product, that is why it is taken as the full heat duty of the FT reactor. Adding the high-pressure steam and municipal heat as products to formula x results in an efficiency of 58.2 %. (bron FT information perhaps handy in bladwijzers)

Chapter 7

Economic analysis

In this last chapter the economic analysis of the process will be performed. In section 7.1 the CAPEX, capital expenditure, of the process will be analyzed. Section 7.2 will cover the OPEX, the operating costs. Lastly section 7.3 will cover the profitability of the process.

7.1 capex

The capital costs will be estimated based on values found in literature. Not only the costs of the physical units are part of the CAPEX. The costs of installing them, overseeing the project by a contractor, transportation of the materials, all has to be paid for.
All of this makes up the total capital investment (TCI). The TCI will be calculated using the factored estimation. This method divides the large installation of the whole plant into different major components, the respective sections of the model. The TCI is made up of sum of the costs and the earlier described installation factor, f, which covers the relevant infrastructure, piping, controls etc. The total of the sum of costs and the installation factor, will be multiplied by another 15%, which will cover contingencies. In formula form it looks as follows:

$$TCI(€) = (1 + 0.15) \cdot \Sigma C_i \cdot (1 + f_i)$$

- Where C_i is the total cost of component i
- Where f_i is the is the installation factor

Equipment costs in literature are quoted in different forms. For example Free on Board (FOB), where the seller of the items delivers the product ready and packaged on a ship, this does not take any costs as transportation into account. Inside battery limits (ISBL) is the second time, which is often reported in literature, this includes the cost of all equipment and piping, instrumentation etc. lastly, outside battery limits (OSBL), which is the most thorough, includes on top of the ISBL, the utilities, common facilities etc. examples are the power lines, land use, sewage etc. Due to this inconsistent way of reporting the costs in the academic world, the installation costs vary widely.

Since the capacity of the equipment determines the price, the costs will be scaled using:

$$\frac{Cost_{original}}{Cost_{scaled}} = \left(\frac{Size_{original}}{Size_{scaled}}\right)^{Scaling\ factor}$$

Lastly to account for the annualized investment costs (AIC) (€), the following formula will be used:

$$AIC = TCI/(1 - DR\% + 1)^{-lifetime}$$

Where,

- DR% is the discount rate percentage
- Lifetime is the lifetime of the unit/equipment

Finding the exact costs of the units is not straightforward and scaling according to the size, is not the most accurate predictor. Since the costs are the main priority of this thesis, it is assumed that sizing is acceptable and representative. Several very comprehensive articles that cover the costs of a BtL process via the FT reaction have already been written. The costs of the gasifier, gas cleaning and FT section, crude-upgrading and power generation can be found in this way. The cost of the SOEC will have to be retrieved separately. Table x contains the units, their quantity and their scaled costs. The costs are calculated using formula x and x, inflation is also incorporated in the final costs, or TCI.

Table 16: total installation cost, inflation, installation factor and contingencies taken into account when determining final costs.

Unit	Base capacity	Base cost (Million €)	Overall installation factor	Scaling factor	Model capacity	TCI (million €)
Gasification, raw syngas cleaning and processing						
EF gasifier[1]	400 MW_{th} (LHV)	129 (2005)	Included	0.7	24 MW_{th} (LHV)	25.50
Particle filters	12.1 $m^3 \cdot s^{-1}$ gas	1.9 (2002)	2	0.65	1.97 $m^3 \cdot s^{-1}$ gas	3.04
Cyclones	12.1 $m^3 \cdot s^{-1}$ gas	3 (2002)	2	0.7	1.97 $m^3 \cdot s^{-1}$ gas	4.80
Scrubbers	12.1 $m^3 \cdot s^{-1}$ gas	3 (2002)	2	0.7	1.97 $m^3 \cdot s^{-1}$ gas	4.80
PSA[2]	9600 $kmol \cdot hr^{-1}$	32.6 (2002)	1.69	0.7	278 $kmol \cdot hr^{-1}$	12.75
Electrolyser						
SOEC[3]	5 MW	10 (2020) €2000/kW	included	1	11.82	27.14
Fischer- Tropsch synthesis						
FT feed compressor	2 MW_e	1.57 (2007)	Included	0.67	0.623 MW_e	1.12
FT slurry bubble column[4]	362 m^3	16.2 (2002)	Included	0.75	60 m^3	7.30
Hydrocracker[5]	13.2 $m^3 \cdot hr^{-1}$	8.22 (2002)	1	0.7	2.64 $m^3 \cdot hr^{-1}$	6.13
Power production						
Boiler steam generator, ductwork, stack	24 MW_{th} boiler duty	1.83 (2007)	included	1	3.07 MW_{th} boiler duty	0.36
Steam cycle (turbine + generator)	30 MW_e	11.0 (2007)	included	0.67	0.62 MW_e	1.27

[1] the price is based on bio-oil as input.
[2] includes both the CO_2 and H_2S PSA.
[3] prices varied from €960-5600 in 2020, costs are expected to drop in the future, €2000/kW chosen to be in the low end of the spectrum and account for price drop in future.
[4] exact source [] confidential
[5] slurry bubble column size in model based on throughput crude oil.

Lastly the costs of more basic units, like pumps, flash drums, decanters, distillation columns, mixers and the heat exchangers were also be retrieved externally. These are summarized in table x:

Unit	Base capacity	Base cost (Million €)	Overall installation factor	Scaling factor	Model capacity	TCI (million €)
Pump	0.14 MW_e	0.12 (2007)	4	1	$4.36 \cdot 10^{-3}$	0.029
Decanter	46.75 $m^3 \cdot h^{-1}$	0.083 (2012)	included	1	9.36 $m^3 \cdot h^{-1}$	0.023
Distillation column	150 $m^3 \cdot h^{-1}$	0.27 (2007)	4	1	23.42 $m^3 \cdot h^{-1}$	0.33
(static) Mixers	50 $L \cdot s^{-1}$	$5.43 \cdot 10^{-3}$ (2007)	included	1	6897 $L \cdot s^{-1}$	1.17
Flash drums	1 MW_{th}	0.22 (2007)	included	1	0.2 Mw	0.044
Heat exchangers	1000 m^2	0.207 (2007)	3.5	1		

Summing up the total of the TCI, the total capital investment is equal to 95.708 Million euros.

7.2 Opex:

The operational expenditure can be found by examining all the cost that are made to keep the operation running. These include rent and utilities, wages, taxes, accounting and legal fees, price of feedstock, maintenance of the equipment and insurance. These can again be divided in fixed and in variable costs. The fixed costs mainly constitute from the maintenance and insurance of the equipment and wages of the employees. The other factors listed are considered variable.

The annual maintenance costs are assumed to be 3% of the TCI. The insurance is assumed to be equal to 0.1% of the TCI. Both these numbers come from []. The wages were also retrieved from Hamelinck et al. They were assumed to be 0.5 % of the TCI at 400 MW_{HHV} of biomass input. The cost of wages scales down with the capacity, a scaling factor of 0.25 is assumed. The HHV of the bio-oil was equal to 30.11 MW, applying the scaling comes results in an estimate of 0.26% of TCI for the wages. Meaning that the annual fixed costs are assumed to be equal to 3.36 % of the TCI.

The variable costs are largely dominated by the electricity consumed and the price of the feedstock, the bio-oil and demineralized water. The costs of the catalysts and solvent are negligible. The degradation of the SOEC performance also has to be taken into account. The hydrogen and oxygen it needs to produce, remains the same, but more electricity is required as the cell performance degrades. Table x summarizes the variable costs.

Unit	Capacity	Total 8000 h·yr^{-1}	Costs per unit	Annual cost (€)
SOEC electricity	11.82 MW	94560 MWh	€100 ·MWh^{-1}	9,456,000
Other electricity	5 MW	40000 MWh	€100 ·MWh^{-1}	4,000,000
Bio-oil	5000 kg·hr^{-1}	40000 tons	€250 ·ton^{-1}	10,000,000
Demi-water	2000 kg	16000 tons	€2 ·ton^{-1}	32,000
SOEC degradation	-0.5% ·1000 hr^{-1}	-4 %	+ 1930 MWH	193,000

The electricity price was taken as presented in May of 2023. The electricity price is capped at €400 per MWh however, meaning that the electricity cost could be quadrupled. The price of the bio-oil is taken to be €250. This is the average price of pyrolysis oil produced by BTG from clean wood and residues, it is assumed that the supplied bio-oil is 50-50 mixture of these. The SOEC cells will degrade 4% annually. A degradation of 2% was taken to calculate the average amount of electricity that will be consumed extra by the electrolyser over the year. The cell stacks can be replaced however. This will be done when the efficiency of the electrolyser has dropped to 80%, it is assumed that this price falls within the maintenance costs.

The fixed annual costs amount to € 3.2 million. The variable costs are equal to € 23.68 million, resulting in a total OPEX of €26.88 million.

Revenue:

The revenue of the plant comes from the gasoline and diesel produced, the high-pressure steam and the municipal heat. These are summarized in table x.

Unit	Capacity	Total 8000 h·yr^{-1}	Costs per unit	Annual proceeds (€)
Gasoline	557.488 kg·hr^{-1} / 884.5 dm^3·hr^{-1}	7.076·10^6 dm^3·hr^{-1}	€0.514·dm^3	3,637,064
Diesel	989.965 kg·hr^1 /1840.4 dm^3·hr^{-1}	14.723 ·10^6 dm^3·hr^{-1}	€0.688 ·dm^3	10,129,424
HP steam	7884.44 kg·hr^{-1}	63,076 tons	€34.1 · ton^{-1}	2,150,892
Municipal heat	2 MW	16000 MWh		

The volume streams of the gasoline and diesel were found using Aspen. The prices were found by looking at the pump prices and subtracting the cost of the excise duties and taxes instilled by the Dutch government. The price of the high-pressure steam is a very general one, since no data could be found on the price for the specified temperature and pressure. The total annual proceeds amount to € 15.92 million.

7.3 Profitability analysis:

Form the total proceeds and the OPEX it can be seen that the project is making a significant net loss of close to €11 million. The main reason is the electricity price and the worth of the products. The latter has to do with the fact that the government makes the most profit on diesel and gasoline bought by the consumer. But the biggest influence is the very high electricity price and need. The war in Ukraine has exploded the electricity prices globally, but mostly in Europe. To make a profit of €1 million, the electricity price would have to be €34.9 per MWh. Under the fast transition scenario, by 2050 1 MWh of solar energy will cost between $2-40, or equivalently €1.82-36.4, which would already mean that the process becomes profitable.

Another factor is the way in which the process is set up. This thesis took the premise that maximizing the amount of diesel and gasoline produced is the best strategy. Similar studies have shown that to maximize profitability the amount of fuel gas produced is so large, that the electricity is sold off as a profitable product as well. However, these studies did not integrate an electrolyser into their system, which is by far the most electricity demanding element of the whole process.

The small scale of the process also results in a relatively high price. For example Rafati et al. have an mixed input of biomass and natural gas equal to 400 MWth. Their FT liquids yield is equal to 2984.6 barrels per day, or 405.9 tons. Meaning that 1014 kg of FT liquids is produced per MW_{th} input. In this study the numbers are 37.14 tons per day for an input of 23.89 MW_{th} based on the LHV of the bio-oil. Meaning that 1555 kg of FT liquids is produced per MW_{th}.

The conclusion that can be drawn in terms of the profitability of the process is that currently it is not a profitable process. But with the energy transition and the development of all the integrated sustainable elements, it can become a competitive production pathway for liquid transportation fuels in the future.

Chapter 8

8.1 Conclusions

The first part of chapter 8 will cover the conclusions that can be drawn from the thesis. The goal was to convert 5000 $kg \cdot hr^{-1}$ of pyrolysis oil into gasoline and diesel, while integrating several sustainable units, to have an overall sustainable and carbon neutral production process. The process runs on renewable electricity, produced by a hybrid wind and solar farm with battery storage. A SOEC electrolyser was used to produce oxygen and hydrogen. The oxygen was sent to an entrained flow gasifier, which turned the bio-oil into syngas. The syngas was upgraded and mixed with the hydrogen gas produced by the electrolyser to obtain the desired H_2:CO ratio. The syngas was transformed to hydrocarbon chains via the Fischer Tropsch process. The hydrocarbons where split in a refinery section to the desired products, a hydrocracker unit was used to increase the yield of the desired products. Lastly heat integration was applied along with the usage of the by-product fuel gas to produce power, to make the overall process as energy efficient as possible. The process was modelled using a software of program developed by AspenTech, Aspen Plus. To assess the quality of the process, it was reviewed from a techno-economical perspective. To do is several research questions were formulated in section 1.3, which will now be answered.

Sub question 1:

What gasifier design and specifications deliver the best quality of syngas, aiming for a high CO yield, for further upgrading while integrating the high-quality heat produced with the provided bio-oil?

An entrained flow gasifier was chosen. The main reasons were its larger production capacity potential, good heat integration properties, little tar production and its compatibility with directly using bio-oil. The gasifier was optimized towards the production of as much CO as possible. The reason being that the only carbon source that would be used for the production of the FT hydrocarbons, was CO. This is the case, since no water gas shift unit was incorporated in the system. The gasifying agent was pure oxygen, coming from the electrolyser. The main factors affecting this goal were the oxygen equivalence ratio and steam to carbon ratio. An OER of 0.498 was chosen and no steam was supplied to the gasifier. The choice of supplying no steam was to create much useful heat in the adiabatically operated gasifier and the mentioned CO yield. A 5% heat loss in the gasifier was considered. The raw syngas coming from the gasifier had a H_2:CO ratio of 0.68 and a molar fraction of 0.37 for CO was reached.

The exiting raw syngas stream reached a temperature of 1343.62 °C, which was able to fully heat up the water going to the SOEC electrolyser and cover the heat demand of one of the distillation columns' reboiler.

Sub question 2:

Which type of electrolyser is most suited for efficient energy integration in this process?

The process has two large heat sources, the gasifier and the FT reactor. On top of that the by-product fuel gas can also be combusted to supply heat where needed. A SOEC electrolyser was therefore chosen. It required a lot of heat, in return its electric efficiency is unmatched. It was found that the electrolyser can be operated below its thermoneutral potential. This allows the electrolyser to 100% efficiently use the renewable electricity supplied. Electricity, especially renewable electricity, is a relatively valuable energy carrier, especially relative to heat. By supplying almost 19% of the energy needed to split the water via heat, less electricity is needed to obtain hydrogen and oxygen. Increasing the overall energy efficiency of the process. So the most suited and energy efficient electrolyser type for this process is the SOEC electrolyser.

Sub question 3:

How to optimize and integrate the Fischer Tropsch process towards the production of gasoline and diesel constituents and use its exothermic reactions in the system?

The FT process is a well-developed and relatively old technology. Many research has been conducted on the process and optimum conditions for the production of diesel and gasoline are known. A low temperature FT process was chosen over a cobalt catalyst. The conditions were 200 °C, 25 bar and a H_2:CO ratio of 2.15:1. These process conditions resulted in a chain growth probability factor of 0.872, allowing for the formation of large hydrocarbon molecules, which yields in the highest amount for the desired products. The carbon conversion was found through a kinetic analysis and literature and equaled 80%. The amount of products formed in the FT reactor, was assumed to obey the Anderson Schulz Flory distribution in terms of their molar fractions. The heat produced by the FT reactor was equal to 6.2 MW. It was used to produce 7884 kg·hr^{-1} of steam at 16.5 bar, which was also sold off as a product. Meaning that the optimization of the FT reactor was mainly based on literature operating conditions and that the heat was used for the production of high pressure steam, which boasted the financial attractiveness of the whole process.

Sub question 4:

How will the FT reactor's products be extracted and converted to the desired products, while maximizing their yield?

Since the FT reactor was optimized towards large hydrocarbon chains production, a hydrocracker unit was used to break down the large chains to hydrocarbons in the desired product range. Distillation columns however preceded the hydrocracker to separate four main categories of molecules. Fuelgas C_2-C_4 , gasoline C_5-C_{10} , diesel C_{11}-C_{21} and wax C_{22+}. In this way high purity gasoline and diesel were obtained. The flowrates where 558 kg·hr^{-1} of gasoline and 990 kg·hr^{-1} of diesel. The diesel contains only paraffinic hydrocarbons, resulting in a very high cetane number and high-grade low sulfur diesel, ready to be blended in. All the distillation columns achieved separations of 95% of the desired compound into its respective steam.

Sub question 5:

Is the process technologically and economically feasible?

The process is indeed technologically feasible. 57.2% of the carbon entering the process is converted to the desired products, diesel and gasoline. The integration of the sustainable units was very successful. Using the pure oxygen as a gasifying agent instead of air, significantly increases the performance of the gasifier. The hydrogen that is formed at the same time makes it possible to optimize the gasifier to maximum CO production. The FTS produces clean and high-quality hydrocarbons.
The process as of now was found to not be economically feasible, the largest factor is the extremely high electricity price at the moment. But future predictions estimate renewable electricity prices to get as low as €2 MWh, which would make the process profitable and a good investment.

The main research question:

How to integrate an as energy efficient possible system that incorporates electrolysis run on renewable electricity and bio-oil as feedstock for the production of diesel and gasoline via the Fischer Tropsch process?

The answer to the main research question is a combination of the answers provided to the sub research questions. Summarized it is as follows. By using a high energy demanding SOEC electrolyser, which operates very electricity efficiently, the energy production of the other units as the gasifier and FT can be used to fuel its energy demands. In return a relatively small amount of renewable electricity is used. By also using excess heat to produce sellable by-products as high-pressure steam and municipal heat, the energy losses are kept to a minimum. The cold utility requirement was equal to 4.91 MW in this way, for a process that produces almost a factor 3 more heat. The answer to the main research questions thus becomes, by choosing units that create products for each other, while being able to supply each other's energy demands.

This concludes the findings of the thesis. Since there is still room for improvement in the process the next section will propose some recommendations for future research.

8.2 Future recommendations

The main reason that many of the recommendations that will now be proposed were not investigated more thoroughly in this thesis is a lack of time. Also the scope of the thesis and its battery limits were determined beforehand and within these limits the research was done. The recommendations will be listed per unit, the same order as throughout the thesis, and ideas of why this should be investigated further will be shared.

- The gasifier unit uses pinewood derived bio-oil as feedstock. This is a relatively clean, at the same time more expensive biomass feedstock. The effects of different, cheaper, bio feedstocks could be investigated. If solid biomass is chosen to be the feedstock, many pre-treatment units will have to be added to the process. It can be investigated if the investing the capital costs needed for these extra units, turns out to be profitable since it would make the biomass unit per unit probably cheaper.

- The gasifier operates at 7 bars. This was done in this thesis to have the raw syngas at the pressure needed in the downstream units, mainly the pressure swing absorber for H_2S removal. Increasing the pressure inside the gasifier would lead to a lower CO yield, but a higher initial H_2:CO ratio, requiring less hydrogen from the electrolyser. The same can be done by introducing steam to the inlet of the gasifier. However, the downside is that with the introduction of steam the outlet temperature of the raw syngas, which played a vital role in the heat exchanger system, would drop significantly. The analysis would thus be if decreasing the amount of hydrogen produced by the electrolyser, since it was the determining factor of the electrolyser production capacity, is worth the heat needed to be supplied, with the benefit of using less electricity.

- If the choice is made to not aim for maximum CO production, the introduction of a water gas shift unit can be investigated. This unit would also use the CO_2 coming from the gasifier to produce more CO. it does add extra costs though and it was found that the molar fraction of the CO_2 was more than a factor 3 lower than that of CO under these conditions. Thus it must be investigated if supplying heat to drive the endothermic reaction of producing CO and water from CO_2 and hydrogen gas is worth the investment of a WGS unit and extra energy demand, while also decreasing the H_2 yield.

- The SOEC electrolyser technology is not well-developed yet, even though great progress is being made in its limitations and stability. It could be investigated if increasing the operating temperature would have additional benefits for the system and what measures could be implemented to counteract the degradation. Also a more thorough financial assessment of this important unit could be made.

- The combustion of the fuel gasses has CO_2 as a major product. Also the CO_2 separated by the PSA is considered waste in the model. These two streams could be captured and fed to the SOEC electrolyser, along with the steam, to directly produce syngas. The potential of the SOEC electrolyser to cofire steam and CO_2, to directly produce syngas could be investigated.

- The main limitation of this thesis is that a standard ASF distribution was assumed for the FT products. An extensive kinetic model using the Aspen Plus simulating software could give a more accurate representation of the performance and products formed in the FT reactor. With a kinetic model a more comprehensive understanding of the influence of the operating conditions could be obtained as well. Sensitivity analysis on varying the pressure and temperature would be the tools for this.

- Observing the effect of changing the cobalt catalyst for an iron catalyst could also be investigated. This would be in combination with the earlier mentioned operating conditions of the gasifier. The iron catalyst has higher activity for the WGS reaction, which would mean that less additional hydrogen is needed. It would also greatly increase the amount of olefins formed, which is beneficial for the gasoline production. Since diesel production was the main target in this thesis this option has not been investigated.

- To improve the economics of the process more fuel gas should be produced to perhaps have a net positive output of electricity, via its combustion towards steam production. This would mean a decrease in the yield of the desired products, but on the other hand a more financially sound process. This can be achieved by optimizing the FT reactor towards a lower chain growth probability factor.

- Since the market share of the relatively small process of this thesis of diesel and gasoline is so limited, the choice was made to have ‘unfinished’ diesel and gasoline, which would be blended with traditional diesel and gasoline produced from fossil fuels. The addition of an isomerization and alkylation plant could be investigated to convert the lower hydrocarbons to mainly gasoline, to have a more finished product.

This covers the future recommendations that could be investigated, as well as the thesis.

Appendix A biomass pre-treatment

The gasification process is made up of different sub-processes which make up a chain from raw biomass or waste up to gasified products. The starting point is having a source of biomass. A list of pre-treatment processes is needed before the biomass is ready for the conversion to the products one wants.

First of all, the obvious types of pre-treatments are harvesting and collecting the biomass and biobased waste. The next step is to store the harvested biomass. The process conditions under which the biomass is stored affect several important parameters for later on, like the dry matter content, the moisture content and most importantly the energy value. There are even some environmental and safety aspects to storing biomass. It can occur that microbiological activity causes degradation to the biomass, which results in mass and volume losses, this process in its turn can emit greenhouse gases and cause self-heating, creating a potential hazard. In most cases a higher original moisture content in the biomass equals a larger loss in dry matter. Dry matter is where the energy is stored, so keeping the losses of thus as minimal as possible is preferable. That's why it is advised to store the biomass when the moisture content is reduced to around 20%. Lastly airtight conditions can also reduce the amount of dry matter lost.

The next two steps, drying and transporting, are somewhat interchangeable. Preferably drying of the biomass is performed in situ, dry biomass has less mass and volume and is thus cheaper to transport. Raw biomass has a high moisture content and in most cases it needs to be dried to reduce this. This high moisture content is unacceptable for most processes because it lowers the effective heating value of the fuel. Drying can be done in several ways, three of them will be briefly discussed. Firstly the biomass can be dried naturally, meaning that dry air is used to take up the water and take it away. This is the slowest way to achieve moisture reduction and is preferred before transportation, if the cost of transportation is affected by volume and mass. The local weather conditions play an important role, but it is a very cheap method to achieve moisture reduction up to around 20% in couple of days. The next method is mechanical drying. As the name suggests machinery is used to reduce the moisture content. A prerequisite is that the biomass is compressible. Different apparatuses are used to squeeze out the moisture from within the biomass structures. It is an energy intensive process, but works much faster than natural drying. Lastly thermal drying can be used, heat is used to remove the moisture. It is the most energy intensive drying technique. There are different types of dryers and techniques available. To choose the most appropriate technique factors as the heat sensitivity of the biomass, its physical form, the throughput capacity, turndown ratio and the pre- and post-drying operations need to be considered. Transportation speaks for itself.

Appendix B Modelling distillation columns

If the molar heat of vaporization for any of the components has the same value, condensation of 1 mole of vapor will vaporize 1 mole of liquid. If the heat losses from the column are limited and the pressure is uniform throughout the column, the vapor and liquid flowrates remain semi-constant. This simplification holds up for many distillations. If constant molar vapor and liquid flow is assumed for each section of the column, energy balances are neither needed in the stripping section nor in the rectifying section. Only a vapor-liquid curve and a material balance are required. These assumptions are used in the McCabe-Thiele method to find the previously mentioned parameters.

First the operating line of the rectifying section needs to be found. The operating line relates the concentrations of one molecule y for vapor and x for liquid, to the flowrate of two passing streams, the vapor and the liquid stream. Following the same line of thought, the operating line of the stripping section can be obtained.

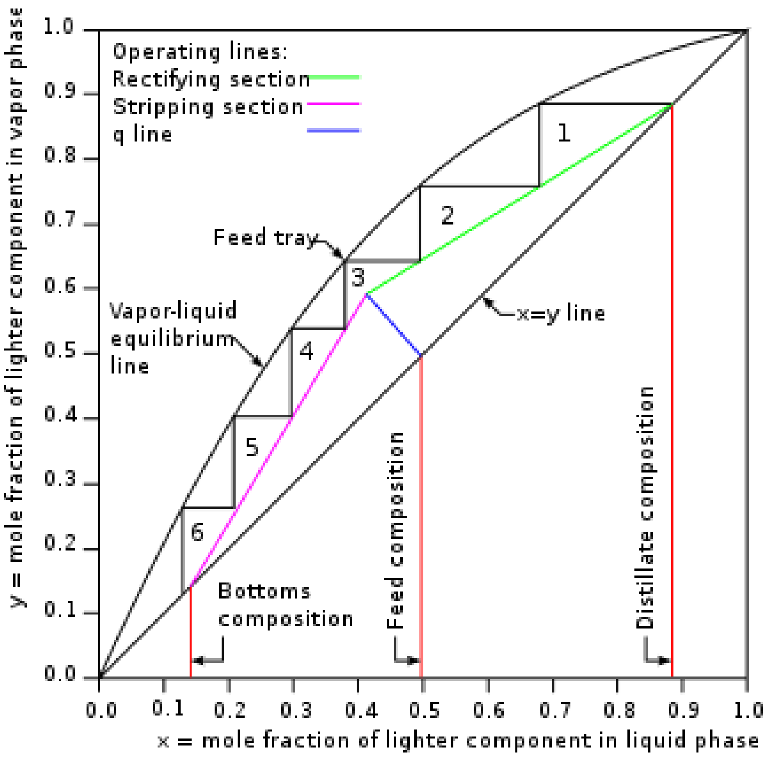

That looks as is seen in figure x

When finding the feed tray the following factors need to be considered. The operating lines for the stripping and the rectifying section are both mass balances. When introducing the feed, these mass balances will change. Nevertheless, the vapor flow in the rectifying section, V', must be larger than the liquid flowrate, L', in the rectifying section. For the stripping section the reverse holds, the liquid flowrate, L'', is higher than the vapor flowrate, V'', between the stages. The following that must hold is that if the feed is mainly liquid the liquid flowrate in the stripping section will be larger than in the rectifying section. If the feed is mainly vapor the vapor flowrate of the rectifying section must be larger than that in the stripping section. These two fixed regularities give rise to an overall mass balance which combines the feed with the respective liquid and vapor flowrates in both sections:

$$F + V'' + L' = L'' + V'$$

If the balance is only applied over the liquid phase it yields:

$$L_F = L'' - L' \equiv q \cdot F$$

Where L_F is the liquid flowrate of the feed and q is defined as the liquid fraction in the feed at feed stage temperature. If the feed is at feed temperature, then q defines the moles of liquid flow in the stripping section resulting from every mole of feed added. Now if the assumption is made that the molar liquid enthalpies and molar vapor enthalpies remain relatively constant a final equation can be made that expresses q in terms of the molar enthalpies:

$$q \equiv \frac{h_V - h_F}{h_V - h_L}$$

h_V, h_L, h_F being the molar enthalpies of the vapor, liquid and feed respectively. Since the molar enthalpies can be estimated a value for q can be obtained. By finding the intersection of the operating lines of the stripping and the rectifying section, for constant molar flow, with q, the so called q-line can be found. It represents a straight line on which every intersection of the other two operating lines must fall. The slope of the q-line is governed by the nature of the feed.

By plotting all three of the operating lines the number of equilibrium stages can be found by constructing a staircase from the first point of the rectifying section to the bottom point of the stripping operating line, or at least over it. This is shown in figure x. What can also be seen in figure x is that the optimum feed stage location can be found at the first opportunity after a horizontal line of the staircase crosses the q line.

For every distillation a target purity of the desired product is specified. Increasing the number of equilibrium stages results in a higher purity but added costs and more complex operation. That is why it was shown how to find the minimum number of equilibrium stages. Another way to increase purity is by increasing the reflux ratio. The reflux ratio is defined as the amount of distillate, for the rectifying section, or the amount of liquid, in the stripping section, that is extracted from the column over the amount that is sent back into the distillation column. A higher reflux ratio requires more energy. The flowrates found for the minimum number of equilibrium stages can be used to find the minimum reflux ratio needed. For the rectifying section that looks like this:

$$R = \frac{(\frac{L'}{V'})_{min}}{1-(\frac{L'}{V'})_{min}}$$

The minimum reflux ratio and the minimum number of stages required are strong tools to find the practical distillation conditions. The operating and fixed costs are a function of the relation between these two minima. For most commercial operations the optimum reflux ratio is between 1.1 and 1.5 the minimum reflux ratio.

1. Flexmill. *Airfoil polishing*. 2021 09-05-2023]; Available from: https://www.flexmill.fi/applications/airfoil-polishing/.
2. Kwack, S.-H., et al., *Development of a kinetic model of the Fischer–Tropsch synthesis reaction with a cobalt-based catalyst.* Reaction Kinetics, Mechanisms and Catalysis, 2011. **104**(2): p. 483-502.
3. Téllez-Anguiano, A., et al., *Continuous-Discrete Observer-based fault detection and isolation system for distillation columns using a binary mixture.* Revista mexicana de ingeniería química, 2016. **15**(1): p. 275-290.
4. Lindsey, R. *Climate Change: Atmospheric Carbon Dioxide*. 2022 27-04-2023]; Available from: https://www.climate.gov/news-features/understanding-climate/climate-change-atmospheric-carbon-dioxide.
5. Friedmann, J., et al., *Net Zero and Geospheric Return: Actions Today for 2030 and Beyond.* 2020.
6. Hames, B.R., *Biomass compositional analysis for energy applications.* Biofuels: methods and protocols, 2009: p. 145-167.
7. Lee, R.A. and J.-M. Lavoie, *From first- to third-generation biofuels: Challenges of producing a commodity from a biomass of increasing complexity.* Animal Frontiers, 2013. **3**(2): p. 6-11.
8. The Geography of Transport Systems. *Global Greenhouse Gas Emissions by the Transportation Sector*. 2014 27-04-2023]; Available from: https://transportgeography.org/contents/chapter4/transportation-and-environment/greenhouse-gas-emissions-transportation/.
9. Holmberg, K. and A. Erdemir, *The impact of tribology on energy use and CO2 emission globally and in combustion engine and electric cars.* Tribology International, 2019. **135**: p. 389-396.
10. International Energy Agency. *Biofuels*. 2022 27-04-2023]; Available from: https://www.iea.org/reports/biofuels.
11. Strezov, V. and T.J. Evans, *Biomass processing technologies*. 2014: CRC Press.
12. AtlasCopco. *What are commercial and industrial uses of carbon dioxide?* 27-04-2023]; Available from: https://www.atlascopco.com/en-ug/compressors/wiki/compressed-air-articles/carbon-dioxide-uses.

13. Wiebren de Jong, R.v.O., *Biomass as a Sustainable Energy Source for the future*. 2014, Hoboken, New Jersey: John Wiley & Sons, American Institute of Chemical Engineers, Inc.
14. Chen, H., *Lignocellulose biorefinery product engineering.* Lignocellulose Biorefinery Engineering, 2015. **11**: p. 125.
15. Leijenhorst, E.J., et al., *Entrained flow gasification of straw-and wood-derived pyrolysis oil in a pressurized oxygen blown gasifier.* Biomass and bioenergy, 2015. **79**: p. 166-176.
16. Zheng, J.-L., et al., *Gasification of bio-oil: Effects of equivalence ratio and gasifying agents on product distribution and gasification efficiency.* Bioresource Technology, 2016. **211**: p. 164-172.
17. Eubia. *Gasification*. 27-04-2023]; Available from: https://www.eubia.org/cms/wiki-biomass/pyrolysis-and-gasification/gasification/.
18. Puig-Arnavat, M., J.C. Bruno, and A. Coronas, *Review and analysis of biomass gasification models.* Renewable and sustainable energy reviews, 2010. **14**(9): p. 2841-2851.
19. Boerrigter, H. and R. Rauch, *Review of applications of gases from biomass gasification.* ECN Biomassa, Kolen en Milieuonderzoek, 2006. **20**: p. 211-230.
20. Nelson, L., S. Park, and M.A. Hubbe, *Thermal depolymerization of biomass with emphasis on gasifier design and best method for catalytic hot gas conditioning.* BioResources, 2018. **13**(2): p. 4630-4727.
21. Van den Aarsen, F., A. Beenackers, and W. van Swaaij, *Modeling of a fluidized bed wood gasifier.* Energy from Biomass, 1983. **5**: p. 255.
22. Choi, W.-K., et al., *Optimal operation of the pressure swing adsorption (PSA) process for CO 2 recovery.* Korean Journal of Chemical Engineering, 2003. **20**: p. 617-623.
23. Adams II, T.A., Y.K. Salkuyeh, and J. Nease, *Processes and simulations for solvent-based CO2 capture and syngas cleanup*, in *Reactor and process design in sustainable energy technology*. 2014, Elsevier. p. 163-231.
24. Rafati, M., et al., *Techno-economic analysis of production of Fischer-Tropsch liquids via biomass gasification: The effects of Fischer-Tropsch catalysts and natural gas co-feeding.* Energy conversion and management, 2017. **133**: p. 153-166.
25. International Renewable Energy Agency. *Hydrogen*. 2022 27-04-2023]; Available from: https://www.irena.org/Energy-Transition/Technology/Hydrogen.
26. Thomas Chrometzka, C.J., Aoibhin Quinn, Tanai Potisat. *H2 View Exclusive – Calculating the Cost of Green Hydrogen*. 2020 27-04-2023]; Available from: https://www.enapter.com/newsroom/h2-view-exclusive-calculating-the-cost-of-green-hydrogen.
27. Todoroki, N. and T. Wadayama, *Electrochemical stability of stainless-steel-made anode for alkaline water electrolysis: Surface catalyst nanostructures and oxygen evolution overpotentials under applying potential cycle loading.* Electrochemistry Communications, 2021. **122**: p. 106902.
28. Schmidt, O., et al., *Future cost and performance of water electrolysis: An expert elicitation study.* International journal of hydrogen energy, 2017. **42**(52): p. 30470-30492.
29. IRENA, *Green Hydrogen Cost Reduction: Scaling up Electrolysers to Meet the 1.50C Climate Goal*. 2020, nternational Renewable Energy Agency
: Abu Dhabi.

30. Sasikumar, G., J. Ihm, and H. Ryu, *Optimum Nafion content in PEM fuel cell electrodes.* Electrochimica Acta, 2004. **50**(2-3): p. 601-605.
31. Hauch, A., et al., *Ni/YSZ electrodes structures optimized for increased electrolysis performance and durability.* Solid State Ionics, 2016. **293**: p. 27-36.
32. Hauch, A., et al., *Recent advances in solid oxide cell technology for electrolysis.* Science, 2020. **370**(6513): p. eaba6118.
33. Bridgwater, A., *Fast pyrolysis of biomass for the production of liquids*, in *Biomass combustion science, technology and engineering*. 2013, Elsevier. p. 130-171.
34. Piemonte, V., et al., *Bio-oil production and upgrading: New challenges for membrane applications.* Membrane Technologies for Biorefining, 2016: p. 263-287.
35. Chakraborty, J.P., S. Singh, and S.K. Maity, *Advances in the conversion of methanol to gasoline*, in *Hydrocarbon Biorefinery*. 2022, Elsevier. p. 177-200.
36. Schulz, H., *Short history and present trends of Fischer–Tropsch synthesis.* Applied Catalysis A: General, 1999. **186**(1-2): p. 3-12.
37. Förtsch, D., K. Pabst, and E. Groß-Hardt, *The product distribution in Fischer–Tropsch synthesis: An extension of the ASF model to describe common deviations.* Chemical Engineering Science, 2015. **138**: p. 333-346.
38. Van Santen, R., et al., *Mechanism and microkinetics of the Fischer–Tropsch reaction.* Physical Chemistry Chemical Physics, 2013. **15**(40): p. 17038-17063.
39. Kim, Y.H., et al., *A simulation study on gas-to-liquid (natural gas to Fischer–Tropsch synthetic fuel) process optimization.* Chemical Engineering Journal, 2009. **155**(1-2): p. 427-432.
40. Sims, R.E., et al., *An overview of second generation biofuel technologies.* Bioresource technology, 2010. **101**(6): p. 1570-1580.
41. Schulz, H., *Comparing Fischer-Tropsch synthesis on iron-and cobalt catalysts: The dynamics of structure and function*, in *Studies in surface science and catalysis*. 2007, Elsevier. p. 177-199.
42. Krishna, R. and S. Sie, *Design and scale-up of the Fischer–Tropsch bubble column slurry reactor.* Fuel processing technology, 2000. **64**(1-3): p. 73-105.
43. Porter, E.A. *Distillation*. 2011 09-05-2023]; Available from: https://www.thermopedia.com/content/703/.
44. Hsu, C.S. and P.R. Robinson, *Petroleum science and technology*. 2019: Springer.
45. Danesh, A., *PVT and phase behaviour of petroleum reservoir fluids*. 1998: Elsevier.
46. Aitani, A.M., *Oil refining and products.* Encyclopedia of energy, 2004. **4**: p. 715-729.
47. Corma, A. and A. Martínez, *Zeolites in refining and petrochemistry.* Stud. Surf. Sci. Catal, 2005. **157**: p. 337-366.
48. Dancuart, L., R. De Haan, and A. De Klerk, *Processing of primary Fischer-Tropsch products.* Studies in Surface Science and Catalysis, 2004. **152**: p. 482-532.
49. Dry den, I.G.C., *The Effienct Use of Energy*. second ed. 1982: Butterworth & Co.
50. Gopal, S., et al., *A Review on Steam Turbine Blade Desing and Its Principle.* International Journal of Science Technology & Engineering, 2015. **2**(5): p. 1-5.
51. Editorial Staff. *Three Phase AC generators*. 09-05-2023]; Available from: https://instrumentationtools.com/three-phase-ac-generators/.
52. Hamelinck, C.N., et al., *Production of FT transportation fuels from biomass; technical options, process analysis and optimisation, and development potential.* Energy, 2004. **29**(11): p. 1743-1771.

53. van den Oever, A., et al., *Systematic review on the energy conversion efficiency of biomass-based Fischer-Tropsch plants.* Fuel, 2022. **324**: p. 124478.
54. Centraal Bureau voor de Statistiek. *Aardoliegrondstoffen- en aardolieproductenbalans; aanbod en verbruik*. 2023 09-05-2023]; Available from: https://www.cbs.nl/nl-nl/cijfers/detail/84596NED.
55. PureTec industrial water. *Water Quality Standards*. 09-05-2023]; Available from: https://puretecwater.com/storage/app/media/downloads/reference/water-quality-standards.pdf.
56. Eurowater. *Water treatment for Hydrogen production*. 2023 09-05-2023]; Available from: https://www.eurowater.com/en/hydrogen-production.
57. Ryu, J., *Catalytic Cracking of Diesel Fuel for Army Field Burners. Part 1. Feasibility of Producing Gaseous Fuel From Diesel Fuel Via Catalytic Cracking*. 1999, ASPEN SYSTEMS INC MARLBOROUGH MA.
58. Khuong, L., et al., *A review on the effect of bioethanol dilution on the properties and performance of automotive lubricants in gasoline engines.* RSC advances, 2016. **6**(71): p. 66847-66869.
59. Jafari, M., et al., *Cost of fouling in full-scale reverse osmosis and nanofiltration installations in the Netherlands.* Desalination, 2021. **500**: p. 114865.
60. Shell. *Opbouw brandstofprijs*. 2020 09-05-2023]; Available from: https://www.shell.nl/consumenten/shell-fuels/opbouw-brandstofprijs.html#:~:text=De%20opslag%2D%20%26%20transportkosten%20liggen%20voor,diesel%20en%2011%25%20voor%20benzine.
61. Shell. *Shell Brandstofprijzen*. 2023 09-05-2023]; Available from: https://www.shell.nl/consumenten/shell-fuels/brandstofprijzen.html.
62. Stempien, J.P., et al., *Physical principles for the calculation of equilibrium potential for co-electrolysis of steam and carbon dioxide in a Solid Oxide Electrolyzer Cell (SOEC).* Electrochimica Acta, 2014. **147**: p. 490-497.